



ECONOMÍA CIRCULAR DE LA INDUSTRIA
AGROALIMENTARIA

TESIS DOCTORAL

D. FRANCISCO JOSÉ SÁNCHEZ BORREGO

Sevilla, 2022



AGRADECIMIENTOS

La realización de esta Tesis Doctoral ha sido posible gracias a la ayuda, apoyo y colaboración de muchas personas.

En primer lugar, quiero agradecer a la tutora de este trabajo, la catedrática Paloma Álvarez Mateos, por su confianza depositada en mí. Todo empezó con mi trabajo fin de grado en 2016, donde desarrollé una gran pasión por el mundo de las energías renovables, y no podría haber sido sin la tutorización de ella, que me metió en un campo del que nunca quiero salir. Gracias por orientarme y transmitirme tus conocimientos durante estos años, además de darme la oportunidad de desarrollar mi pensamiento crítico. Y por supuesto, gracias por pelear contra viento y marea para que la Tesis Doctoral siguiera adelante, ya que sin tu tenacidad nada habría sido posible.

Agradecer también a mi director de la Tesis Doctoral, el doctor Juan Francisco García Martín, por ayudarme a replantear y reformular cada uno de los párrafos que iba escribiendo en los artículos. Gracias por tu inconmensurable ayuda a la hora de redactar dichos artículos, ya que me ayudaste a mejorar mucho mi redacción científica, a la par que me enseñaste desde cero a como presentar artículos en revistas científicas de alto impacto.

Asimismo, a las profesoras Titulares de Universidad Francisca Romero Sarria y M.^a Dolores Alcalá González, y al profesor Titular de Universidad José Manuel Córdoba Gallego, por haberme enseñado como poner el equipo de pirólisis en funcionamiento, así como su conservación y mantenimiento. De igual forma, por haberme dejado utilizar el equipo de Espectroscopía Infrarroja, así como el medidor de Superficie Específica (BET).

Por supuesto, quiero destacar la labor de *Kaura Coproducts*, *Biosel* y *Coopvcampo*, ya que, sin el suministro de las distintas materias primas, el trabajo descrito en esta Tesis Doctoral no hubiera sido posible.

No puede faltar la mención a todos los compañeros de trabajo con los que he entablado una amistad y han hecho mi trabajo durante estos años mucho más sencillo y llevadero. Gracias a Noelia García Criado, Salvatore Romano y a Tomás Barea de Hoyos

Limón por los buenos momentos, así como las discusiones sobre los temas técnicos generados en el laboratorio.

A mi familia por todo su apoyo durante estos años, ya que cada fin de semana que volvía a casa, me encontraba con un apoyo incondicional. Y en especial a mi pareja, por aguantar muchas de nuestras conversaciones en las que le contaba lo que iba haciendo diariamente, y aunque ella no entendía la mitad siempre me escuchaba, y me alentaba a seguir trabajando duro.

Por último, pero no menos importante, a mis amigos por todo vuestro apoyo y ayuda. Los viajes que hemos ido realizando durante estos años, las salidas, las conversaciones... cada momento ha ayudado a llevar el desarrollo de la Tesis Doctoral, así como la redacción de ésta mucho más fácil.

ÍNDICE

RESUMEN	7
MARCO DE LA TESIS	9
1. INTRODUCCIÓN	10
1.1. Residuos Agroalimentarios	11
1.2. Tratamientos y/o usos actuales	13
1.3. Pirólisis	14
2. OBJETIVOS DEL TRABAJO	17
3. RESULTADOS Y DISCUSIÓN	18
3.1. CAPÍTULO 1: CARACTERIZACIÓN DEL PROCESO	18
3.1.1. Análisis Termogravimétrico (TGA)	19
3.1.2. Distribución de los productos de la pirólisis	19
3.2. CAPÍTULO 2: APLICACIÓN DE LOS BIOCARBONES	22
3.2.1. Absorción de azufre utilizando los biochars obtenidos de naranja dulce y rama de naranjo	23
3.2.2. Aplicación de los biochars obtenidos de hueso de aceituna como catalizador en la reacción de esterificación	24
3.3. CAPÍTULO 3: CARACTERIZACIÓN DE LOS BIO-OILS	27
4. CONCLUSIONES	30
5. REFERENCIAS BIBLIOGRÁFICAS	32
6. Biodiesel and Other Value-Added Products from Bio-Oil Obtained from Agrifood Waste	34
7. Determination of the Composition of Bio-Oils from the Pyrolysis of Orange Waste and Orange Pruning and Use of Biochars for the Removal of Sulphur from Waste Cooking Oils	50
8. Production of Bio-Oils and Biochars from Olive Stones: Application of Biochars to the Esterification of Oleic Acid	71

RESUMEN

Los residuos de la industria agroalimentaria, como son los residuos de naranjo y del aceite de oliva, tienen una gran repercusión debido a su gran producción anual a nivel global. En los países del mediterráneo (Italia, Grecia, España...), la producción de dichas industrias es mayor que en el resto del mundo. Esto hace especialmente importante el estudio de nuevas formas de aprovechamiento de dichos residuos, con el fin de contribuir al “*zero waste*” mediante la economía circular. Dentro de los residuos anteriormente descritos, algunos como los huesos de aceituna, ramas y hojas, pueden ser usados como combustibles directamente.

No obstante, existen otros tratamientos termoquímicos como torrefacción, gasificación, pirólisis, etc., que aportan una nueva visión del aprovechamiento de dichos residuos lignocelulósicos para la producción y obtención de productos de alto valor añadido. En la presente Tesis Doctoral se ha optado por la pirólisis de los huesos de aceituna, las podas de naranjas y los residuos generados en la extracción del zumo de naranjas dulces.

La pirólisis en la última década ha sido una técnica muy empleada para la reutilización de residuos lignocelulósicos y obtención de productos de alto valor como son un sólido poroso (biocarbón o biochar), un líquido viscoso (bio-oil o bioaceite) y un gas (syngas o gas de síntesis). La pirólisis está tomando mucha importancia por los usos que tienen estos productos. Por un lado, el bio-oil junto al syngas tienen gran valor para la obtención de biocombustibles. El biocarbón es un material que tiene una alta superficie específica, lo que le confiere un gran uso como bioadsorbente y biocatalizador.

En el desarrollo de esta Tesis Doctoral, todos los biocarbones obtenidos a partir de las distintas materias primas fueron caracterizados por microscopía infrarroja, así como su superficie específica (método BET). Una vez caracterizados todos los biocarbones, fueron utilizados con distintos fines. En primer lugar, una parte de ellos fue utilizada para la adsorción de sustancias contaminantes (en este caso azufre) de aceite usado, con el fin de adecuarlo a las condiciones exigidas de venta para producción de biodiésel. En segundo lugar, otros biocarbones se utilizaron para la obtención de biocatalizadores ácidos para la reacción de esterificación de ácidos grasos libres con metanol, para la producción de ésteres metílicos (biodiésel).

Por otro lado, el bio-oil obtenido fue analizado, con el objetivo de identificar los compuestos con mayor valor añadido, aportando un gran valor al bio-oil. Se encontraron

algunos muy interesantes, tales como la levoglucosanona y el catecol, que tienen un gran interés en la industria orgánica.

MARCO DE LA TESIS

La presente Tesis Doctoral se ha realizado gracias a la financiación del proyecto FEDER Interconecta “*Economía Circular aplicada a la producción eficiente de biocombustibles y bioenergía*” (CARBOENERGY), realizado con las empresas *Kaura Coproducts, S.L.*, *Bioenergía y Biomasa de Andalucía S.L.*, y *Agrícola Olivarera Virgen Del Campo S.c. Andaluza*. El proyecto está dentro del marco de la potencialización de la economía circular en las industrias agroalimentarias, concretamente en la búsqueda de alternativas viables, tanto técnica como económicamente, de residuos de naranjos y olivar. Dicho proyecto ha sido subvencionado por la Unión Europea dentro del Fondo Europeo de Desarrollo Regional para el periodo 2018-2021, gestionado por el CDTI.

Este objetivo viene englobado en el marco de la sostenibilidad de los recursos agroalimentarios mediante la economía circular, principio recogido en el Programa Marco Horizonte 2020 (H2020) de la Unión Europea.

El trabajo experimental se ha llevado a cabo durante los años 2019-2021 en el Departamento de Ingeniería Química de la Facultad de Química, dentro del grupo de investigación AGR155 “Obtención de biocombustibles”.

Los trabajos han tenido un claro enfoque multidisciplinar, realizando experiencias a escala laboratorio, y posteriormente evaluándose los resultados aplicando técnicas de química analítica (FTIR, cromatografía de gases, superficie específica BET...).

Los resultados que se muestran son fruto de la realización de una serie de trabajos de investigación que se presentan como compendio de artículos en revistas científicas de alto impacto, de acuerdo con la normativa reguladora de los estudios de doctorado en la Universidad de Sevilla, dentro del programa de doctorado en Química.



1. INTRODUCCIÓN

1.1. Residuos Agroalimentarios

De entre todas las materias primas de la industria alimentaria, las frutas y verduras son las que más residuos producen. En Europa, España lidera el ranking de producción de naranja y zumo de naranja, y ocupa el sexto lugar en el ranking mundial, según la Organización de las Naciones Unidas para la Agricultura y la Alimentación (2018) [1]. En España, esta actividad agrícola se encuentra principalmente en Valencia y Andalucía, produciendo casi 2×10^6 t al año de naranjas dulces, fruto del naranjo dulce (*Citrus sinensis*). Según el Ministerio de Agricultura, Pesca y Alimentación de España (2018) [2], la recolección, manipulación, transporte y comercialización de la naranja es responsable de miles de empleos [3].

La poda es realizada por los agricultores, con el objetivo de eliminar ramas viejas y poder regenerar los naranjos. En España, se producen anualmente más de 5×10^6 t de poda de naranjos, que son considerados residuos y, por tanto, deben eliminarse para evitar la contaminación, el crecimiento de plagas y el retraso de las prácticas agrícolas [4]. La poda del naranjo está compuesta principalmente por celulosa, hemicelulosa y lignina.

La industria de los cítricos, en particular el sector del zumo de naranja produce más de $2,2 \times 10^6$ t de residuos en España cada año [2]. Los residuos de naranja generados en la producción de zumo de naranja suponen alrededor del 50-60% (p/p) en base húmeda [5] de la fruta procesada, con una cantidad de humedad de aproximadamente el 82% (p/p) [6], conteniendo el residuo alrededor del 60-65% de piel, 30-35% de pulpa y 0-10% de semillas [7]. Actualmente, estos residuos no tienen un uso comercial rentable. Tradicionalmente, se utilizan para la alimentación de los animales, como abono [8] o como cama para el ganado, opciones que no aportan ningún beneficio ni económico ni medioambiental, por lo que muchos de ellos van a parar a los vertederos creando un problema logístico [9] y aumentando el problema económico y medioambiental [10].

Otra de las materias primas más importantes a nivel global es la relacionada con la industria del olivo, que supone 11×10^6 ha en el mundo, la mayor parte en países mediterráneos, como España, Italia, Grecia, Marruecos, etc. Se producen 20×10^6 t [11] de aceitunas al año (Fig. 2). La principal explotación es la producción de aceite de oliva, que produce grandes cantidades de subproductos. Otro de los principales productos son las aceitunas de mesa, conocidas en todo el mundo como encurtido y utilizadas como ingrediente en la cocina.

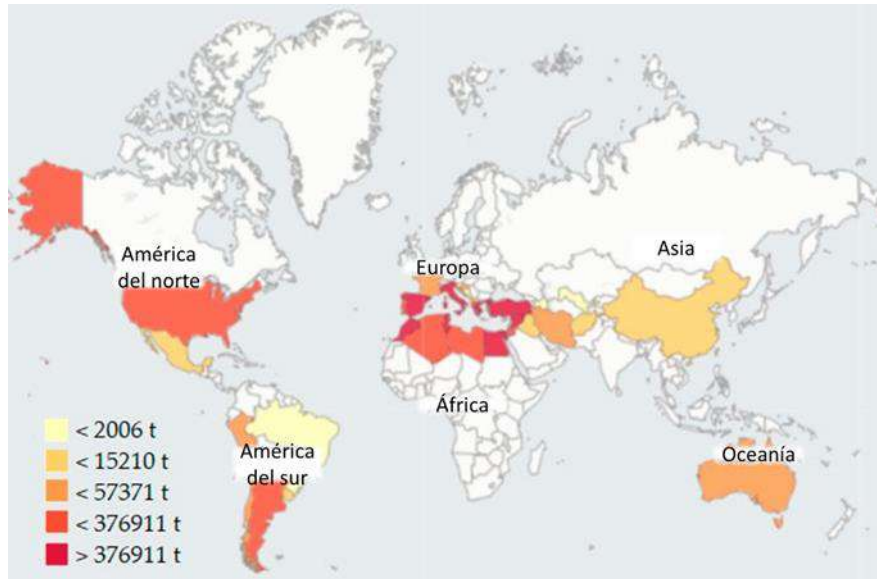


Figura 2. Producción media de aceitunas por países entre 1994 y 2017 [11].

En la industria olivarera, el proceso de extracción del aceite puede realizarse con decánters de 2 o 3 fases, dando lugar a diferentes tipos de residuos (2 fases alperujo y aceite; 3 fases orujo, alpechín y aceite). En general, se puede decir que los subproductos principales de las almazaras son el orujo, las aguas residuales de la almazara, el alpeorujo y el hueso de aceituna. De este último se estima que son unas 42.900 t/año [12], lo que hace esencial la búsqueda de su aprovechamiento para obtener productos de alto valor. En la Fig. 3 se muestra la generación de subproductos de la industria del aceite de oliva por ha de cultivo.

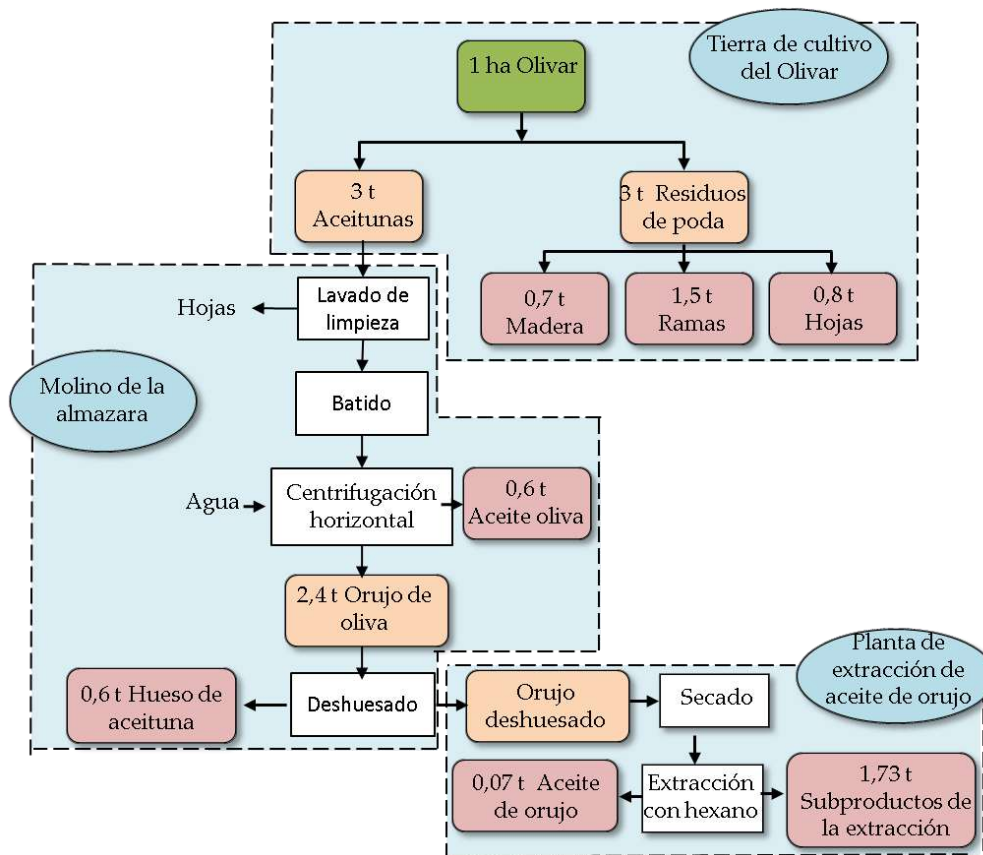


Figura 3. Producto y subproducto por ha de olivar obtenidos de las almazaras [11].

Como se puede observar en la Fig.3, los mayores subproductos son el hueso de aceituna (OS) con 0,6 t/ha y los residuos de poda (3t/ha).

El hueso de aceituna está formado por celulosa, hemicelulosa y lignina. Su composición en estos componentes es diferente según la variedad de la aceituna, pero tiene un rango entre 27,1%-36,4% (p/p) de celulosa; 24,5%-32,2% (p/p) de hemicelulosa y 23,1%-40,4% (p/p) de lignina [11,13–15].

1.2. Tratamientos y/o usos actuales

Hoy en día, existen muchos tratamientos para estos residuos. Respecto a los residuos de naranja, en los últimos años, se han propuesto diferentes vías de recuperación y reutilización. Entre ellas, destacan los procesos bioquímicos como la fermentación para la producción de bioetanol [16], la digestión anaeróbica [17,18] y la recuperación de flavonoides y productos químicos [19]. Recientemente, también se han investigado métodos de conversión térmica, como la gasificación, el tostado y la pirólisis de cáscaras de cítricos [20].

Los huesos de aceituna tienen usos muy variados, que van desde su conversión en pellets para su uso en calderas, hasta su transformación en biocombustibles (bioetanol) [21]. Otro campo en el que pueden ser útiles es en la construcción, donde pueden ser usados como materiales de construcción [22]. Finalmente, unos usos menos conocidos son la obtención de harinas ricas en omega 3 y fibra [23] y la producción de bioplásticos [24].

No obstante, el uso principal de este subproducto es su combustión directa en calderas. Este tratamiento es ampliamente utilizado en la industria agroalimentaria para la obtención de energía térmica. La combustión directa genera unos graves problemas ambientales, debido a la emisión de CO₂, CO, SO y SO₂, generando así una grave contaminación atmosférica. No obstante, hay otros tratamientos termoquímicos menos dañinos para el medio ambiente, como pueden ser la torrefacción, gasificación, licuefacción hidrotermal y la pirólisis.

La torrefacción es un proceso caracterizado por un calentamiento en atmósfera no oxidante. La temperatura máxima de operación en dicho proceso es 300 °C [11]. Este tipo de proceso suele ser utilizado para obtener de la biomasa un material enriquecido en carbón con una alta energía y un bajo contenido en oxígeno.

La gasificación es otro proceso termoquímico basado en la oxidación de la biomasa, normalmente sólidos compuestos por lignocelulosa, llevada a cabo con oxígeno o vapor de agua a altas temperaturas (800-1000 °C). El objetivo principal es la obtención del gas de síntesis (syngas), compuesto principalmente por N₂, CO y H₂, que se puede utilizar en procesos como el de Fischer-Tropsch para la fabricación de biocombustibles.

La licuefacción hidrotermal (HTL) es un proceso usado para convertir biomasa con humedad en un bio-oil utilizando temperatura moderada (150-350 °C) y altas presiones (50-200 bar). Este bio-oil puede ser transformado en biogás por digestión anaerobia. Además, se obtiene un carbón con un alto poder calorífico (puede ser utilizado para la producción de energía) y un syngas (que como hemos visto antes es útil en obtención de biocombustibles) [25].

1.3. Pirólisis

El proceso de pirólisis es llevado a cabo a altas temperaturas (entre 300 y 700°C), en ausencia de oxígeno (atmósfera inerte de Ar, N₂...). Durante el proceso de pirólisis, cada material lignocelulósico (celulosa, hemicelulosa y lignina) experimenta distintos

mecanismos de reacción (descarboxilación, deshidratación y desmetilación), produciendo una fracción líquida (bio-oil), una fracción gaseosa (syngas), y un sólido rico en carbono (biochar) [26].

Hay numerosos factores que afectan al proceso de pirólisis, de entre los que se incluyen las características de la materia prima, la temperatura de pirólisis, la rampa de calentamiento y el flujo de gas inerte [27]. Cabe recalcar la influencia de la temperatura en los productos obtenidos, ya que, a mayor temperatura del proceso, mayor es la producción de bio-oil. No obstante, a menores temperaturas, la producción de biochar se ve favorecida [28].

La pirólisis puede ser rápida o lenta, dependiendo de la rampa de calentamiento y del tiempo de residencia. Menores temperaturas de pirólisis y rampas de calentamiento, así como mayor tiempo de residencia, favorecen la producción de biochar. Aproximadamente un 35% del peso total de la biomasa seca puede ser transformado en biochar, aunque un aumento de la presión puede aumentar el rendimiento de producción de dicho producto [29].

Los gases no condensables (syngas) son una mezcla de componentes básicos, tales como monóxido de carbono (CO) e hidrógeno (H₂). El alto poder calorífico del syngas (4,37-5,68 MJ/m³) hace que tenga un papel importante en plantas de cogeneración [30].

El bio-oil es una mezcla de compuestos orgánicos, como ésteres, ácidos y aromáticos, que varían según la composición de la materia prima. Así, otros estudios han sido llevados a cabo en los últimos años para la utilización de dichos componentes. Una de las aplicaciones puede ser la extracción de algunos compuestos aromáticos, tales como fenoles y otros de alto valor añadido (levoglucosanona o catecol). Adicionalmente, es necesario mencionar que los bio-oils pueden ser usados como aditivos de alta calidad en gasolinas dentro de motores de combustión [31]. No obstante, los bio-oils deberán ser analizados para, en función de su composición, poder darle un uso u otro.

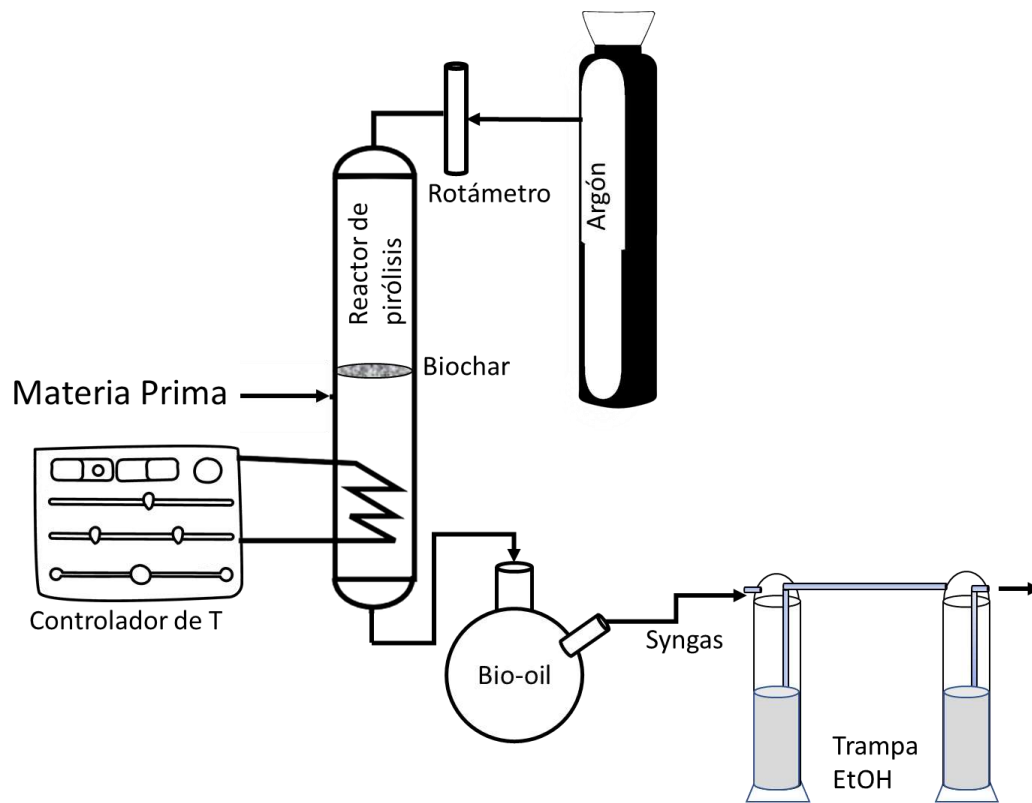
Finalmente, el biochar es un sólido no volátil rico en carbono, compuesto por el residuo no hidrocarbonado de la biomasa, formado principalmente por lignina, óxidos metálicos y metales pesados. Dentro de las aplicaciones actuales del biochar, el uso como biocatalizador puede ser resaltado, ya que por ejemplo puede ser utilizado en la reacción de esterificación del ácido oleico con metanol para la obtención de biodiesel [32,33]. Por otro lado, se ha estudiado también su capacidad absorbente de distintos contaminantes,

como metales pesados o químicos farmacéuticos de mezclas acuosas [34]. No obstante, muchos de los biochars obtenidos a partir de distintas materias primas tienen una baja superficie específica o baja actividad catalítica, por lo que tienen que ser pre-tratados con ácidos, tales como el ácido sulfúrico [35] o el ácido fosfórico [36].

2. OBJETIVOS DEL TRABAJO

Los objetivos de la Tesis Doctoral han sido los siguientes:

- ✓ Valorizar los residuos de naranja y huesos de aceituna a través de la pirólisis.
- ✓ Evaluar las condiciones óptimas de pirólisis para la producción de biochar y bio-oil a partir de los residuos de naranja y del hueso de aceituna.
- ✓ Caracterizar los biocarbones y bio-oils obtenidos.
- ✓ Establecer las condiciones óptimas para la obtención de sustancias de alto valor añadido (levoglucosanona, catecol).
- ✓ Encontrar las condiciones óptimas de operación en la reacción de esterificación de ácidos grasos libres con metanol, utilizando los biochars obtenidos en la pirólisis de las distintas materias primas como biocatalizador ácido heterogéneo de la reacción de esterificación.
- ✓ Eliminar el azufre en aceites usados de cocina para que puedan ser utilizados como materia prima en la producción de biodiésel.



3. RESULTADOS Y DISCUSIÓN

3.1. CAPÍTULO 1: CARACTERIZACIÓN DEL PROCESO

En primer lugar, se llevó a cabo una caracterización de la materia prima mediante un análisis termogravimétrico, con el objetivo de estimar la composición de esta, y tener una idea de los rangos de temperatura a utilizar para los tratamientos termoquímicos.

3.1.1. Análisis Termogravimétrico (TGA)

En la TGA de la rama de naranja, se observó en primer lugar la pérdida de agua (12% p/p.), seguida de la pérdida de celulosa y hemicelulosa (41% p/p.) y, finalmente la pérdida de lignina (20% p/p.).

Por el lado contrario, en la TGA del residuo de naranja dulce, se observó la pérdida de agua (45% p/p.), seguido de la pérdida de celulosa y hemicelulosa (14% p/p.). La degradación de la pectina se sitúa en 12% (p/p.), llegando finalmente a la lignina (5% p/p.). Con ambos datos, se pudo estimar que la temperatura óptima de pirólisis sería sobre 400-600 °C, debido a que con estas temperaturas un 70-80% de la materia prima habría sido degradada.

Finalmente, en la TGA del hueso de aceituna, se observó una pérdida de humedad sobre los 100 °C (15% p/p.). En segundo lugar, entre 150-200 °C se degrada la hemicelulosa (24% p/p.), mientras que la degradación de la celulosa se observa entre 200-250 °C (27% p/p.). Finalmente, el proceso de degradación de la lignina es gradual desde los 200 hasta los 800 °C (15% p/p.). Además, se puede observar que sobre los 400 °C un 70% de la materia prima inicial ha sido degradada, mientras que a 600 °C se alcanza un 80% de degradación.

Tras la obtención de una idea general del rango de temperatura adecuado, se llevaron a cabo las distintas pirólisis, con el objetivo de encontrar las condiciones óptimas de operación.

3.1.2. Distribución de los productos de la pirólisis

Los bio-oils y biochars obtenidos fueron pesados, para poder obtener los porcentajes de los productos después de la pirólisis (Tabla 1). Los biochars fueron almacenados en envases individuales. A los biochars se les analizó la superficie específica BET (S_{BET}). Algunas muestras iniciales se pretrataron con ácido sulfúrico (H_2SO_4) con el objetivo de aumentar la superficie específica, y ver las diferencias con la materia prima sin tratar.

Tabla 1. Rendimientos (η) de biochar, bio-oil y syngas obtenidos a distintas condiciones de pirólisis.

Materia Prima	T (°C)	Rampa T (°C/min)	Flujo Ar (mL/h)	$\eta_{\text{Bio-oil}}$ (% p/p)	$\eta_{\text{Biocarbón}}$ (% p/p)	$\eta_{\text{Biogás}}$ (% p/p)	Superficie específica BET (m²/g)
Naranja dulce	600	10	150	19,56	32,44	48,00	≤1,00
Naranja dulce	600	10	30	10,67	32,11	57,22	≤1,00
Naranja dulce	600	10	300	22,00	30,89	47,11	≤1,00
Naranja dulce	400	10	150	21,67	34,33	44,00	≤1,00
Naranja dulce	400	5	150	26,00	37,67	36,33	≤1,00
Rama naranjo	400	5	150	58,20	35,10	6,70	2,82
Rama naranjo	400	10	150	57,27	35,33	7,39	5,44
Rama naranjo	600	10	150	65,59	27,94	6,47	9,56
Rama naranjo	600	10	30	67,21	24,71	8,08	24,28
Rama naranjo	600	10	300	57,51	29,10	13,39	12,01
Rama naranjo	600	20	150	55,20	28,18	16,63	10,42
Hueso Aceituna+H ₂ SO ₄	600	10	150	17,10	44,60	38,20	418,60
Hueso Aceituna+H ₂ SO ₄	500	10	150	13,50	51,20	35,20	263,38
Hueso Aceituna+H ₂ SO ₄	400	10	150	6,70	57,80	35,60	5,80
Hueso Aceituna+H ₂ SO ₄	400	5	150	7,00	59,60	33,40	13,75
Hueso Aceituna+H ₂ SO ₄	400	20	150	8,20	60,20	31,60	21,50
Hueso Aceituna+H ₂ SO ₄	400	10	150	7,00	60,00	33,00	42,09
Hueso Aceituna+H ₂ SO ₄	400	20	300	1,60	57,20	41,20	106,65
Hueso Aceituna+H ₂ SO ₄	400	20	50	5,00	57,80	37,20	52,95
Hueso Aceituna+H ₂ SO ₄	600	10	150	2,17	41,67	56,14	367,93
Hueso Aceituna	600	10	150	20,26	27,17	52,57	242,71
Hueso Aceituna	500	10	150	23,57	27,67	48,76	230,38
Hueso Aceituna	400	10	150	23,36	31,17	45,50	4,55
Hueso Aceituna	400	20	150	30,83	29,33	39,83	8,18
Hueso Aceituna	400	5	150	32,17	31,67	36,17	8,90
Hueso Aceituna	400	5	50	36,10	33,50	30,40	6,57
Hueso Aceituna	400	5	300	25,33	30,33	44,33	12,38

La producción de biochar a partir de todas las materias primas fue inversamente proporcional a la temperatura de pirólisis, y directamente proporcional a la producción de fluidos.

Con una temperatura de 400 °C en las pirólisis de naranja dulce, al aumentar la rampa de temperatura (de 5 a 10 °C·min⁻¹), hay un descenso en el porcentaje de biochar y bio-oil, así como un aumento del syngas. Por el contrario, en la misma temperatura de pirólisis a partir de rama de naranjo, al aumentar la rampa, los porcentajes de biochar se mantienen constantes.

Al aumentar el flujo de argón en las pirólisis de naranja dulce, se observa una disminución del biochar y del syngas, así como un aumento del bio-oil. En cambio, en las pirólisis de rama de naranjo, al aumentar el flujo de argón los porcentajes de biochar y syngas aumentan, disminuyendo así la de bio-oil.

Conforme a las pirólisis de hueso de aceituna pretratado, se observó que la rampa de temperatura no influyó en la producción de biochar en las distintas pirólisis. No obstante, la producción de bio-oil fue directamente proporcional a la rampa de temperatura. Por otro lado, los rendimientos de bio-oil obtenidos a partir de los huesos de aceituna, fueron inversamente proporcional a la rampa de temperatura.

Además, en relación con el flujo de argón, la pirólisis de hueso de aceituna pretratado que mayor rendimiento de biochar y bio-oil tiene es la realizada con 150 mL Ar·min⁻¹. Por otro lado, los rendimientos de biochar y bio-oil en las pirólisis a partir de hueso de aceituna tienen una relación inversamente proporcional al flujo utilizado.

Finalmente puede observarse que los rendimientos de biochar obtenidos pirólisis con hueso de aceituna pretratado son mayores que en las del hueso sin tratar.



3.2. CAPÍTULO 2: APLICACIÓN DE LOS BIOCARBONES

3.2.1. Absorción de azufre utilizando los biochars obtenidos de naranja dulce y rama de naranjo

Finalmente, los biocarbones obtenidos y caracterizados fueron utilizados para la eliminación de azufre de aceites usados de cocina, con el objetivo de ver cuál de ellos daba un mayor rendimiento de desulfuración.

Tabla 2. Rendimientos (η) de desulfuración de aceites de cocina con biocarbones obtenidos a partir de naranja dulce bajo distintas condiciones de pirólisis.

T (°C)	Rampa T (°C·min ⁻¹)	Flujo de argón (mL·min ⁻¹)	Superficie específica (m ² ·g ⁻¹)	$\eta_{\text{desulfuración}}$ (%)
400	5	150	≤1	78,3 ± 0,01
400	10	150	≤1	77,4 ± 0,03
600	10	30	≤1	76,3 ± 0,01
600	10	150	≤1	75,5 ± 0,03
600	10	300	≤1	76,2 ± 0,02

En primer lugar, se vio que la superficie específica no tuvo influencia en la absorción de azufre con biocarbones de naranja dulce (Tabla 2).

Tabla 3. Rendimientos (η) de desulfuración de aceites de cocina con biocarbones obtenidos a partir de rama de naranjo bajo distintas condiciones pirolíticas.

T (°C)	Rampa T (°C·min ⁻¹)	Flujo de argón (mL·min ⁻¹)	Superficie específica (m ² ·g ⁻¹)	$\eta_{\text{desulfuración}}$ (%)
400	5	150	2,82	76,5 ± 0,01
400	10	150	5,44	77,5 ± 0,03
600	10	30	24,28	66,4 ± 0,01
600	10	150	7,52	78,8 ± 0,01
600	10	300	12,01	72,0 ± 0,03
600	20	150	10,42	75,0 ± 0,04

Por el contrario, la superficie específica de los biocarbones de rama de naranjo (Tabla 3) sí que tuvo influencia en la absorción de azufre del aceite usado. De hecho, la absorción de azufre fue inversamente proporcional a la superficie específica. Este hecho puede explicarse según experiencias previas [37] donde se indica que, al aumentar la superficie

específica, el tamaño de poro disminuye, lo que hace que el azufre sea menos absorbido en dichos poros.

Finalmente, se compararon los espectros de infrarrojos obtenidos de los biocarbones utilizados para la desulfuración de azufre, tras su tratamiento.

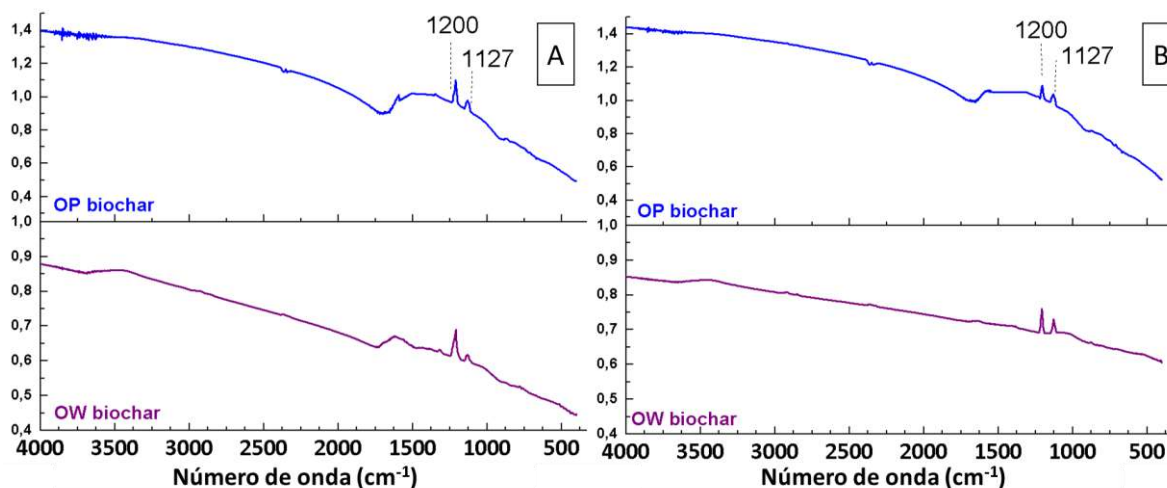


Figura 4. Espectros de los biocarbones de naranja dulce (OW) y de la rama de naranjo (OP) después de la eliminación de azufre del aceite de fritura. Se representan los biocarbones que proporcionan una mayor reducción de azufre (A) y los biocarbones que conducen a una menor desulfuración (B).

En los espectros de infrarrojo, se pudieron observar dos bandas, la primera a 1127 cm^{-1} (relacionada con el enlace C=S), y la segunda a 1200 cm^{-1} (relacionada con el enlace O=S=O) [38]. Ambas bandas fueron más intensas en los biocarbones con una mayor absorción de azufre.

3.2.2. Aplicación de los biochars obtenidos de hueso de aceituna como catalizador en la reacción de esterificación

El índice de acidez se utilizó para medir la evolución de la reacción. El índice de acidez inicial fue $182,2\text{ mg KOH/g}$ aceite.

Tabla 4. Resultados del índice de acidez, rendimiento (η) de esterificación y porcentajes de fase orgánica y acuosa tras la esterificación en el aceite de fritura.

Biochar	Índice de acidez	$\eta_{\text{esterificación}}$	Fase orgánica (%)	Fase acuosa (%)
1	172,2	5,5	-	-
2	180,7	0,3	-	-

4	13,1	92,8	63,9	32,1
5	16,1	91,2	64,1	22,8
6	183,7	0,0	-	-
6	26,7	85,3	52,1	26,9
7	17,4	90,4	60,8	36,8
8	12,9	92,9	58,5	26,5
9	8,8	95,2	61,0	28,5
10	9,8	94,6	62,8	23,7
11	7,1	96,1	55,3	25,3
12	7,0	96,2	63,7	26,6
13	10,3	94,3	57,7	23,0
15	8,7	95,2	49,2	28,9
16	8,4	95,4	67,3	24,8
17	7,8	95,7	59,9	25,7

Los biochars obtenidos a partir de hueso de aceituna, aun teniendo una menor superficie específica que los biochars obtenidos a partir de hueso de aceituna pretratado (Tabla 4), promovieron mejor rendimiento en la reacción de esterificación ácidos grasos con metanol.

La experiencia que mejor rendimiento proporcionó fue la realizada con el biochar 12, cuya fase orgánica (compuesta por ésteres metílicos) fue analizada, y representada en la Tabla 5.

Tabla 5. Composición de la fase orgánica obtenida tras la esterificación de ácido oleico comercial.

Área (%)	Componente
5,65	Dodecanoato de metilo
2,78	Miristoleato de metilo
9,49	Palmoleato de metilo
12,79	Palmitoleato de metilo
5,83	Ester metílico del ácido cis-10-heptadecenoico
48,78	Oleato de metilo
13,50	Linoleato de metilo
1,18	Ester metílico del ácido 11-Eicosenoico

A la vista de dichos resultados (Tabla 5), se pudo comprobar que la fase orgánica de la reacción de esterificación estaba compuesta por ésteres metílicos (biodiesel).



3.3. CAPÍTULO 3: CARACTERIZACIÓN DE LOS BIO-OILS

Tabla 6. Composición de los bio-oils obtenidos a partir de las distintas materias primas, así como principales usos.

Materia Prima	Componente principal Bio-oil	Concentración (%)	Usos
Naranja dulce	Ácido propanoico	3,00-4,00	Inhibidor del crecimiento de moho y algunas bacterias, sirviendo para conservación de piensos
	Tolueno	25,00-30,00	Disolvente utilizado para pinturas, esmalte de uñas, barnices
	4-Hidroxi-4-metil-2-pentanona	3,10-5,95	Síntesis orgánica de productos
	Furfural	3,00-8,00	Disolvente selectivo en la refinación de aceites lubricantes para la industria petrolera
	5-Hidroximetilfurfural	23,00-31,00	Usado en envasado, la construcción, el textil, los cosméticos, los alimentos y la salud
Rama de naranjo	Tolueno	2,15-2,60	Disolvente utilizado para pinturas, esmalte de uñas, barnices
	4-Hidroxi-4-metil-2-pentanona	92,60-94,70	Síntesis orgánica de productos
	2-Furanmetanol	1,30	Se utiliza como monómero en cementos, adhesivos, revestimientos y resinas de fundición
	2,6-Dimetoxi-fenol	1,30-2,20	Potenciador del sabor
Hueso de Aceituna	Furfural	3,80	Disolvente selectivo en la refinación de aceites lubricantes para la industria petrolera
	O-xileno	3,40	Se usa como disolvente en la imprenta y en las industrias de caucho y cuero
	Levogluosenona	-	Precursor quirral de síntesis orgánica
	Catecol	3,33	Astringente y antiséptico
	Creosol	7,32	Desinfectante menos tóxico que el fenol
	Vanilina	1,50	Saborizante en alimentos, bebidas y elementos farmacéuticos
Hueso de Aceituna+H ₂ SO ₄	Furfural	5,30	Disolvente selectivo en la refinación de aceites lubricantes para la industria petrolera
	O-xileno	6,26	Se usa como disolvente en la imprenta y en las industrias de caucho y cuero
	Levogluosenona	9,57	Precursor quirral de síntesis orgánica
	Catecol	6,17	Astringente y antiséptico
	Creosol	6,94	Desinfectante menos tóxico que el fenol
	Vanilina	3,65	Saborizante en alimentos, bebidas y elementos farmacéuticos

Los bio-oils fueron caracterizados usando un cromatógrafo de gases acoplado a un espectrómetro de masas, con el objetivo de llevar a cabo un análisis tentativo-cualitativo de los principales componentes de los bio-oils bajo distintas condiciones de pirólisis.

Los bio-oils obtenidos a partir de naranja dulce (Tabla 6), tuvieron como componente principal el tolueno y el 5-hidroximetilfurfural (HMF), siendo estas concentraciones mayores a una menor temperatura de pirólisis. También se observó furfural, 4-hidroxi-4-metil-2-pentanona y ácido propanoico.

Por otro lado, los bio-oils obtenidos a partir de rama de naranjo (Tabla 6), presentaron como componentes principales el 4-hidroxi-4-metil-2-pentanona y el tolueno.

Por último, se estudió la influencia del pretratamiento ácido en la composición de los bio-oils (Tabla 6). En líneas generales, se pudo observar que el bio-oil obtenido a partir de hueso de aceituna pretratado tenía una composición más interesante en compuestos de alto valor añadido, tales como levoglucosanona, catecol o vanilina. Esto puede ser explicado por la transformación de compuestos lignocelulósicos en levoglucosanona mediante el pretratamiento ácido. Este producto es un compuesto de alta importancia en la industria orgánica, debido a su quiralidad.

Por este motivo, y debido a su alto precio y demanda en el mercado (10 mg de levoglucosena (95%) tienen un precio de 165 euros, Sigma Aldrich, 03/2022), la utilización y aprovechamiento de los bio-oils producidos a partir de hueso de aceituna es muy interesante, por lo que encontrar las condiciones óptimas de operación en unas futuras investigaciones sería necesario para la implantación de dicho aprovechamiento a escala industrial.

A la vista de los resultados obtenidos (Tabla 6), se puede decir que la composición de los bio-oils depende en gran medida de la materia prima, siendo éste el factor más influyente. No obstante, otros factores como la temperaturas, rampa de temperatura y flujo de gas inerte, juegan también un papel importante (3.4. del artículo de la revista Agronomy).

4. CONCLUSIONES

- La rama de naranjo tuvo una mayor estabilidad térmica que la naranja dulce y que el hueso de aceituna, debido a su mayor contenido en lignina (20% vs 5% vs 15% p/p, respectivamente).
- Hubo una correlación inversamente proporcional entre la temperatura de pirólisis y la producción de biochar a partir de rama de naranja, residuo de naranja dulce o hueso de aceituna.
- Las condiciones óptimas para la producción de biochar a partir de rama de naranja fueron 400 °C, 150 mL Ar·min⁻¹ y 10 °C·min⁻¹. Por otro lado, las condiciones óptimas para la producción de biochar a partir de residuo de naranja dulce fueron 400 °C, 150 mL Ar·min⁻¹ y 5 °C·min⁻¹. Las condiciones óptimas para la producción de biochar a partir de hueso de aceituna pretratado fueron 400 °C, 20 °C·min⁻¹ y 150 mL Ar·min⁻¹. Finalmente, las condiciones óptimas para la obtención de biochar a partir de hueso de aceituna fueron 400 °C, 5 °C·min⁻¹ y 50 mL Ar·min⁻¹.
- Los biochars producidos a partir de hueso de aceituna pretratado tuvieron la mayor superficie específica, seguidos de los obtenidos a partir de hueso de aceituna, seguidos a su vez de los obtenidos a partir de rama de naranjo, y finalmente los obtenidos a partir del residuo de la naranja dulce.
- Los biochars obtenidos a partir de naranja dulce y rama de naranjo se usaron con éxito para la eliminación de azufre del aceite de fritura.
- El uso del biochar obtenido a partir de hueso de aceituna, proporcionó un mayor rendimiento de esterificación que el biochar de hueso de aceituna pretratado.
- Con respecto a los bio-oils obtenidos a partir del residuo de la naranja dulce, se componían principalmente de tolueno y 5-hidroximetilfurfural. Por otro lado, los bio-oils obtenidos a partir de rama de naranjo se componían principalmente por 4-hidroxi-4-metil-2-pentanona. Finalmente, los bio-oils obtenidos a partir de hueso de aceituna estaban compuestos por una amplia gama de compuestos, destacando el catecol y la levoglucosenona por su alto valor añadido.

5. REFERENCIAS BIBLIOGRÁFICAS

1. FAOSTAT Available online: <https://www.fao.org/faostat/es/#data/QC> (accessed on 2 December 2021).
2. Ministerio de Agricultura, Pesca y Alimentación Available online: <https://www.mapa.gob.es/es/> (accessed on 2 December 2021).
3. García-Martín, J.F.; Olmo, M.; García, J.M. Effect of Ozone Treatment on Postharvest Disease and Quality of Different Citrus Varieties at Laboratory and at Industrial Facility. *Postharvest Biology and Technology* **2018**, *137*, 77–85, doi:10.1016/j.postharvbio.2017.11.015.
4. Rodríguez, A.; Rosal, A.; Jiménez, L. Biorefinery of Agricultural Residues by Fractionation of Their Components through Hydrothermal and Organosolv Processes. *Afinidad* **2010**, *67*, 14–20.
5. Wilkins, M.R.; Suryawati, L.; Maness, N.O.; Chrz, D. Ethanol Production by *Saccharomyces cerevisiae* and *Kluyveromyces marxianus* in the Presence of Orange-Peel Oil. *World Journal of Microbiology and Biotechnology* **2007**, *23*, 1161–1168, doi:10.1007/s11274-007-9346-2.
6. Rezzadori, K.; Benedetti, S.; Amante, E.R. Proposals for the Residues Recovery: Orange Waste as Raw Material for New Products. *Food and Bioproducts Processing* **2012**, *90*, 606–614, doi:10.1016/j.fbp.2012.06.002.
7. Crawshaw, R. Co-Product Feeds: Animal Feeds from the Food and Drink Industries 2001.
8. Correia Guerrero, C.; Carrasco de Brito, J.; Lapa, N.; Santos Oliveira, J.F. Re-Use of Industrial Orange Wastes as Organic Fertilizers. *Bioresource Technology* **1995**, *53*, 43–51, doi:10.1016/0960-8524(95)00050-O.
9. Elias, X. *Reciclaje de Residuos Industriales: Residuos Sólidos Urbanos y Fangos de Depuradora*; **2012**; ISBN 9788499693668.
10. Restrepo Duque, A.M.; Rodríguez Sandoval, E.; Manjarrés Pinzón, K. Edible Orange Peels: An Approximation to the Development of Products with Added Value from Agricultural Products. *Producción + Limpia* **2011**, *6*, 47–57.
11. García Martín, J.F.; Cuevas, M.; Feng, C.H.; Álvarez Mateos, P.; Torres García, M.; Sánchez, S. Energetic Valorisation of Olive Biomass: Olive-Tree Pruning, Olive Stones and Pomaces. *Processes* **2020**, *8*, 511, doi:10.3390/PR8050511.
12. Sánchez, F.; San Miguel, G. Improved Fuel Properties of Whole Table Olive Stones via Pyrolytic Processing. *Biomass and Bioenergy* **2016**, *92*, 1–11, doi:10.1016/j.biombioe.2016.06.001.
13. Rodríguez, G.; Lama, A.; Rodríguez, R.; Jiménez, A.; Guillén, R.; Fernández-Bolaños, J. Olive Stone an Attractive Source of Bioactive and Valuable Compounds. *Bioresource Technology* **2008**, *99*, 5261–5269, doi:10.1016/j.biortech.2007.11.027.
14. Martín Lara, M.A.; Hernáinz, F.; Calero, M.; Blázquez, G.; Tenorio, G. Surface Chemistry Evaluation of Some Solid Wastes from Olive-Oil Industry Used for Lead Removal from Aqueous Solutions. **2009**, *44*, 151–159, doi:10.1016/j.bej.2008.11.012.

15. Fernández Bolaños, J.; Felizón, B.; Heredia, A.; Rodríguez, R.; Guillén, R.; Jiménez, A. Steam-Explosion of Olive Stones : Hemicellulose Solubilization and Enhancement of Enzymatic Hydrolysis of Cellulose. **2001**, *79*, 53–61.
16. Boluda-Aguilar, M.; López-Gómez, A. Production of Bioethanol by Fermentation of Lemon (*Citrus Limon L.*) Peel Wastes Pretreated with Steam Explosion. *Industrial Crops and Products* **2013**, *41*, 188–197, doi:10.1016/j.indcrop.2012.04.031.
17. Siles, J.Á.; Martín, M.D.L.Á.; Martín, A.; Raposo, F.; Borja, R. Anaerobic Digestion of Wastewater Derived from the Pressing of Orange Peel Generated in Orange Juice Production. *Journal of Agricultural and Food Chemistry* **2007**, *55*, 1905–1914, doi:10.1021/jf0630623.
18. Calabrò, P.S.; Fazzino, F.; Sidari, R.; Zema, D.A. Optimization of Orange Peel Waste Ensiling for Sustainable Anaerobic Digestion. *Renewable Energy* **2020**, *154*, 849–862, doi:10.1016/j.renene.2020.03.047.
19. Feng, C.H.; García-Martín, J.F.; Broncano Lavado, M.; López Barrera, M. del C.; Álvarez-Mateos, P. Evaluation of Different Solvents on FLavonoids Extraction Efficiency from Sweet Oranges and Ripe and Immature Seville Oranges. **2020**, *55*, 3123–3134.
20. Volpe, M.; Panno, D.; Volpe, R.; Messineo, A. Upgrade of Citrus Waste as a Biofuel via Slow Pyrolysis. *Journal of Analytical and Applied Pyrolysis* **2015**, *115*, 66–76, doi:10.1016/j.jaap.2015.06.015.
21. El Hanandeh, A. Energy Recovery Alternatives for the Sustainable Management of Olive Oil Industry Waste in Australia: Life Cycle Assessment. *Journal of Cleaner Production* **2015**, *91*, 78–88, doi:10.1016/j.jclepro.2014.12.005.
22. Merino, M. del R.; Guijarro Rodríguez, J.; Fernández Martínez, F.; Santa Cruz Astorqui, J. Viability of Using Olive Stones as Lightweight Aggregate in Construction Mortars. *Revista de la Construcción* **2017**, *16*, 431–438, doi:10.7764/RDLC.16.3.431.
23. Jahanbakhshi, R.; Ansari, S. Physicochemical Properties of Sponge Cake Fortified by Olive Stone Powder. *Journal of Food Quality* **2020**, *2020*, doi:10.1155/2020/1493638.
24. Bioplastic Packaging from Olive Waste Available online: <https://bioplasticsnews.com/2020/05/08/bioplastic-packaging-olive-waste/> (accessed on 7 December 2021).
25. Evcil, T.; Simsir, H.; Ucar, S.; Tekin, K.; Karagoz, S. Hydrothermal Carbonization of Lignocellulosic Biomass and Effects of Combined Lewis and Brønsted Acid Catalysts. *Fuel* **2020**, *279*, 118458, doi:10.1016/j.fuel.2020.118458.
26. Collard, F.X.; Blin, J. A Review on Pyrolysis of Biomass Constituents: Mechanisms and Composition of the Products Obtained from the Conversion of Cellulose, Hemicelluloses and Lignin. *Renewable and Sustainable Energy Reviews* **2014**, *38*, 594–608, doi:10.1016/j.rser.2014.06.013.
27. Bhattacharjee, N.; Baran Biswas, A. Pyrolysis of Orange Bagasse: Comparative Study and Parametric Influence on the Product Yield and Their Characterization. *Journal of Environmental Chemical Engineering* **2019**, *7*, 102903, doi:10.1016/j.jece.2019.102903.
28. Guo, J.; Zheng, L.; Li, Z.; Zhou, X.; Cheng, S.; Zhang, L.; Zhang, Q. Effects of Various Pyrolysis Conditions and Feedstock Compositions on the Physicochemical Characteristics of Cow Manure-

Derived Biochar. *Journal of Cleaner Production* **2021**, *311*, 127458, doi:10.1016/j.jclepro.2021.127458.

29. Basu, P. *Pyrolysis and Torrefaction*; First Edit.; Elsevier Inc., **2010**; ISBN 9780123749888.
30. Bradley, D.; Svebio, B.H.; Ab, H.; Wild, M.; Deutmeyer, M.; Schouwenberg, P.P.; Essent, R.; Hess, R.; Tumuluru, J.S.; Bradburn, K. Low Cost, Long Distance Biomass Supply Chains. In Task 40: Sustainable International Bioenergy Trade; Goh, C.S., Junginger, M., Eds.; IEA Bioenergy: Paris, France, **2013**; pp. 1–65.
31. Sánchez Borrego, F.J.; Álvarez Mateos, P.; García Martín, J.F. Biodiesel and Other Value-Added Products from Bio-Oil Obtained from Agrifood Waste. **2021**, *9*, 797. doi.org/10.3390/pr9050797
32. Álvarez-Mateos, P.; García-Martín, J.F.; Guerrero-Vacas, F.J.; Naranjo-Calderón, C.; Barrios, C.C.; Pérez Camino, M. del C.; Barrios, C.C. Valorization of a High-Acidity Residual Oil Generated in the Waste Cooking Oils Recycling Industries. *Grasas y Aceites* **2019**, *40*, e335, doi:10.3989/gya.1179182.
33. Roy, M.; Mohanty, K. Valorization of De-Oiled Microalgal Biomass as a Carbon-Based Heterogeneous Catalyst for a Sustainable Biodiesel Production. *Bioresource Technology* **2021**, *337*, 125424, doi:10.1016/j.biortech.2021.125424.
34. Sun, Y.; Gao, B.; Yao, Y.; Fang, J.; Zhang, M.; Zhou, Y.; Chen, H.; Yang, L. Effects of Feedstock Type, Production Method, and Pyrolysis Temperature on Biochar and Hydrochar Properties. *Chemical Engineering Journal* **2014**, *240*, 574–578, doi:10.1016/j.cej.2013.10.081.
35. Islam, M.K.; Rehman, S.; Guan, J.; Lau, C.Y.; Tse, H.Y.; Yeung, C.S.; Leu, S.Y. Biphasic Pretreatment for Energy and Carbon Efficient Conversion of Lignocellulose into Bioenergy and Reactive Lignin. *Applied Energy* **2021**, *303*, 117653, doi:10.1016/j.apenergy.2021.117653.
36. Laurenza, A.G.; Losito, O.; Casiello, M.; Fusco, C.; Nacci, A.; Pantone, V.; D'Accolti, L. Valorization of Cigarette Butts for Synthesis of Levulinic Acid as Top Value-Added Chemicals. *Scientific Reports* **2021**, *11*, 1–8, doi:10.1038/s41598-021-95361-4.
37. Wu, L.; Wan, W.; Shang, Z.; Gao, X.; Kobayashi, N.; Luo, G.; Li, Z. Surface Modification of Phosphoric Acid Activated Carbon by Using Non-Thermal Plasma for Enhancement of Cu(II) Adsorption from Aqueous Solutions. *Separation and Purification Technology* **2018**, *197*, 156–169, doi:10.1016/j.seppur.2018.01.007.
38. Huang, S.; Liang, Q.; Geng, J.; Luo, H.; Wei, Q. Sulfurized Biochar Prepared by Simplified Technic with Superior Adsorption Property towards Aqueous Hg(II) and Adsorption Mechanisms. *Materials Chemistry and Physics* **2019**, *238*, doi:10.1016/j.matchemphys.2019.121919.

Review

Biodiesel and Other Value-Added Products from Bio-Oil Obtained from Agrifood Waste

Francisco José Sánchez-Borrego *, Paloma Álvarez-Mateos  and Juan F. García-Martín * 

Departamento de Ingeniería Química, Facultad de Química, Universidad de Sevilla, C/Profesor García González, 1, 41012 Seville, Spain; palvarez@us.es

* Correspondence: frasanbor@alum.us.es (F.J.S.-B.); jfgarmar@us.es (J.F.G.-M.); Tel.: +34-954-557-183 (F.J.S.-B.)

Abstract: Bio-oil is a promising source of chemicals and renewable fuels. As the liquid phase obtained from the pyrolysis of biomass, the composition and amount of bio-oil generated depend not only on the type of the biomass but also on the conditions under which pyrolysis is performed. Most fossil fuels can be replaced by bio-oil-derived products. Thus, bio-oil can be used directly or co-fed along with fossil fuels in boilers, transformed into fuel for car engines by hydrodeoxygenation or even used as a more suitable source for H₂ production than biomass. On the other hand, due to its rich composition in compounds resulting from the pyrolysis of cellulose, hemicellulose and lignin, bio-oil co-acts as a source of various value-added chemicals such as aromatic compounds. This review presents an overview of the potential applications of bio-oils and the pyrolysis conditions under which they are obtained. Then, different extraction methods for value-added chemicals, along with the most recent developments, are discussed and future research directions for bio-oil upgrades are highlighted.

Keywords: biofuels; bio-oil; bioplastic; hydrodeoxygenation; pyrolysis; renewable fuel; recyclable plastics



Citation: Sánchez-Borrego, F.J.; Álvarez-Mateos, P.; García-Martín, J.F. Biodiesel and Other Value-Added Products from Bio-Oil Obtained from Agrifood Waste. *Processes* **2021**, *9*, 797. <https://doi.org/10.3390/pr9050797>

Academic Editor:
Elsayed Elbeshbishy

Received: 30 March 2021
Accepted: 28 April 2021
Published: 30 April 2021

Publisher's Note: MDPI stays neutral with regard to jurisdictional claims in published maps and institutional affiliations.



Copyright: © 2021 by the authors. Licensee MDPI, Basel, Switzerland. This article is an open access article distributed under the terms and conditions of the Creative Commons Attribution (CC BY) license (<https://creativecommons.org/licenses/by/4.0/>).

1. Biofuels: The Search for Alternative Fuels for Transportation

Fossil fuels are still the main energy source worldwide; their overexploitation is resulting in their depletion and increases in global warming [1]. With the increase in energy demand, the price of fossil fuels is also increasing, as their supply is dominated by a few Middle Eastern countries. According to the International Energy Agency report, the energy demand in Asia (the most populated continent) will increase by 76% by 2030 [1].

Dependence on imported fossil fuels thus poses a serious threat to the energy security and economic stability of all countries as the world is expected to run out of petroleum in the next 50 years [1]. Due to these limited reserves of conventional fossil fuels and their negative impact on global climate and human health, much research is focused on the search for alternative energy sources. Along with other energy resources, such as solar, wind, hydroelectric, and nuclear energy, biodiesel can help reduce fossil fuel dependence. Biodiesel is a non-toxic renewable energy source that is gaining attention globally due to its direct applicability in preexisting engines without any modification, since its properties are similar to those of conventional diesel fuel.

Biodiesel is a renewable biofuel free of sulphur and polycyclic aromatic compounds, which are major advantages. Brazil, USA, Malaysia, Argentina, Spain, Belgium and Germany are among the top producers, meeting 80% of the biodiesel demand [1]. Blending, thermal cracking, micro-emulsification and transesterification are four basic approaches for production of biodiesel [2–4]. Among them, transesterification is the most commonly used method at the industrial scale due to less expensive operation and high product yield.

The availability of various oil resources (edible, non-edible and waste cooking oils) has been discussed elsewhere [1], along with the advancements in technology related to oil extraction. Palm oil and waste cooking oils are the main raw materials used nowadays for biodiesel production. *Jatropha curcas* oil (non-edible oil) is also regarded as a potential

alternative to these raw materials [5]. Despite some drawbacks, such as poorer oxidation stability due to the high amount of unsaturated fatty acids, the high availability of oxygen in jatropha biodiesel reduces hydrocarbons, CO and particulate matter emissions. The comprehensive assessment of the performance and emissions of compression ignition engines operated on jatropha biodiesel and its blends can be found elsewhere [2,5]. On the other hand, the lower calorific value of jatropha biodiesel is responsible for a decrease in brake thermal efficiency and an increase in brake specific fuel consumption [2].

Various technologies, from the laboratory scale to industrial production, have been developed and many facilities have been established for biodiesel production using various feedstocks [1]. Thus, various innovative process intensification technologies (biological reactors, microreactors, membrane reactors, oscillatory flow reactors, microwave reactors, reactive distillation, centrifugal contractors, etc.) can be found in the literature [6–10]. On the other hand, the use of bio-based technologies in biodiesel production is regarded as advantageous as these methods generate less waste and are considered ecofriendly. To be specific, bio-based methods, such as those using immobilized enzymes and heterogeneous catalysts derived from biomass, have been reported to efficiently catalyze the transesterification reaction for biodiesel production [11,12]. The use of bio-oils as a source of biodiesel is still in its infancy. Nevertheless, it could represent a potential alternative for lignocellulose residues without any current feasible application.

2. Agrifood Industry Waste

Forestry and agricultural residues represent the typical lignocellulose raw material, these being the most plentiful sources of biomass in the world, generating around 200 billion tons per year [13]. For this reason, it is essential to develop new technologies to treat this biomass; otherwise, its accumulation as waste would affect the environment. Production of biofuels has already reached commercial scale. However, the industrial production costs of those biofuels, such as bioethanol, are still high, so they have to be cut down. Wood and straw were widely used as household fuels until charcoal began to replace wood from the beginning of the 20th century. Currently, the typical uses of lignocellulose at the commercial scale are syngas production by gasification and electricity generation.

In the last few decades, the use of lignocellulose biomass as a raw material for energy production, as well for materials for energy storage, has gained interest among researchers. Another important reason for the use of biomass is based on its renewability together with the reduction of the net carbon dioxide emission and wide distribution and availability. The major chemical components of lignocellulose biomass are cellulose, hemicelluloses and lignin. All of them have shown great potential as raw materials for energy generation [14]. For instance, cellulose can be described as a long-chain homopolymer consisting of D-glucose units with cellobiose as a repeating unit. Therefore, cellulose which can be fermented into bioethanol [15,16] plays the main role in the production of biofuels from biomass.

A huge variety of enforcements have been implemented for functional materials derived from lignocellulose [17]. Hemicelluloses are known to be a group of polysaccharides consisting of short-branched chains. Hemicelluloses are also essential for the production of biofuels because they can represent up to 35% of the weight of biomass on a dry basis [14]. To be specific, the production of bioethanol from hemicellulose-rich biomasses, such as olive stones and olive tree-pruning residues, requires the use of non-conventional yeasts capable of fermenting not only D-glucose, but also pentoses (mainly D-xylose) [14,15,18]. Lignin has received less attention than the other lignocellulose constituents in biofuels production due to its composition, which is mainly based on aromatic compounds. Nevertheless, the modifications assayed in recent years to alter lignin structure have increased the interest in producing carbon materials for super capacitors or energy-storage materials from lignin [19].

Thermochemical conversion is a very important method when converting biomass into energy and fuels. Thermochemical conversion could be defined as the controlled

heating or oxidation of raw materials, generating heat and energy products. This includes a wide range of techniques, including pyrolysis, liquefaction, gasification and combustion. Among all the thermochemical conversion techniques, the differences among them are based on their oxidation range and temperature [14,20].

Pyrolysis is a process of thermal decomposition of biomass that is carried out in the absence of oxygen, using instead inert atmospheres (e.g., argon or nitrogen). It is an endothermic process, so the products generated through this process have high energy content. The products generated in the pyrolysis are very heterogeneous and are mainly composed of volatile products (synthesis gas or syngas), a liquid fraction (bio-oil) and a solid carbonized waste (biochar). In turn, syngas consists of a mixture of CO and H₂ (along with other compounds such as CO₂, CH₄, C₂H₆, C₂H₄ and H₂O) [14].

Another thermal pretreatment is torrefaction, which is characterized by being carried out at a low temperature (200–300 °C) and is designed to remove water and other volatile compounds [14]. With this procedure, a solid product is obtained with a lower oxygen content and a higher energy density than the original raw material. Torrefaction begins when the temperature reaches 200 °C, and ends when the temperature drops below 200 °C, utilizing a very short heating time. It could be considered a softer version of pyrolysis, as well as being less destructive structurally as a carbonization method [21]. The main gases produced by gasification are CO, H₂, CH₄ and CO₂. Compared to pyrolysis, the final products obtained from torrefaction require less post-treatment to use them.

When the process is carried out under air, which is a reactive atmosphere, complete gasification occurs at higher temperatures (500 °C), resulting in the formation of gaseous fuel and a solid residue (ash). High temperatures inhibit the formation and condensation of liquid products [22]. Gasification is composed of three steps. The first is called drying and it takes place at temperatures up to 120 °C. In this step, all the moisture from the raw material is removed to produce steam. The second step is called devolatilization and it occurs at temperatures up to 350 °C: the volatile matter from the raw material is lost, leading to char formation. Finally, the third step is the gasification of the char, which takes place at temperatures above 350 °C. The process finishes when it reaches the temperature of 500 °C [23].

When air is introduced in the reaction, combustion of char and volatile products takes place, with these products reacting with oxygen. In the gasification reaction, char reacts with carbon dioxide and steam, generating hydrogen gas and carbon monoxide. The high temperatures used in this process bring the reversible water-gas shift reaction into equilibrium [24].

Among these thermal techniques, pyrolysis can be highlighted because of the bio-oil produced. It is an interesting source of biofuels and other high added-value products, such as syn-gas and aromatic compounds, which are described in detail in Section 4.4. The pyrolysis conditions under which bio-oils have been obtained from different biomasses are listed in Table 1.

Table 1. Fiber composition on a dry basis and pyrolysis conditions of biomasses used for bio-oil production.

Biomass	CEL (%)	HEM (%)	Lignin (%)	Temperature (°C)	Time (h)	Reference
Olive stones	26.5	35.4	34.7	450–700	2	[16]
Olive tree pruning	36.6	19.7	20.8	300–650	2	[14]
Corn stover	34.5	33.2	21.3	350–700	2	[20]
Corn cob	45.1	33.4	15.9	300–650	2	[20]
Rice straw	44.5	27.2	22.7	400–700	2	[20]
Sugarcane bagasse	35.3	24.1	28.5	450–700	2	[20]
Reed canary grass	39.2	21.8	8.05	300–600	2	[20]

CEL: cellulose; HEM: hemicellulose.

3. Pyrolysis

As mentioned above, pyrolysis is a form of thermal decomposition carried out under an inert atmosphere, i.e., without oxygen.

Bio-oil or pyrolysis oil, which is the liquid phase, consists of water and oxygenated aliphatic and aromatic chemicals [25]. The composition of bio-oils can vary significantly, although they tend to have similar features. The moisture content is usually between 15 and 30% wt, while the oxygen content ranges between 35 and 40% wt. Due to the presence of carboxylic acids, bio-oils tend to have low pH values (2–3). Other components that are usually found in bio-oils are alcohols, esters, aldehydes, ketones, phenols, furans and sugars [14,25].

The chosen conditions of the pyrolysis vary depending on the product to be obtained, resulting in different pyrolysis processes. To favor the formation of carbon, slow pyrolysis processes are used. These are characterized by having a long residence time (from hours to days) as well as a low heating rate. In this type of process, roughly 35% wt biochar, 35% wt syngas and 30% wt bio-oil are usually obtained [26]. On the other hand, to increase the production of bio-oil over biochar, fast pyrolysis is more suitable (Figure 1) [27]. In this type of process, the use of a smaller particle size is required in order to obtain uniform heating. Therefore, the use of raw materials with small particle sizes favors the production of bio-oil [27,28].

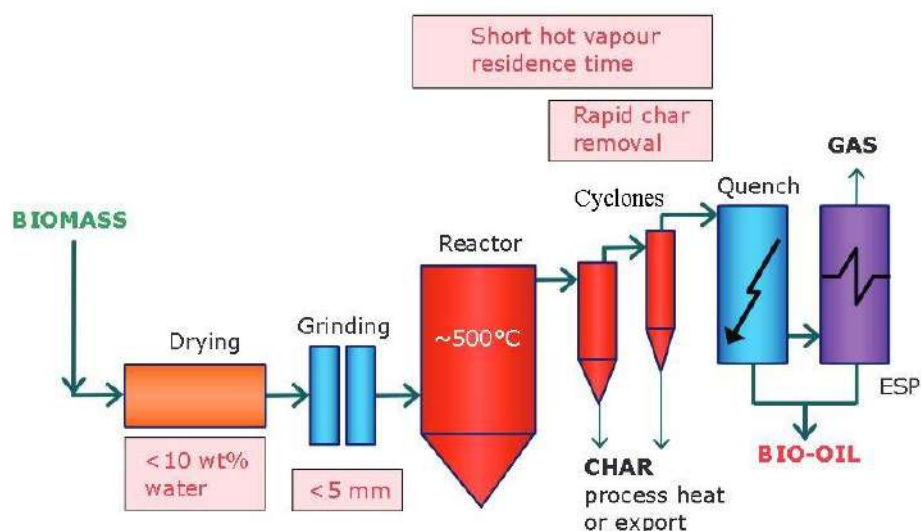


Figure 1. Typical scheme for production of bio-oil via fast pyrolysis [27].

Another essential factor to take into account is the final temperature. A temperature higher than 650 °C increases the proportion of gaseous product, while heating at low temperatures increases the proportion of biochar. Taking into account these factors, the optimum temperature for the production of bio-oil has to be determined for a specific biomass in order to maximize the formation of the desired product [27].

For instance, in bio-oil production, yields close to 75% of the weight of the initial biomass (with small amounts of solid carbon and gases) can be obtained. Fast pyrolysis produces bio-oils with lower viscosity and greater miscibility in water than those produced with slow pyrolysis [29].

While it is true that temperature is a factor that plays a key role in the final composition of the products, the temperature ramp, residence time and particle size, together with the heterogeneity of the biomass, mean that pyrolysis reactions have great chemical complexity. Each of the biomass components has characteristic thermal conditions and thus to degrade them they must be subjected to pyrolysis at different temperatures. At the lowest temperatures, in the range of 210–310 °C, hemicellulose is pyrolyzed. Subsequently, cellulose tends to degrade from 300–315 °C, its end point being around 360–380 °C. Finally,

lignin usually begins its degradation at the same temperature as hemicellulose, over 200 °C, but its pyrolysis range is much higher, since it can be degraded up to 1000 °C [30].

Furthermore, these pyrolytic processes can be modified through the use of catalysts. For example, some of these catalysts have the objective of reducing the oxygen content of the final bio-oil. Currently, pyrolysis is carried out by thermal depolymerization, together with a subsequent decomposition of the raw material into volatile compounds. However, the deoxygenation reactions that are catalyzed by acid catalysts render a greater formation of hydrocarbon products. This process includes decarboxylation, decarbonylation and dehydration [31].

4. Applications of Bio-Oils

Various studies on the uses of bio-oil can be found in the literature from the last 15 years [32–34]. The applications of bio-oil include its direct use [33,34], the production of high-quality biofuels for the automotive industry [35], and its use as a raw material for obtaining high-value chemical compounds, such as aromatic compounds (phenol) [36,37]. With regard to this latter application, one point to note is that some of the organic components of bio-oil are regarded as high added-value products. Bio-oil is a mixture of organic compounds, some of which are fine chemicals with added value. For this reason, the production of organic compounds, such as aromatic chemicals, esters and acids, from bio-oil has gained great importance in recent years [37,38].

On the other hand, the production of certain families of chemical products has also been investigated, since some of them, such as phenols, have plenty of applications. For example, phenols can be used as a raw material to produce binder through crosslinking reactions [32,39,40].

In earlier assays, the pyrolysis of biomass was carried out with the aim of producing a renewable fuel and replacing fossil fuels (gasoline and diesel). Different configurations of pyrolysis and pyrolyzers were proposed for this process. Bubbling, circulation, cone rotation and grinding have been varied in these assays [41]. Some research groups and companies have developed the industrial production of bio-oil. Among them, Red Arrow's Ensyn in Canada and the UPM refinery in Finland can be highlighted.

However, bio-oils also have some characteristics—such as high acidity, low thermal stability and less calorific power and higher viscosity than diesel—that can cause operation problems when they are used in diesel or gasoline engines [42,43]. To deal with these hindrances, researchers have developed a method that converts bio-oil into a fuel similar to fossil fuels (gasoline and diesel) through the hydrodeoxygenation (HDO) reaction. This is performed to decrease the oxygen content in bio-oil, which increases the calorific value and its thermal stability [26,35,41]. Through hydrodeoxygenation problems related to the high oxygen content of bio-oil can be solved [41]. Despite these advantages, the process is still very expensive since external hydrogen is needed in the engine and a metal oxide catalyst is needed for the process, in addition to the potential rapid deactivation of the catalyst due to the formation of coke.

4.1. Bio-Oil as Fuel for Boilers and Heavy-Duty Engines

One use of the various kinds of bio-oils is directly burning them together with fossil fuels as furnace and boiler fuels. Furthermore, bio-oil may be more suitable than heavy fossil fuels when it comes to combustion in boilers.

The combustion of bio-oil leads to less pollution by CO₂, NO_x and SO_x and thus can result in a reduction of air pollution, avoiding the use of subsequent processes to reduce these pollutants in boilers [44]. From the comparison of the data provided in Table 2, it can be seen that bio-oil has poor fuel properties when compared to fossil fuels. One of the most remarkable differences might be that bio-oil has higher water content compared to heavy fossil fuels (20–30% wt vs. 0.32% wt).

Table 2. Typical fuel properties of bio-oil and fossil fuels [45].

Property	Bio-Oil	Gasoline	Diesel	Heavy Fossil Fuel Oil
Density at 15 °C (kg/dm ³)	1.11–1.13	0.72–0.76	0.78–0.86	0.95
Pour point (°C)	−9 up to −36	–	−40	12
Water content (% wt)	20–30	–	0.05	0.32
Flash point (°C)	40–110	−43	50	110
Viscosity (cSt)	15–40 at 10 °C	0.5 at 20 °C	3 at 40 °C	130 at 10 °C
Higher heating value (MJ/kg)	14–19	45.7	47.0	42.9
Lower heating value (MJ/kg)	13–18	42.9	43.0	40.6
Elemental composition (% wt)	50–60% C	86% C	87.4% C	88.1% C
	7–8% H	12.8% H	12.1% H	10.85% H
	≤0.5% N	0% N	0.039% N	0.5% N
	35–40% O	1% S	1.39% S	0.35–0.64% O

Nevertheless, the higher heating value of bio-oil is similar to other biomasses, such as olive pruning residues, olive stones or olive pomaces, that are currently used in boilers [14].

It can be concluded from Table 2 that the bio-oil produced from pyrolysis cannot be used directly in current burner designs, which are designed for heavy fossil fuels. The primary reason is that, despite having the same flash point, the viscosity of bio-oil is lower than that of heavy fossil fuel oil. Therefore, it is necessary to redesign the current burners in order to use bio-oil as fuel, as the properties of bio-oil are different from those of its fossil analogue. One of the main differences is that the flash point and the pour point are lower for bio-oil compared with heavy fossil fuel, indicating that the storage and pumping components in boilers must be redesigned. In addition, the materials of the components of the boiler that are in contact with the bio-oil (such as the engine and the burner) have to be resistant against corrosion.

To summarize, bio-oil could be used as boiler fuel but the structure and design of current engines would have to be modified for optimal operation.

4.2. Bio-Oil to Biofuel by Hydrodeoxygenation

As mentioned earlier, one of the main characteristics of bio-oil is that it contains large amounts of water and heavy aromatic compounds, which results in instability and a low energy content [46–49]. Due to this, its transportation, storage and use in engines are very complicated. A proposed method to treat the product in order to improve its properties is shown in Figure 2 [50].

Hydrodeoxygenation could be used as a process to change the properties of bio-oil for its use as engine fuel and solve some problems. The process is characterized by operating at high temperature and high pressure, with the aim of reducing the oxygen in the bio-oil [51,52].

The deoxygenated stream consists of hydrocarbons, which can be used as gasoline, naphtha and aviation fuel, or as additives for these fuels, as long as the upgraded bio-oil is fractionated [49]. The main drawback is that the viscosity of biofuel (1–5 cP) is less than that of the fuel oil (180 cP). Due to the influence of this low viscosity, current pumping systems might require some modifications to allow the use of biofuel feeding.

The combustion of these biofuels in automotive engines has been investigated. For instance, the combustion of a hydrotreated bio-oil from pine wood has been assayed in a 20 kWe engine over a period of 40 h [52]. The engine was able to run without any problems when diesel was replaced with biofuel from bio-oil. By contrast, the operation of the engine was not entirely successful when using 100% raw bio-oil as feedstock.

This process has yet to be further developed since it requires a catalyst to reduce the formation of coke and increase the rate of hydrodeoxygenation. For this reason, the viability of the industrial-scale catalyzed HDO process for bio-oil production must be verified. The HDO process is hampered due to the formation of coke, which causes the

rapid deactivation of the catalyst. It has been reported that aromatic compounds and sugars are primarily responsible for the formation of coke [49].

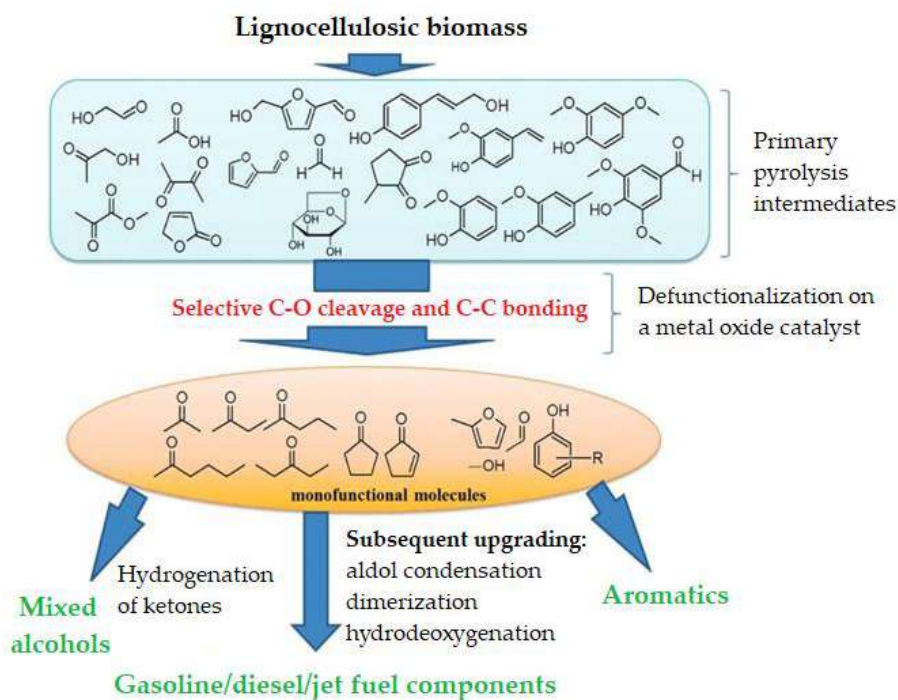
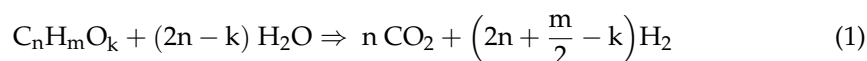


Figure 2. Biofuel production through bio-oil enhancement [50].

4.3. Bio-Oil to Hydrogen

Hydrogen is characterized by being a fuel as well as an energy carrier due to its high energy content (120.7 MJ/kg) [53]. Furthermore, the only product or waste generated from hydrogen combustion is water, so H_2 combustion does not contribute to the emission of greenhouse gases.

Hydrogen is produced on a large scale mainly through reforming with steam generated from fossil fuels [54]. Due to the poor features of fossil fuels, such as their great atmospheric pollution, and their impeding depletion, researchers are paying attention to the use of biomass as an alternative feedstock to produce hydrogen. The bio-oil steam-reforming reaction (Equation 1) can be described as follows [55]:



The direct gasification of biomass to produce hydrogen can be performed in a simple process. However, transporting bio-oil over long distances is very expensive due to its low calorific density. One alternative that would reduce the transportation costs could be the use of bio-oil instead of biomass to produce hydrogen, since bio-oil has higher energy density than biomass.

Another advantage of bio-oil is that the hydrogen produced by reforming the bio-oil with steam in the HDO reaction can be used as a reagent in reforming reactions [53,54,56]. The main scheme for bio-oil steam reforming is shown in Figure 3.

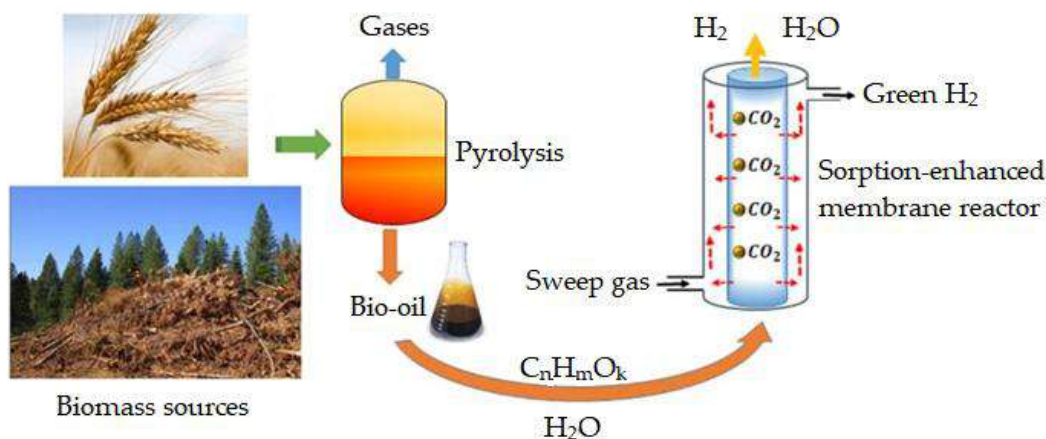


Figure 3. Hydrogen production scheme via steam reforming of bio-oil [55].

Different types of reactors have been tested with regard to the reforming reaction of bio-oil with steam. The design of the reactor plays a key role in avoiding the formation of coke in the previously described reaction, since the coke production reaction is very fast [53]. For instance, the first reactors tested in the reforming reaction were fixed-bed and fluidized-bed reactors. The durability of fluidized-bed reactors is greater than that of fixed-bed ones, since the coke formed during the above-described process can be gasified.

The largest formations of coke are generally observed in the bio-oil injection line and in the reactor inlet section. To overcome this problem, some researchers have used a nozzle to feed bio-oil into the reactor, which increases the feeding rate [57]. These researchers found that the use of a nozzle, under the assayed conditions, prevented the formation of coke for 35 h. Furthermore, the injection point was located at a considerable distance from the catalytic bed in order to keep the inlet temperature as low as possible, thus minimizing coke production at the nozzle outlet.

Furthermore, to achieve high reaction rates and increase hydrogen selectivity, catalysts have been used in steam reforming. This also minimizes the formation of coke. The main catalysts assayed so far have been those based on Ni doped with transition metals [53]. Noble metals, such as Pt and Ru, apart from being very selective and stable over time in a stream, are less prone to coke deposition on their catalytic surface. Nevertheless, their high prices prevent their use at a large scale.

4.4. Bio-Oil to High-Value Chemicals

Currently, most industrial chemicals as well as those used in daily life are obtained from fossil fuel feedstocks. Nevertheless, research on the production and separation of chemicals from bio-oil has been stimulated in the last few years [58]. Different methods have been applied to separate chemicals from bio-oil. Among them, the two outstanding and most widely used methods are the distillation and solvent extraction techniques.

4.4.1. Distillation of Bio-Oil

The high added-value chemicals of bio-oil can be separated by distillation at high temperatures and atmospheric pressure [33]. Due to high concentrations of reactive organic oxygen compounds, such as aromatics, ketones and aldehydes, the polymerization of these compounds takes place at these high distillation temperatures. Therefore, vacuum distillation is recommended in order to decrease the distillation temperature, and avoid these undesirable reactions.

Furthermore, it has been proved that separation efficiency is improved under vacuum distillation and that this technique can separate smaller molecules, such as various types of acids (acetic and formic), as well as hydroxyacetone [59].

4.4.2. Solvent Extraction

Various solvents for the extraction of chemicals from bio-oil have been assayed, including alkaline solutions, ketones, ethers, water, super-critical CO₂, ethyl acetate, toluene and n-hexane [60,61].

In one method, phenols were extracted from a bio-oil produced from the pyrolysis of sawdust, which was carried out by means of a solvent [60]. The phenols were extracted by adding ethyl ether and 10% wt caustic soda, finally obtaining sodium phenoxide. Furthermore, phenols have also been extracted with hydrochloric acid. Other researchers have carried out the extraction of different organic compounds from the bio-oil of forest residues by adding n-hexane, water and dichloromethane [62].

4.5. Conversion of Bio-Oil to Carbonaceous Materials

The applications of carbonaceous materials, which are usually produced from coal or biomass, cover a wide range, especially at the industrial scale [63]. The production of these carbonaceous materials from bio-oil is an attractive proposition in light of the fact that they have a positive impact on the environment due to their sustainability as raw materials. Furthermore, biomass generally has low or zero sulphur content and nitrogen content has been reported to be much lower than that in coal. The porous structure of activated carbon is also responsible for its low mechanical resistance.

In order to increase the mechanical resistance of carbonaceous materials made from biomass, a methodology has been developed for their manufacture from bio-oil and biochar [63]. When the pores of biochar are filled with the solids resulting from the polymerization of the bio-oil, the above-described mechanical resistance increases.

From the studies available in the literature on the production of carbonaceous materials from bio-oil, it can be concluded that the technology has to be improved and developed through further investigation in order to identify feasible pathways and their mechanisms. This could provide an overview of the possibilities for the production of specific carbonaceous materials under the most suitable conditions.

4.6. Electrodes

Pitch is regarded as one of the most abundant raw materials available to obtain electrodes. In industry, the tar produced from coal is used as pitch. Nevertheless, in recent years a part of the tar produced from the pyrolysis of biomass—called biopitch—has been investigated, which could replace the tar derived from coal [64]. One advantage is that its oxygen content is higher than that of pitch (20% wt instead of 2% wt). This higher content can improve the softening point during heating, mainly due to water vapor and the presence of some light compounds in the material during heating.

Furthermore, the higher oxygen content is translated into an increase in the reactivity of the pitch, with the ultimate goal of polymerization during heating [64]. Furthermore, the production of solid products from bio-oil is favored due to the high oxygen content.

4.7. Bio-Oil in Asphalt

The use of bio-oil as a source of binder for asphalt could overcome the uncertainty in the supply of petroleum-based binders [65]. Bio-oil from the pyrolysis of biomass can be used as a binder in asphalt, not only because it is renewable, but also due to its low levels of heterogeneous atoms, such as sulphur (almost nil) and nitrogen (0.5% wt) [26,41,42,44], as well as the presence of high levels of phenols, such as phenolic monomers and pyrolytic lignin in the bio-binder structure, which are derived from the degradation of lignin to some extent. These compounds account for the potential of the use of bio-oil in asphalt [66]. The rheological properties of bio-oil as a bio-binder have been compared with those of petroleum resources [67]. The authors of one study pyrolyzed oak wood to obtain bio-oil and studied the specifications of this bio-binder and a mixture of the same with polyethylene at 2 and 4% wt, added to control the viscosity in the binder derived from coal.

The authors found that both the bio-binder and its mixture with polyethylene had great potential for substituting asphalt binders derived from coal [67].

4.8. Pesticides

Another example of the use of bio-oil is the production of pyroligneous acid, also known as wood vinegar, which is obtained from the slow pyrolysis liquid fraction obtained as a byproduct of charcoal production. It is one of the most valuable products of the pyrolysis of biomass and has biocide properties that make the bio-oil containing it a potential pesticide. For instance, it has been reported that wood vinegar obtained from the pyrolysis of bamboo is effective in controlling fungi at concentrations between 0.1 and 1% wt [68]. This wood vinegar includes acetic acid, one of the organics acids produced from pyrolysis. This acid can account for around 15% wt in wood bio-oil.

4.9. Polyurethane Foams Formation

Polyurethane (PU) has many of different uses in industry, including as feedstock for the production of insulation materials, medicine and furniture [69]. Normally, it is produced from fossil fuel resources through the reaction between isocyanates and polyols.

Recently, some researchers have investigated how to produce PU from bio-oil, looking at the viability and profitability of the process [68]. Biopolyol was extracted from bio-oil using an organic solvent (ethyl acetate), which was mixed with bio-oil at the same ratio. The authors of this study claimed to have obtained PU foam with some properties similar to those of commercial PU through the use of condensation reactions among biopolyol, polymethylene polyphenyl isocyanate, polymeric diphenyl methane diisocyanate and some additives.

4.10. Plastics

One of the less well-known uses of fossil fuels, from within the great variety of their uses, is the production of plastics. Due to their low degradation kinetics, the huge amount of plastics produced in the world is accumulated in the environment, generating a huge environmental problem [69,70]. Furthermore, the production of additives causes environmental problems, such as the production of toxins (phthalates and plasticizers), during the process of plastic de-composition. As a result, researchers have paid attention to the production of biodegradable plastics over the last few decades [70–72]. Fractionation of bio-oil has been carried out successfully, giving rise to various chemical products such as ethanol, xylose, acetic acid, ethylene and others. Some of these can be used as monomers for the production of different plastics [70]. However, their high price, lower mechanical properties and low-quality appearance narrow their potential for production at a large scale.

4.11. Biodiesel

As mentioned earlier, bio-oils produced from lignocellulose residues by fast pyrolysis or catalytic fast pyrolysis are regarded as suitable raw materials to produce renewable diesel [73].

In order to stabilize the hydrotreated bio-oil, butane and other light compounds are removed with a lights removal column [74]. Later, the stable bio-oil stream is separated into light and heavy fractions. The heavy fraction (boiling point above 350 °C) is then sent to a hydrocracker to completely convert the bio-oil into gasoline and diesel blend components. The main process might occur as shown in Figure 4.

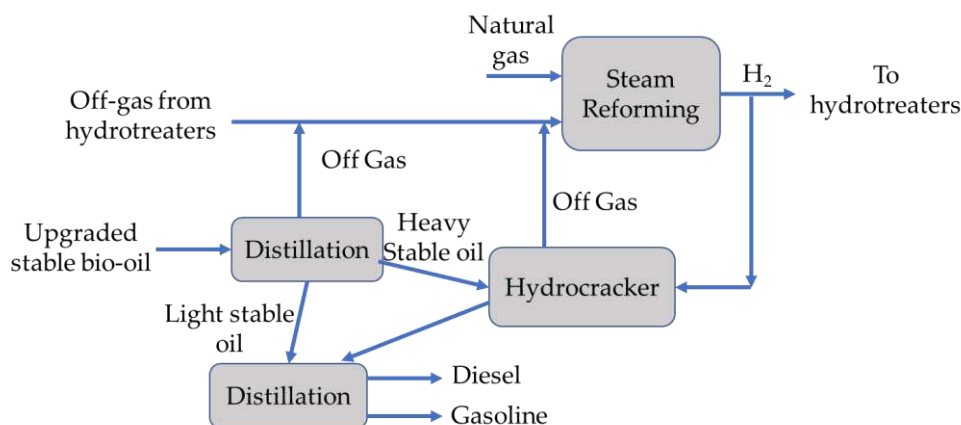


Figure 4. Block diagram for hydrocracking and product separation [74].

The final product is a mixture of liquids spanning the gasoline and diesel range and some gaseous byproducts. The gasoline and diesel products can be separated by distillation. While biodiesel from transesterification of triglycerides from vegetal oils or animal fats is composed of methyl (or ethyl) esters, biodiesel from bio-oil has a similar composition to that of fossil diesel (hydrocarbons, mainly paraffins, aromatics and naphthenes). Methyl-ester biodiesel is commercially found mixed with commercial diesel in varying percentages ranging from 5% to 30%, although 100% methyl-ester biodiesel can also be found to a lesser extent. As a result, the presence of biodiesel from the transesterification of triglycerides in the fuel affects its physical and chemical properties. On the contrary, biodiesel obtained from hydrocracking of bio-oil is regarded as suitable for blending with petroleum diesel [74]. The yield of fuel products based on 100% renewable raw material has been reported to be approximately 65% wt [74]. Furthermore, the carbon balance is shown in Table 3. As can be seen, researchers achieved a 55% wt conversion of the carbon in the combined feed (biomass plus natural gas) into fuel products.

Table 3. Carbon balance of product fuel from wood [74].

Raw material	Biomass	88% wt
	Natural gas	12% wt
Fuel products	Gasoline pool	23% wt
	Diesel pool	32% wt
Waste products	Pyrolysis unit exhaust	23% wt
	Upgrading wastewater	0% wt
	Upgrading heaters exhaust	2% wt
	Reformer exhaust	20% wt

Another strategy might be burning a blend of bio-oil and diesel in an oil-fired furnace [75]. Although using bio-oil to replace fossil fuels has limitations due to undesirable properties of bio-oil, such as high water, acidity and oxygen contents, low heating value, and so on, a low blend ratio of bio-oil used to substitute petroleum-derived oil has advantages. For instance, it can be easily combusted in furnaces without any modifications. Thus, bio-oil blended with 5% (v/v) diesel achieved a stable combustion, emitting less CO₂, NO, SO₂ and CO than pure diesel. Furthermore, a study on the life cycle assessment of the production of bio-fuels from bio-oil showed that the life cycle assessment for diesel produced by fast pyrolysis of forest residues and subsequent hydrotreating and hydrocracking indicated greenhouse gases emissions of 0.142 kg CO₂-eq per km and a net energy value of 1.00 MJ per km, which are lower than those obtained for fossil fuels. [76].

5. Conclusions

Due to the interesting features of bio-oil, such as higher energetic density and less pollution compared with fuels from fossil feedstocks, it is being widely used nowadays at both laboratory and industrial scales.

Bio-oil is a firm alternative to fossil fuels feedstocks with a wide range of applications but, in order to achieve a better quality process, further investigations have to be carried out to enhance its properties. However, it is also essential to highlight the important role that bio-oil could play nowadays in global industry, with fossil fuels getting closer to depletion every day.

In this context, the most feasible way to improve and use bio-oil might be hydrotreatment, which can transform waste such as residual forestry biomass into a byproduct with real applications. Thus, the renewable fuels obtained by hydrotreatment of bio-oil can be used for direct combustion or in biorefineries.

However, other potential uses of bio-oil, such as in the production of bioplastics, are less attractive since their production costs are higher than those of fossil fuels and, specifically for bioplastics, their mechanical properties and the quality of appearance are worse. However, the production of asphalt from bio-oil is attractive due to its lack of sulphur content, but this has to be further developed in the future.

Author Contributions: F.J.S.-B., P.Á.-M., J.F.G.-M. are equally participated in the writing of this review paper. F.J.S.-B., P.Á.-M., J.F.G.-M. have read and agreed to the published version of the manuscript. All authors have read and agreed to the published version of the manuscript.

Funding: This review paper is within the LIFE 13-Bioseville ENV/1113 project, funded by the European Union.

Institutional Review Board Statement: Not applicable.

Informed Consent Statement: Not applicable.

Conflicts of Interest: The authors declare no conflict of interest.

References

1. Bhatia, S.K.; Bhatia, R.K.; Jeon, J.M.; Pugazhendhi, A.; Awasthi, M.K.; Kumar, D.; Kumar, G.; Yoon, J.J.; Yang, Y.H. An overview on advancements in biobased transesterification methods for biodiesel production: Oil resources, extraction, biocatalysts, and process intensification technologies. *Fuel* **2021**, *285*, 119117. [[CrossRef](#)]
2. García Martín, J.F. *Recent Developments in Jatropha Research*; Nova Science Publishers, Inc.: Hauppauge, NY, USA, 2021; ISBN 978-1-53619-132-5.
3. Álvarez-Mateos, P.; García-Martín, J.F.; Guerrero-Vacas, F.J.; Naranjo-Calderón, C.; Barrios, C.C.; Pérez Camino, M.d.C. Valorization of a high-acidity residual oil generated in the waste cooking oils recycling industries. *Grasas Aceites* **2019**, *70*, e335. [[CrossRef](#)]
4. Kumar, H.; Sarma, A.K.; Kumar, P. A comprehensive review on preparation, characterization, and combustion characteristics of microemulsion based hybrid biofuels. *Renew. Sustain. Energy Rev.* **2020**, *117*, 109498. [[CrossRef](#)]
5. Singh, D.; Sharma, D.; Soni, S.L.; Inda, C.S.; Sharma, S.; Sharma, P.K.; Jhalani, A. A comprehensive review of physicochemical properties, production process, performance and emissions characteristics of 2nd generation biodiesel feedstock: *Jatropha curcas*. *Fuel* **2021**, *285*, 119110. [[CrossRef](#)]
6. García-Martín, J.F.; Barrios, C.C.; Alés-Álvarez, F.J.; Domínguez-Sáez, A.; Álvarez-Mateos, P. Biodiesel production from waste cooking oil in an oscillatory flow reactor. Performance as a fuel on a TDI diesel engine. *Renew. Energy* **2018**, *125*, 546–556. [[CrossRef](#)]
7. Hassan, A.A.; Smith, J.D. Investigation of microwave-assisted transesterification reactor of waste cooking oil. *Renew. Energy* **2020**, *162*, 1735–1746. [[CrossRef](#)]
8. Carbajal, E.M.T.; Hernández, E.M.; Linares, L.F.; Maldonado, E.N.; Ballesteros, R.L. Techno-economic analysis of Scenedesmus dimorphus microalgae biorefinery scenarios for biodiesel production and glycerol valorization. *Bioresour. Technol. Rep.* **2020**, *12*, 100605. [[CrossRef](#)]
9. Athar, M.; Zaidi, S. A review of the feedstocks, catalysts, and intensification techniques for sustainable biodiesel production. *J. Environ. Chem. Eng.* **2020**, *8*, 104523. [[CrossRef](#)]
10. Mondal, B.; Jana, A.K. Techno-economic feasibility of reactive distillation for biodiesel production from algal oil: Comparing with a conventional multiunit system. *Ind. Eng. Chem. Res.* **2019**, *58*, 12028–12040. [[CrossRef](#)]




11. Shuai, W.; Das, R.K.; Naghdi, M.; Brar, S.K.; Verma, M. A review on the important aspects of lipase immobilization on nanomaterials. *Biotechnol. Appl. Biochem.* **2017**, *64*, 496–508. [[CrossRef](#)]
12. Bhatia, S.K.; Gurav, R.; Choi, T.R.; Kim, H.J.; Yang, S.Y.; Song, H.S.; Park, J.Y.; Park, Y.L.; Han, Y.H.; Choi, Y.K.; et al. Conversion of waste cooking oil into biodiesel using heterogenous catalyst derived from cork biochar. *Bioresour. Technol.* **2020**, *302*, 122872. [[CrossRef](#)]
13. Zhang, Y.H.P. Reviving the carbohydrate economy via multi-product lignocellulose biorefineries. *J. Ind. Microbiol. Biotechnol.* **2008**, *35*, 367–375. [[CrossRef](#)]
14. García Martín, J.F.; Cuevas, M.; Feng, C.H.; Álvarez Mateos, P.; Torres García, M.; Sánchez, S. Energetic valorisation of olive biomass: Olive-tree pruning, olive stones and pomaces. *Processes* **2020**, *8*, 511. [[CrossRef](#)]
15. Cuevas, M.; Saleh, M.; García-Martín, J.F.; Sánchez, S. Acid and enzymatic fractionation of olive stones for ethanol production using *Pachysolen tannophilus*. *Processes* **2020**, *8*, 195. [[CrossRef](#)]
16. Cuevas, M.; García Martín, J.F.; Bravo, V. Ethanol production from olive stones through liquid hot water pre-treatment, enzymatic hydrolysis and fermentation. Influence of enzyme loading, and pre-treatment temperature and time. *Fermentation* **2021**, *7*, 25. [[CrossRef](#)]
17. Zhang, J.; Cai, D.; Qin, Y.; Liu, D.; Zhao, X. High value-added monomer chemicals and functional bio-based materials derived from polymeric components of lignocellulose by organosolv fractionation. *J. Chem. Inf. Model.* **2019**, *53*, 1689–1699. [[CrossRef](#)]
18. García Martín, J.F.; Cuevas, M.; Bravo, V.; Sánchez, S. Ethanol production from olive prunings by autohydrolysis and fermentation with *Candida tropicalis*. *Renew. Energy* **2010**, *35*, 1602–1608. [[CrossRef](#)]
19. Zhu, H.; Luo, W.; Ciesielski, P.N.; Fang, Z.; Zhu, J.Y.; Henriksson, G.; Himmel, M.E.; Hu, L. Wood-derived materials for green electronics, biological devices, and energy applications. *Chem. Rev.* **2016**, *116*, 9305–9374. [[CrossRef](#)] [[PubMed](#)]
20. Tanger, P.; Field, J.L.; Jahn, C.E.; DeFoort, M.W.; Leach, J.E. Biomass for thermochemical conversion: Targets and challenges. *Front. Plant Sci.* **2013**, *4*, 1–20. [[CrossRef](#)]
21. van der Stelt, M.J.C.; Gerhauser, H.; Kiel, J.H.A.; Ptasiński, K.J. Biomass upgrading by torrefaction for the production of biofuels: A review. *Biomass Bioenergy* **2011**, *35*, 3748–3762. [[CrossRef](#)]
22. Reed, T.B. Combustion, pyrolysis, gasification and liquefaction of biomass. In Proceedings of the Energy from Biomass Conference, Brighton, UK, 4–7 November 1980.
23. Najeeb, K.; Dustin, D.; Xianglan, B.; Kwang, H.K.; Robert, C.B. Pyrolytic sugars from cellulosic biomass. *ChemPubSoc Eur.* **2012**, *5*, 2228–2236.
24. Kirubakaran, V.; Sivaramakrishnan, V.; Nalini, R.; Sekar, T.; Premalatha, M.; Subramanian, P. A review on gasification of biomass. *Renew. Sustain. Energy Rev.* **2009**, *13*, 179–186. [[CrossRef](#)]
25. Yaman, S. Pyrolysis of biomass to produce fuels and chemical feedstocks. *Energy Convers. Manag.* **2004**, *45*, 651–671. [[CrossRef](#)]
26. Kan, T.; Strezov, V.; Evans, T.J. Lignocellulosic biomass pyrolysis: A review of product properties and effects of pyrolysis parameters. *Renew. Sustain. Energy Rev.* **2016**, *57*, 1126–1140. [[CrossRef](#)]
27. Bridgwater, T. Challenges and opportunities in fast pyrolysis of biomass: Part II. *Johns. Matthey Technol. Rev.* **2018**, *62*, 150–160. [[CrossRef](#)]
28. Onay, O.; Kockar, O.M. Slow, fast and flash pyrolysis of rapeseed. *Renew. Energy* **2003**, *28*, 2417–2433. [[CrossRef](#)]
29. Bridgwater, A.V. Catalysis in thermal biomass conversion. *Appl. Catal. A Gen.* **1994**, *116*, 5–47. [[CrossRef](#)]
30. Zhou, H.; Long, Y.; Meng, A.; Li, Q.; Zhang, Y. The pyrolysis simulation of five biomass species by hemi-cellulose, cellulose and lignin based on thermogravimetric curves. *Thermochim. Acta* **2013**, *566*, 36–43. [[CrossRef](#)]
31. Wang, K.; Kim, K.H.; Brown, R.C. Catalytic pyrolysis of individual components of lignocellulosic biomass. *Green Chem.* **2014**, *16*, 727–735. [[CrossRef](#)]
32. Mirkouei, A.; Haapala, K.R.; Sessions, J.; Murthy, G.S. A review and future directions in techno-economic modeling and optimization of upstream forest biomass to bio-oil supply chains. *Renew. Sustain. Energy Rev.* **2017**, *67*, 15–35. [[CrossRef](#)]
33. Czernik, S.; Bridgwater, A.V. Overview of applications of biomass fast pyrolysis oil. *Energy Fuels* **2004**, *18*, 590–598. [[CrossRef](#)]
34. Brammer, J.G.; Lauer, M.; Bridgwater, A.V. Opportunities for biomass-derived “bio-oil” in European heat and power markets. *Energy Policy* **2006**, *34*, 2871–2880. [[CrossRef](#)]
35. Xu, X.; Li, Z.; Sun, Y.; Jiang, E.; Huang, L. High-quality fuel from the upgrading of heavy bio-oil by the combination of ultrasonic treatment and mutual solvent. *Energy Fuels* **2018**, *32*, 3477–3487. [[CrossRef](#)]
36. Rashid, U.; Nizami, A.-S.; Rehan, M. Waste biomass utilization for value-added green products. *Curr. Org. Chem.* **2019**, *23*, 1497–1498. [[CrossRef](#)]
37. Wang, Y.; Li, X.; Mourant, D.; Gunawan, R.; Zhang, S.; Li, C.Z. Formation of aromatic structures during the pyrolysis of bio-oil. *Energy Fuels* **2012**, *26*, 241–247. [[CrossRef](#)]
38. Rehan, M.; Nizami, A.S.; Rashid, U.; Naqvi, M.R. Editorial: Waste biorefineries: Future energy, green products and waste treatment. *Front. Energy Res.* **2019**, *7*, 3–5. [[CrossRef](#)]
39. Maneffa, A.; Prielcel, P.; Lopez-Sanchez, J.A. Biomass-derived renewable aromatics: Selective routes and outlook for p-xylene commercialisation. *ChemSusChem* **2016**, *9*, 2736–2748. [[CrossRef](#)]
40. Vélez, D.C.P.; Magalhães, W.L.E.; Capobianco, G. Carbon fiber from fast pyrolysis bio-oil. *Sci. Technol. Mater.* **2018**, *30*, 16–22. [[CrossRef](#)]

41. Hu, X.; Gholizadeh, M. Biomass pyrolysis: A review of the process development and challenges from initial researches up to the commercialisation stage. *J. Energy Chem.* **2019**, *39*, 109–143. [[CrossRef](#)]
42. Hughey, C.A.; Hendrickson, C.L.; Rodgers, R.P.; Marshall, A.G. Elemental composition analysis of processed and unprocessed diesel fuel by electrospray ionization fourier transform ion cyclotron resonance mass spectrometry. *Energy Fuels* **2001**, *15*, 1186–1193. [[CrossRef](#)]
43. Gholizadeh, M.; Gunawan, R.; Hu, X.; Mercader, F.D.M.; Westerhof, R.; Chaitwat, W.; Hasan, M.M.; Mourant, D.; Li, C.Z. Effects of temperature on the hydrotreatment behaviour of pyrolysis bio-oil and coke formation in a continuous hydrotreatment reactor. *Fuel Process. Technol.* **2016**, *148*, 175–183. [[CrossRef](#)]
44. Hou, S.S.; Huang, W.C.; Rizal, F.M.; Lin, T.H. Co-firing of fast pyrolysis bio-oil and heavy fuel oil in a 300-kW_{th} furnace. *Appl. Sci.* **2016**, *6*, 326. [[CrossRef](#)]
45. Hu, X.; Gholizadeh, M. Progress of the applications of bio-oil. *Renew. Sustain. Energy Rev.* **2020**, *134*, 110124. [[CrossRef](#)]
46. Lehto, J.; Oasmaa, A.; Solantausta, Y.; Kytö, M.; Chiaramonti, D. Review of fuel oil quality and combustion of fast pyrolysis bio-oils from lignocellulosic biomass. *Appl. Energy* **2014**, *116*, 178–190. [[CrossRef](#)]
47. Chiaramonti, D.; Prussi, M.; Buffi, M.; Tacconi, D. Sustainable bio kerosene: Process routes and industrial demonstration activities in aviation biofuels. *Appl. Energy* **2014**, *136*, 767–774. [[CrossRef](#)]
48. Chiaramonti, D.; Bonini, M.; Fratini, E.; Tondi, G.; Gartner, K.; Bridgwater, A.V. Development of emulsions from biomass pyrolysis liquid and diesel and their use in engines—Part 2: Tests in diesel engines. *Fuel Energy Abstr.* **2004**, *45*, 48. [[CrossRef](#)]
49. Han, Y.; Gholizadeh, M.; Tran, C.C.; Kaliaguine, S.; Li, C.Z.; Olarte, M.; Garcia-Perez, M. Hydrotreatment of pyrolysis bio-oil: A review. *Fuel Process. Technol.* **2019**, *195*, 106140. [[CrossRef](#)]
50. Mante, O.D.; Rodriguez, J.A.; Senanayake, S.D.; Babu, S.P. Catalytic conversion of biomass pyrolysis vapors into hydrocarbon fuel precursors. *Green Chem.* **2015**, *17*, 2362–2368. [[CrossRef](#)]
51. Wildschut, J. Pyrolysis oil upgrading to transportation fuels by catalytic hydrotreatment. Ph.D. Thesis, University of Groningen, Groningen, The Netherlands, 2009.
52. Van De Beld, B.; Holle, E.; Florijn, J. The use of pyrolysis oil and pyrolysis oil derived fuels in diesel engines for CHP applications. *Appl. Energy* **2013**, *102*, 190–197. [[CrossRef](#)]
53. Kumar, A.; Chakraborty, J.P.; Singh, R. Bio-oil: The future of hydrogen generation. *Biofuels* **2017**, *8*, 663–674. [[CrossRef](#)]
54. Kirtay, E. Recent advances in production of hydrogen from biomass. *Energy Convers. Manag.* **2011**, *52*, 1778–1789. [[CrossRef](#)]
55. Soria, M.A.; Barros, D.; Madeira, L.M. Hydrogen production through steam reforming of bio-oils derived from biomass pyrolysis: Thermodynamic analysis including in situ CO₂ and/or H₂ separation. *Fuel* **2019**, *244*, 184–195. [[CrossRef](#)]
56. Zhang, L.; Hu, X.; Hu, K.; Hu, C.; Zhang, Z.; Liu, Q.; Hu, S.; Xiang, J.; Wang, Y.; Zhang, S. Progress in the reforming of bio-oil derived carboxylic acids for hydrogen generation. *J. Power Sources* **2018**, *403*, 137–156. [[CrossRef](#)]
57. Basagiannis, A.C.; Verykios, X.E. Steam reforming of the aqueous fraction of bio-oil over structured Ru/MgO/Al₂O₃ catalysts. *Catal. Today* **2007**, *127*, 256–264. [[CrossRef](#)]
58. Hu, X.; Zhang, Z.; Gholizadeh, M.; Zhang, S.; Lam, C.H.; Xiong, Z.; Wang, Y. Coke formation during thermal treatment of bio-oil. *Energy Fuels* **2020**, *34*, 7863–7914. [[CrossRef](#)]
59. Zhang, X.S.; Yang, G.X.; Jiang, H.; Liu, W.J.; Ding, H.S. Mass production of chemicals from biomass-derived oil by directly atmospheric distillation coupled with co-pyrolysis. *Sci. Rep.* **2013**, *3*, 1–7. [[CrossRef](#)]
60. Shah, Z.; CV, R.; AC, M.; DS, R. Separation of Phenol from Bio-oil produced from pyrolysis of agricultural wastes. *Mod. Chem. Appl.* **2017**, *5*, 1000199. [[CrossRef](#)]
61. Wang, J.; Cui, H.; Wei, S.; Zhuo, S.; Wang, L.; Li, Z.; Yi, W. Separation of biomass pyrolysis oil by supercritical CO₂ extraction. *Smart Grid Renew. Energy* **2010**, *01*, 98–107. [[CrossRef](#)]
62. Oasmaa, A.; Kuoppala, E.; Solantausta, Y. Fast pyrolysis of forestry residue. 2. Physicochemical composition of product liquid. *Energy Fuels* **2003**, *17*, 433–443. [[CrossRef](#)]
63. Hu, X.; Nango, K.; Bao, L.; Li, T.; Mahmudul Hasan, M.D.; Li, C.Z. High yields of solid carbonaceous materials from biomass. *Green Chem.* **2019**, *21*, 1128–1140. [[CrossRef](#)]
64. Rocha, J.D.; Coutinho, A.R.; Luengo, C.A. Biopitch produced from eucalyptus wood pyrolysis liquids as a renewable binder for carbon electrode manufacture. *Braz. J. Chem. Eng.* **2002**, *19*, 127–132. [[CrossRef](#)]
65. Aziz, M.M.A.; Rahman, M.T.; Hainin, M.R.; Bakar, W.A. An overview on alternative binders for flexible pavement. *Constr. Build. Mater.* **2015**, *84*, 315–319. [[CrossRef](#)]
66. Wang, H.; Ma, Z.; Chen, X.; Hasan, M.R.M. Preparation process of bio-oil and bio-asphalt, their performance, and the application of bio-asphalt: A comprehensive review. *J. Traffic Transp. Eng.* **2020**, *7*, 137–151. [[CrossRef](#)]
67. Raouf, M.A.; Williams, R.C. Temperature and shear susceptibility of a nonpetroleum binder as a pavement material. *Transp. Res. Rec.* **2010**, *2180*, 9–18. [[CrossRef](#)]
68. Tiilikkala, K.; Fagernäs, L.; Tiilikkala, J. History and use of wood pyrolysis liquids as biocide and plant protection product. *Open Agric. J.* **2014**, *4*, 111–118. [[CrossRef](#)]
69. Wu, J.; Wang, Y.; Wan, Y.; Lei, H.; Yu, F.; Liu, Y.; Chen, P.; Yang, L.; Ruan, R. Processing and properties of rigid polyurethane foams based on bio-oils from microwave-assisted pyrolysis of corn stover. *Int. J. Agric. Biol. Eng.* **2009**, *2*, 40–50. [[CrossRef](#)]
70. Laycock, B.; Nikolić, M.; Colwell, J.M.; Gauthier, E.; Halley, P.; Bottle, S.; George, G. Lifetime prediction of biodegradable polymers. *Prog. Polym. Sci.* **2017**, *71*, 144–189. [[CrossRef](#)]

71. Asghari, F.; Samiei, M.; Adibkia, K.; Akbarzadeh, A.; Davaran, S. Biodegradable and biocompatible polymers for tissue engineering application: A review. *Artif. Cells Nanomed. Biotechnol.* **2017**, *45*, 185–192. [[CrossRef](#)]
72. Kargarzadeh, H.; Huang, J.; Lin, N.; Ahmad, I.; Mariano, M.; Dufresne, A.; Thomas, S.; Gałęski, A. Recent developments in nanocellulose-based biodegradable polymers, thermoplastic polymers, and porous nanocomposites. *Prog. Polym. Sci.* **2018**, *87*, 197–227. [[CrossRef](#)]
73. Spatari, S.; Larnaudie, V.; Mannoh, I.; Wheeler, M.C.; Macken, N.A.; Mullen, C.A.; Boateng, A.A. Environmental, exergetic and economic tradeoffs of catalytic- and fast pyrolysis-to-renewable diesel. *Renew. Energy* **2020**, *162*, 371–380. [[CrossRef](#)]
74. Jones, S.; Valkenburg, C.; Walton, C. *Production of Gasoline and Diesel from Biomass via Fast Pyrolysis, Hydrotreating and Hydrocracking: A Design Case*; Pacific Northwest National Lab.: Springfield, MO, USA, 2009.
75. Hou, S.S.; Huang, W.C.; Lin, T.H. Co-combustion of fast pyrolysis bio-oil derived from coffee bean residue and diesel in an oil-fired furnace. *Appl. Sci.* **2017**, *7*, 1085. [[CrossRef](#)]
76. Hsu, D. Life cycle assessment of gasoline and diesel produced via fast pyrolysis and hydroprocessing. *Contract* **2011**, *303*, 275–3000. [[CrossRef](#)]

Article

Determination of the Composition of Bio-Oils from the Pyrolysis of Orange Waste and Orange Pruning and Use of Biochars for the Removal of Sulphur from Waste Cooking Oils

Francisco-José Sánchez-Borrego , Noelia García-Criado, Juan F. García-Martín *  and Paloma Álvarez-Mateos * 

Departamento de Ingeniería Química, Facultad de Química, Universidad de Sevilla, C/Profesor García González s/n, 41012 Seville, Spain; fsanchez25@us.es (F.-J.S.-B.); noegarcia@gmail.com (N.G.-C.)

* Correspondence: jfgarmar@us.es (J.F.G.-M.); palvarez@us.es (P.Á.-M.)

Abstract: Waste generated in the agri-food sector is a potential source of biomass and other products of high added value. In this work, the pyrolysis of orange waste and orange pruning was carried out to produce adsorbent biochars and characterise the bio-oils aiming for high-added-value compounds. Pyrolysis was carried out in a vertical tubular furnace on the laboratory scale modifying the temperature (400–600 °C), the heating ramp (5–20 °C·min⁻¹) to reach the previous temperature and the inert gas flow rate (30–300 mL Ar·min⁻¹) throughout the furnace. The most suitable conditions for obtaining biochar were found to be 400 °C, 5 °C·min⁻¹, and 150 mL Ar·min⁻¹ for orange waste, and 400 °C, 10 °C·min⁻¹, and 150 mL Ar·min⁻¹ for orange pruning. Thermogravimetric analysis showed higher thermal stability for orange pruning due to its higher lignin content (20% vs. 5% wt. on a wet basis). The bio-oil composition was determined by GC-MS. Toluene and 5-hydroxymethylfurfural were the main compounds found in orange waste bio-oils, while orange pruning bio-oils were composed mainly of 4-hydroxy-4-methyl-2-pentanone. Finally, the removal of the sulphur content from waste cooking oil was assayed with the biochars from both orange waste and orange pruning, whose BET surface areas were previously determined. Despite their low specific surface areas (≤ 1 m²·g⁻¹ for orange waste biochars and up to 24.3 m²·g⁻¹ for orange pruning biochars), these biochars achieved a reduction of the initial sulphur content of the waste cooking oil between 66.4% and 78.8%.

Keywords: biochar; bio-oil; oil desulphurisation; orange pruning; orange waste; pyrolysis



Citation: Sánchez-Borrego, F.-J.; García-Criado, N.; García-Martín, J.F.; Álvarez-Mateos, P. Determination of the Composition of Bio-Oils from the Pyrolysis of Orange Waste and Orange Pruning and Use of Biochars for the Removal of Sulphur from Waste Cooking Oils. *Agronomy* **2022**, *12*, 309. <https://doi.org/10.3390/agronomy12020309>

Academic Editors: Kyoung S. Ro and Ariel A. Szogi

Received: 21 December 2021

Accepted: 21 January 2022

Published: 25 January 2022

Publisher's Note: MDPI stays neutral with regard to jurisdictional claims in published maps and institutional affiliations.



Copyright: © 2022 by the authors. Licensee MDPI, Basel, Switzerland. This article is an open access article distributed under the terms and conditions of the Creative Commons Attribution (CC BY) license (<https://creativecommons.org/licenses/by/4.0/>).

1. Introduction

Among all raw materials in the food industry, fruits and vegetables produce the most waste. In Europe, Spain leads the orange and orange juice production ranking, and is sixth in the global ranking, according to the Food and Agriculture Organization (2018) [1]. In Spain, this agricultural activity can be found mainly in Valencia and Andalusia, producing almost 2×10^6 t per year of sweet oranges, the fruit of the sweet orange tree (*Citrus sinensis*). According to the Spanish Ministry of Agriculture, Fishing, and Food [2], the orange harvesting, handling, transport, and marketing are responsible for thousands of jobs [3].

Farmers prune to remove old branches and regenerate orange trees. In Spain, more than 5×10^6 t of orange pruning are produced annually, which are considered as waste and therefore must be disposed of to avoid contamination, pest growth, and delay in agricultural practices [4]. As a lignocellulose material, orange-tree pruning is mainly composed of cellulose, hemicellulose, and lignin.

The citrus industry, in particular the orange juice sector, produces more than 2.2×10^6 t of waste in Spain each year [2]. The orange waste (OW) generated in the production of orange juice accounts for around 50–60 wt.% in wet basis [5] of the processed fruit, with an amount of moisture of approximately 82% wt.% [6], the waste containing approximately 60–65% peel, 30–35% pulp, and 0–10% seeds [7]. These residues have no profitable

commercial use. Traditionally, they are used for animal feed, as fertiliser [8], or as cattle bedding, options that provide no benefit either economically or for the environment, so many of them go to dumps, creating a logistic problem [9] and increasing the economic and environmental problems [10].

Therefore, a profitable alternative for these orange residues is needed. In recent years, different recovery and reuse pathways have been proposed. Among them, biochemical processes such as fermentation for bioethanol production [11], anaerobic digestion [12,13], and recovery of flavonoids and chemical products [14] are highlighted. Recently, thermal conversion methods, such as gasification, roasting, pyrolysis [15], and catalytic hydrotreating [16] have also been researched.

Pyrolysis is one of the main thermochemical processes for converting biomass into valuable products [17]. It is the thermal degradation of organic material in the absence of oxygen. During the pyrolysis process, each lignocellulose material undergoes different reaction mechanisms (i.e., decarboxylation, dehydration, and demethylation), resulting in biochar, bio-oil, and syngas production [18]. Pyrolysis can be fast or slow, depending mainly on the heating ramp and residence time, and other factors such as pressure and the type of process (batch or continuous) [19]. The performance, composition, and distribution of the products depend on the pyrolysis conditions, mainly on factors such as the nature of the biomass (starting raw material), previous treatments, particle size, reactor type, maximum reaction temperature, heating ramp, residence time, pressure, use of a mineral catalyst, etc. [20]. Lower process temperatures and heating ramps and longer gas residence times improve biochar production [21]. Approximately 35% of the weight of dry biomass can be turned into biochar, although higher pressures can provide significantly higher performance.

The liquid part, bio-oil, is a dark brown polar fluid that flows freely and is similar to biomass in its elemental composition. It is composed of a very complex mixture of oxygenated derivatives of hydrocarbons, which result from the incomplete degradation of long-chain hydrocarbons, cellulose, hemicellulose, and part of lignin, which is decomposed during pyrolysis into smaller and lighter molecules, such as tars, oils, phenols, and waxes [17]. It has a distinctive smoky smell due to the presence of low-molecular-weight aldehydes and acids. The bio-oil from orange peel contains valuable compounds such as phenols, benzenes, toluene, p-xylene, styrene, carboxylic acid, and d-limonene (its main component) [21]. D-limonene can be used in the food and pharmaceutical industries. As for bio-oils from the pyrolysis of orange pruning, no data is available in the literature.

Non-condensable gases (syngas) are a mixture of basic components such as carbon monoxide (CO) and hydrogen (H₂). Their higher heating value has been reported to be 4.37–5.68 MJ/m³ [21]. Both bio-oil and syngas have the heating potential to be used as a cogeneration energy source in biomass waste pyrolysis plants.

Biochar is a non-volatile solid waste rich in carbon, composed of the remaining biomass that is not hydrocarbons, mainly parts of lignin, oxides (usually metallic), and heavy metals, depending on the composition of the raw material. It is used as fuel (briquettes) [22], as an alternative adsorbent to remove different types of contaminants, including heavy metals, nutrients, and pharmaceuticals from aqueous solution [23], as an amendment to improve soil fertility, as a raw material for the preparation of activated carbon [24] and, mainly, as a biocatalyst. For example, biochars from different raw materials were used to catalyse the esterification reaction of free fatty acids with methanol [25–27] or with glycerol [28], and the esterification of glycerol with acetic acid or acetic anhydride [29], all of them within the biodiesel production framework.

The sulphur content in fuels is of major importance due to the formation of sulphur oxides during fuel combustion in engines, which in turn react with water steam to produce sulphuric acid. Regarding biodiesel, its maximum sulphur content as established by the EN14214 standard is 10 mg·kg⁻¹. This is of great importance for companies dealing with the recycling of waste cooking oils (WCO). Thus, the sale price of the WCO of these companies to biodiesel industries depends on the sulphur content [30]. Sulphur removal in vegetable

oils and WCO has been studied mainly in relation to the subsequent biodiesel production, considering the above-mentioned environmental problems associated with SO_x emissions and the corrosion in the engines [30]. The most widely used treatments for sulphur removal are adsorption, solvent extraction, precipitation, and oxidation reaction [31]. As previously stated, biochars can act as adsorbent. Hence, they could be used for the removal of sulphur in WCO. To the best of our knowledge, this possibility has not been explored yet. Based on all the aforementioned considerations, the objectives of this work were the following:

- (1) Valorising orange tree pruning and sweet orange waste (currently used for the production of boiler pellets and cattle feed, respectively) through the production of biochar and bio-oil by slow pyrolysis.
- (2) Characterise the biochars and bio-oils obtained.
- (3) Apply the biochars obtained for the removal of sulphur from waste cooking oils.

2. Materials and Methods

2.1. Raw Materials

The company Export Orange S.L. (Salteras, Spain) provided orange tree pruning (OP) and sweet oranges (SO), while Grupo BIOSEL S.L. (Aznalcóllar, Spain) supplied the waste cooking oil (WCO) used throughout this research.

2.2. Pretreatment of Sweet Oranges

SO were weighted, superficially washed with distilled water, dried, and ground in a Thermomix TM 21 (Vorwerk, Wuppertal, Germany) to obtain 1 × 1 cm section. Subsequently, the juice was separated from the peel and the pulp by sieving. Afterward, the mixture of peel and pulp (orange waste, OW) was dried at 45 °C in a laboratory oven. Most of the moisture (80% wt.) of the OW was removed. The OW was then weighed, ground in a ball mill at 500 rpm for 20 min, and passed through a sieve to achieve a particle size of less than 1 mm. Finally, the OW was dried in the oven at 45 °C.

2.3. Pretreatment of Orange Pruning

First, the leaves were separated from the branches, and then the latter (OP) were chopped and introduced in an oven at 45 °C. Subsequently, the OP was milled in a ball mill at 500 rpm for 20 min to achieve a particle size of less than 1 mm and introduced again in the oven at 45 °C until constant weight.

2.4. Pyrolysis

OW and OP were subjected to thermal treatment under an inert atmosphere (Ar). Pyrolysis was carried out in a vertical tubular pyrolytic furnace (16 cm height, 3.5 cm diameter). The reactor was a quartz tube with a porous plate and a ground nozzle, into which 9 g of OW or 4.33 g of OP, respectively, were introduced (Figure 1).

The heating ramp was programmed using a CN300-P temperature regulator (Conatec, Irún, Spain), connected to the oven through a thermocouple. A heating wire was placed around the bottom of the quartz tube (supported by aluminum foil) to prevent condensation of the liquid in the tube, which was intended to occur in the round bottom flask (Figure 1). Two ethanol traps were used to remove pollutants from syngas. A rotameter was used to control the flow rate of the inert gas (Ar) through the pyrolysis reactor.

The operational variables to study were the flow rate of the inert gas (30, 150, and 300 mL Ar·min⁻¹), the maximum pyrolysis temperature (400 and 600 °C) and the heating ramp (5, 10 and 20 °C·min⁻¹), maintaining the maximum temperature for 2 h. Subsequently, the system was cooled to room temperature. These conditions were selected based on previous work on citrus pyrolysis available in the literature [15,20,32–34]. Each experiment was carried out in duplicate. The experimental set of pyrolysis carried out is illustrated in Table 1.

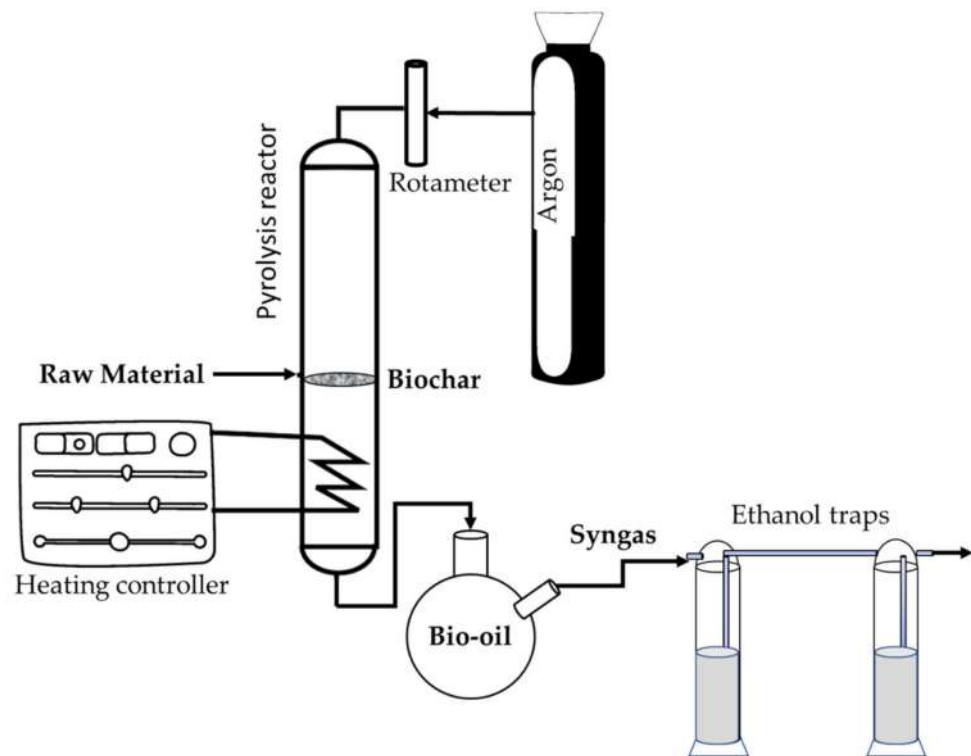


Figure 1. Pyrolysis equipment.

Table 1. Pyrolysis conditions for orange pruning (OP) and orange waste (OW).

Raw Material	Initial Mass (g)	T (°C)	H _{ramp} (°C·min ⁻¹)	Ar Flow Rate (mL·min ⁻¹)
OW	9.00	400	5	150
OW	9.00	400	10	150
OW	9.00	600	10	30
OW	9.00	600	10	150
OW	9.00	600	10	300
OP	4.33	400	5	150
OP	4.33	400	10	150
OP	4.33	600	10	30
OP	4.33	600	10	150
OP	4.33	600	10	300
OP	4.33	600	20	150

H_{ramp}: heating ramp.

2.5. Adsorption of Sulphur in Oils by the Produced Biochars

The study of the sulphur adsorption by the biochars was carried out in a 250 mL stirred batch reactor, in which 50 mL WCO were introduced along with 5 g biochar (10% *w/v*). The temperature, stirring and residence time were set to 50 °C, 700 rpm and 120 min, respectively. All the experiences were carried out in duplicate. Subsequently, the biochar was removed from the WCO by filtration, and the sulphur content in the oil was analysed.

2.6. Products Characterisation

2.6.1. Thermogravimetric Analysis

Thermogravimetric analysis was used to determine the lignin, hemicellulose, and cellulose content of the samples and to obtain information on the optimal carbonisation temperature. To perform the analysis, an SDT Q600 electrobalance (TA Instruments, Inc., New Castle, DE, USA) with a sensitivity of $\pm 0.5 \mu\text{g}$ was used. The sample heating system consisted of a vertical furnace capable of reaching a maximum temperature of 1200 °C.

The samples were first heated under an Ar atmosphere to decompose the organic matter, leaving only inorganic ash. The analyses were carried out at a $10\text{ }^{\circ}\text{C}\cdot\text{min}^{-1}$ constant heating ramp until reaching $800\text{ }^{\circ}\text{C}$ under a flow rate of $100\text{ mL Ar}\cdot\text{min}^{-1}$ until constant weight.

2.6.2. Fourier-Transform Infrared Spectroscopy (FTIR)

A Nicolet iS5 FTIR spectrometer (Thermo Fisher Scientific, Waltham, MA, USA) was used to characterise the raw materials as well as the biochars obtained before and after the desulphurisation of WCO. The powder compaction was carried out on a uniaxial press applying a pressure of $10\text{ t}\cdot\text{cm}^{-2}$. For transmission measurements, 13 mm capsules were prepared using potassium bromide (KBr) as diluent, 5% wt. being the final sample concentration. Spectra were recorded in the $500\text{--}4000\text{ cm}^{-1}$ range.

2.6.3. Biochar Texture Characterisation

The BET method was used to calculate the specific surface area (SBET). A Gemini V-2365 adsorption equipment (Micromeritics Instrument Corporation, Norcross, GA, USA) was used. The biochars were previously degassed at $170\text{ }^{\circ}\text{C}$ for 2 h under N_2 atmosphere.

2.6.4. Gas Chromatography–Mass Spectrometry

A qualitative analysis of the bio-oil composition from pyrolysis was performed with a TSQ8000 mass spectrometer (Thermo Fisher Scientific, Waltham, MA, USA) coupled to a triple quadrupole gas chromatograph (GC-MS), equipped with an autosampler. A Zebron ZB-5MS column ($30\text{ m} \times 0.25\text{ mm} \times 0.25\text{ }\mu\text{m}$; 5% phenyl-arylene, 95% dimethylpolysiloxane) and N_2 as carrier gas were used. Analyses were carried out under the following conditions: $50\text{ }^{\circ}\text{C}$ initial temperature, $7\text{ }^{\circ}\text{C}\cdot\text{min}^{-1}$ heating ramp for 30 min, and final temperature of $310\text{ }^{\circ}\text{C}$.

The identification of the peaks was performed using the database of the Quan Browser tool of the XCalibur software (Thermo Fisher Scientific, Waltham, MA, USA). To limit the compounds, several factors were taken into account: that the area of the compound had a value greater than 1, that the probability of the compound was greater than 40%, and that the compound were present in a greater number of samples. The area of each compound was calculated using the internal standard method.

2.6.5. Determination of Sulphur in Oils

The WCO samples were subjected to acid digestion in a microwave digestion system (UltraWAVE, Milestone Inc., Santa Clara, CA, USA). Briefly, 0.25 g WCO were weighted and digested in 25 mL closed glass beakers at $200\text{ }^{\circ}\text{C}$ with 4 mL HNO_3 and 1 mL H_2O_2 , to finally making up to a volume of 25 mL with distilled water. After digestion, the sulphur content in the samples was determined using a Spectroblue TI (Spectro Analytical Instruments GmbH, Kleve, Germany) inductively coupled plasma-optical emission spectrometer.

3. Results and Discussion

3.1. Characterisation of the Raw Material

Thermogravimetric Analysis (TGA)

Three stages of mass loss were observed in the TGA of orange pruning (Figure 2A). The first stage was related to moisture removal, which could be divided in turn into two stages: one until $92\text{ }^{\circ}\text{C}$ (4 wt.%) and the other until $120\text{ }^{\circ}\text{C}$, suggesting the presence of at least two types of water bonding in the samples. The latter (8% mass loss) was related to adsorbed water molecules, weakly linked by hydrogen bonds. The second stage of mass loss, which ranges from 130 to $210\text{ }^{\circ}\text{C}$ and reached a mass loss of 41%, is the active zone, generally related to the degradation of hemicellulose and cellulose polymers [35]. The third stage of mass loss, from 210 to $600\text{ }^{\circ}\text{C}$, is the passive zone, attributed to lignin decomposition, with the highest mass loss occurring between 210 and $300\text{ }^{\circ}\text{C}$.

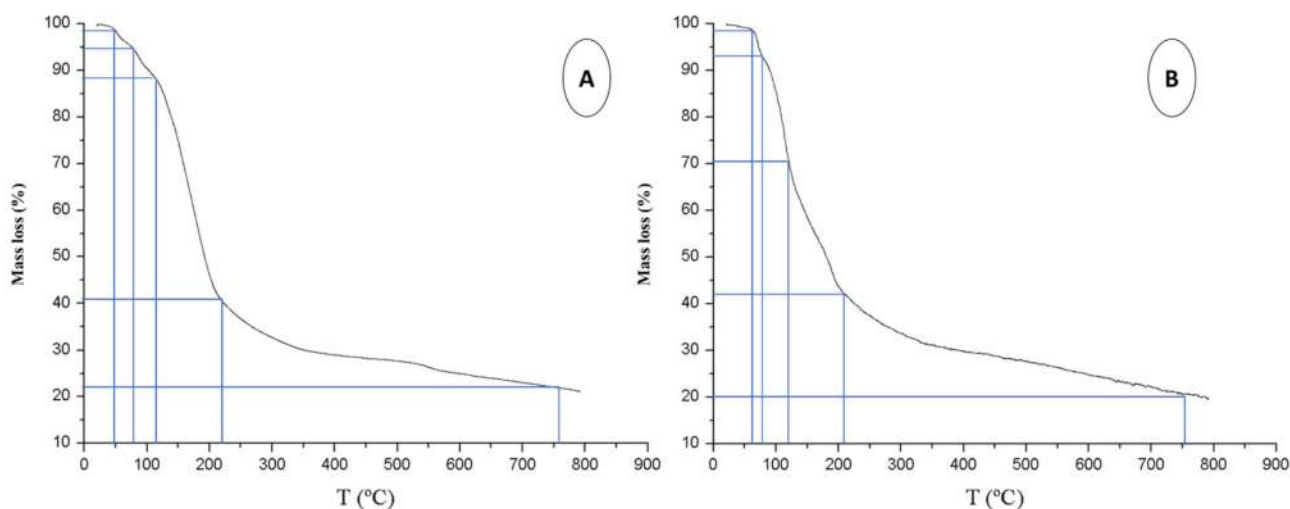


Figure 2. Thermogravimetric curve obtained in the pyrolysis of orange tree pruning (A) and orange waste (B).

Assuming the data depicted in Figure 2A, the lignin content could account for 20 wt.%, taking into account the large limitations of TGA for quantitative analysis. Beyond this stage, the mass loss up to 800 °C can be attributed to the total degradation of the biomass. The non-degraded remaining mass at 800 °C could correspond to inorganic salts.

Similarly to what occurred for OP, mass loss up to roughly 100 °C in the TGA of orange waste was associated with moisture removal. Again, a slope close to 73 °C and another close to 114 °C were observed, corresponding to physically absorbed and adsorbed water molecules, respectively (Figure 2B). There was also another mass loss due to pectin water ranging from 87 to 165 °C, which corresponds to a mass loss of 36% [36]. Therefore, the sample had approximately 45 wt.% moisture.

Cellulose and hemicellulose polymers degraded between 165 and 205 °C for OW and showed a maximum degradation rate at 188 °C, as observed in Figure 2B. In the literature, studies carried out on sweet oranges and under the same conditions assume that cellulose and hemicellulose begin their degradation together, presenting a maximum degradation rate at 213 °C. This trend was also noted in the study of the pyrolysis of six species of tropical hardwoods under an N₂ atmosphere [37].

According to the literature, cellulose degrades between 315 and 400 °C [36], and hemicellulose begins its degradation at a slightly lower temperature (220–315 °C), due to the more disordered nature of the polymer [38]. From the thermogravimetric curve (Figure 2B), it could be assumed that the degradation of cellulose and hemicellulose began at 165 °C and ended at 205 °C, corresponding to a loss of mass of 14%. Pectin degradation showed several continuous and prolonged weight losses at various temperatures (226, 305, 394, and 475 °C) [34]. In this case, pectin would degrade between approximately 205 and 400 °C, leading to various weight losses (overlapping peaks). This range would correspond to a loss of mass of 12 wt.%, according to the literature [35].

In Figure 2B, the lignin degradation process began at room temperature and gradually degrades up to 800 °C [36], a temperature at which 80 wt.% decomposition of the initial mass was reached. It would correspond to a lignin content of roughly 5% wt. At 800 °C, 20 wt.% raw material would remain undegraded, which corresponds to carbon residues and metallic compounds. The ash content was 3 wt.%, a value that agrees with the data available in literature [7].

In summary, the greatest weight loss occurred up to 400 °C (Figure 2A,B), which indicates that the samples are mainly made up of water, cellulose, and hemicellulose, while 72–78% degradation of the initial mass was achieved at 600 °C, which coincides with what is reported in the literature [38].

3.2. Product Distribution after Pyrolysis

The bio-oils and biochars obtained were weighed to obtain their percentages after pyrolysis (Table 2). The biochars obtained were stored in individual containers. Subsequently, the BET specific surface area (S_{BET}) of each biochar was measured, and the FTIR spectra were acquired. The bio-oils were analysed by GC-MS.

Table 2. Material balance of the performed pyrolyses.

Raw Material	T (°C)	H _{ramp} (°C·min ⁻¹)	Ar Flow Rate (mL·min ⁻¹)	Biochar (% wt.)	Bio-Oil (% wt.)	Syngas (% wt.)	S _{BET} (m ² /g)
OW	400	5	150	37.7	57.8	4.6	≤1
OW	400	10	150	34.3	56.7	7.9	≤1
OW	600	10	30	32.1	56.6	11.2	≤1
OW	600	10	150	31.3	58.9	9.8	≤1
OW	600	10	300	30.9	62.2	6.9	≤1
OP	400	5	150	35.1	58.2	6.7	2.8
OP	400	10	150	35.3	57.3	7.4	5.4
OP	600	10	30	24.7	67.2	8.1	24.3
OP	600	10	150	27.9	65.6	6.5	9.6
OP	600	10	300	29.1	57.5	13.4	12.0
OP	600	20	150	28.2	55.2	16.6	10.4

OW: orange waste; OP: orange pruning; H_{ramp}: heating ramp; S_{BET}: BET-specific surface.

The trends reported by other authors can be observed in Table 2 for OW biochars [15,39]. At 400 °C, moving from different heating ramps (5 and 10 °C·min⁻¹), there is a decrease in the percentages obtained of biochar and bio-oil, as well as an increase in syngas with the increase in the ramp. In contrast, at 400 °C and different heating ramps (5 and 10 °C·min⁻¹), the percentages remain stable for the OP biochar samples.

For OW biochars, at different pyrolysis temperatures (400 and 600 °C), there is a decrease in biochar percentages and an increase in biogas when the temperature is higher (Table 2). No significant differences were observed in the bio-oil percentages. Furthermore, for OP biochars, at 600 °C, there was a higher bio-oil proportion and less biochar than those produced at 400 °C. In general, the percentage of biochar decreases and those of the fluids increase as the temperature increases. This trend is in agreement with the available literature using orange peel [40] or coffee silverskin [41].

When increasing the flow rate of the inert gas (30, 150, and 300 mL Ar·min⁻¹), a decrease in the percentages of biochar and syngas (and therefore an increase in bio-oil) is observed for OW, as Charusiri et al., pointed out in the pyrolysis of sugarcane leaves [40]. On the contrary, as Ar flow increases in OP pyrolysis at 600 °C and 10 °C·min⁻¹, the percentages of syngas and biochar also increase, thus decreasing the bio-oil fraction.

Finally, for OP pyrolysis at 600 °C with the same Ar flow (150 mL·min⁻¹), as the heating ramp increases, the percentage of biochar does not change, bio-oil decreases, and syngas increases. A low heating ramp implies an enhanced heat transfer [41]; this could be the reason why the percentage of bio-oil decreases as the heating ramp increases, because the degradation of the raw material is lower.

3.3. Characterisation of Biochars

3.3.1. Temperature Influence

In order to assess the effect of temperature, the FTIR spectra of the raw materials were compared with those of the biochars obtained from OW and OP at different maximum pyrolysis temperatures, one at 400 °C and the other at 600 °C, keeping in both cases the rest of the conditions constant (Figure 3).

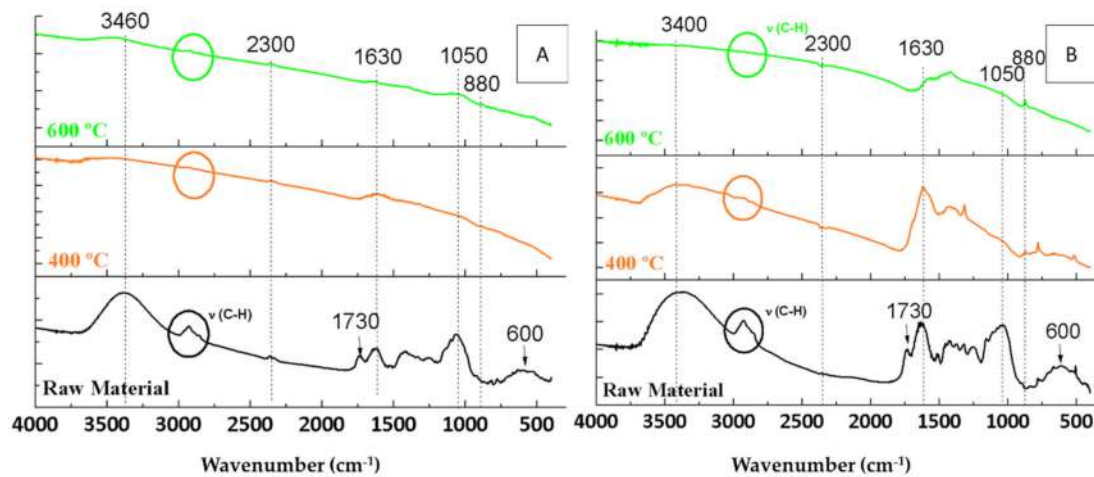


Figure 3. FTIR spectra of the raw materials and the biochars resulting from the pyrolyses under $150 \text{ mL Ar}\cdot\text{min}^{-1}$ flow rate and $10 \text{ }^\circ\text{C}\cdot\text{min}^{-1}$ heating ramp for 2 h of orange waste (A) and orange pruning (B) at different temperatures.

Regarding the OW biochars, it was observed that thermal treatment led to a decrease in the intensity of the FTIR bands present in the raw material. Bands associated with the presence of water adsorbed on the surface (a wide band around 3400 cm^{-1} and a band at 1630 cm^{-1}) decreased considerably in OW biochars (Figure 3A). These bands shifted slightly towards higher wavenumbers after pyrolysis. For example, the water band observed at 3380 cm^{-1} for OW could be found at 3640 cm^{-1} in its biochars (indicated by an arrow in Figure 3A).

In addition to water, it was observed that the C-H vibration bands in the C-H vibrations region (2900 cm^{-1}) [24] were more intense for the highest pyrolysis temperature ($600 \text{ }^\circ\text{C}$), which could indicate that a hydrocarbon skeleton may be formed at this temperature. The band at 2300 cm^{-1} corresponds to the asymmetric tension vibration of the CO_2 molecule. Although its intensity was low in the raw material, it decreased with an increase in the pyrolysis temperature.

Furthermore, with respect to OP biochars (Figure 3B), the bands related to water (3400 and 1630 cm^{-1}) at $400 \text{ }^\circ\text{C}$ had a smaller decrease in intensity, while at $600 \text{ }^\circ\text{C}$, they completely disappeared. In addition to water, the band in the C-H vibrations region (2900 cm^{-1}) [24] was more intense for the lowest pyrolysis temperature, which could indicate that a hydrocarbon skeleton may be formed at this temperature. The band at 2300 cm^{-1} (CO_2) remained almost constant. Finally, for both OP and OW biochars, the band attributed to C=O bonds (for example of lactones) at 1730 cm^{-1} disappeared completely after pyrolysis, as did the band that corresponds to calcium compounds (600 cm^{-1}), due to their decomposition with increasing temperature [34]. Finally, the intensity of the band at 880 cm^{-1} , corresponding to aromatic compounds [35], increased with increasing temperature.

3.3.2. Influence of the Inert Gas Flow Rate

To evaluate the influence of flow, the FTIR spectra of the raw materials were compared with those of the biochars obtained from OW and OP at different flow rates, namely 30 , 150 , and $300 \text{ mL Ar}\cdot\text{min}^{-1}$, maintaining constant the rest of the pyrolysis conditions (Figure 4).

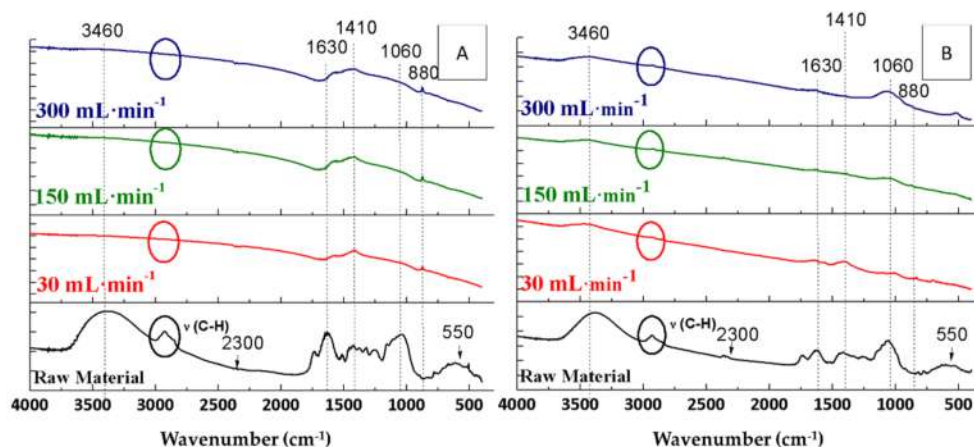


Figure 4. FTIR spectra of the raw materials and the biochars resulting from pyrolyses of orange waste (A) and orange pruning (B) carried out at 600 °C for 2 h with a heating ramp of 10 °C·min⁻¹ using different Ar flow rates.

Regarding orange waste, the water bands (3460 and 1630 cm⁻¹) of the resulting biochars had the same intensity under the three assayed conditions (Figure 4A). It was remarkable that the bands in the region of the C-H vibrations (at 2900 cm⁻¹) [24] were only found at higher flow rates, whereas the band at 2300 cm⁻¹ (CO₂) did not depend on the flow rate. The intensity of the band at 1410 cm⁻¹ (carboxylic acid band) [42] was inversely proportional to the flow rate. Therefore, the highest intensity was observed in the experience carried out under 30 mL Ar·min⁻¹ flow rate (Figure 4A). In contrast, of note is that the intensity of the 1060 cm⁻¹ band (C-O bond) was directly proportional to the flow rate, corresponding to the band that appeared with the highest intensity in the biochar pyrolysed under 300 mL Ar·min⁻¹. The band at 880 cm⁻¹, corresponding to aromatic compounds [37], did not appear in the OW biochars. Finally, the band related to calcium was observed at 550 cm⁻¹ [43], which only appeared in OW biochars when working under 300 mL Ar·min⁻¹.

On the other hand, with respect to the OP biochars, the band at 3460 cm⁻¹ was barely noticeable, while there was a small band at 1630 cm⁻¹. The band at 2900 cm⁻¹ disappeared completely. Similarly to OW biochars, the band at 2300 cm⁻¹ (CO₂) was not related to the assayed flow rate during the pyrolysis process. The band at 1730 cm⁻¹ completely disappeared from the OP after pyrolysis. The band at 1410 cm⁻¹ was also inversely proportional to the flow rate. However, there were no differences in the band at 1060 cm⁻¹ in the FTIR spectra of the three biochars. Finally, the band at 880 cm⁻¹, which appeared after pyrolysis, could be seen in the FTIR spectra of OP biochars, while the band at 550 cm⁻¹ did not appear.

3.3.3. Influence of the Heating Ramp

To study the influence of the heating ramp, the FTIR spectra of the raw materials were compared with those of the OW and OP biochars (Figures 5 and 6) obtained at different heating ramps, to be specific, 5, 10, and 20 °C·min⁻¹, keeping the rest of the conditions constant.

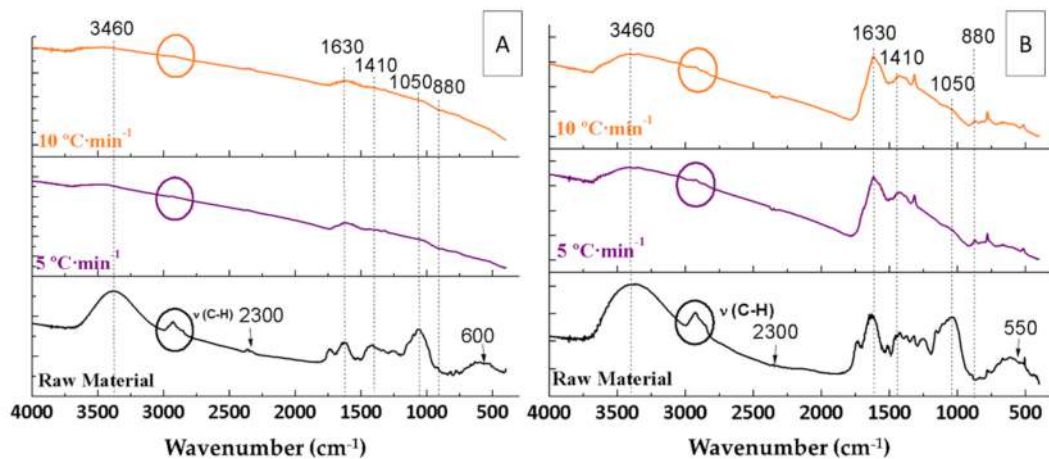


Figure 5. IR spectra of the raw materials and the biochars resulting from the pyrolyses of orange waste (A) and orange pruning (B) performed at 400 °C for 2 h under 150 mL Ar·min⁻¹ flow rate using different heating ramps.

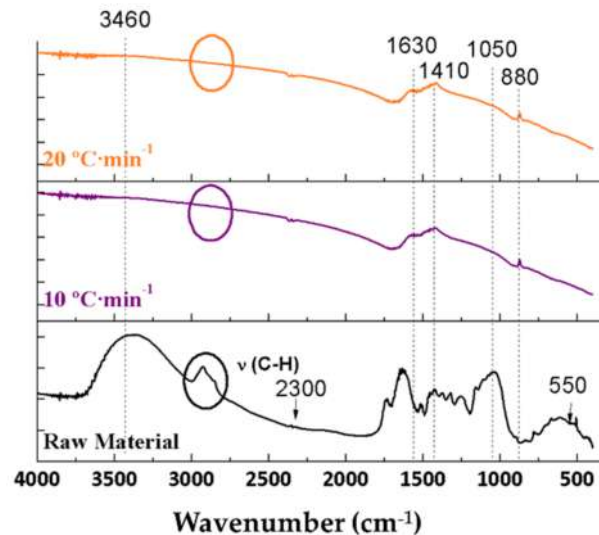


Figure 6. FTIR spectra of the raw material and the biochars resulting from the pyrolyses of orange pruning performed at 600 °C for 2 h under 150 mL Ar·min⁻¹ flow rate using different heating ramps.

All bands marked in Figures 5 and 6 and described in Sections 3.3.1 and 3.3.2 were not affected by varying the flow rate. These bands included the bands at 3460 and 1630 cm⁻¹ (water), at 2900 cm⁻¹ (C-H), at 2300 cm⁻¹ (CO₂), at 1730 cm⁻¹ (C=O), at 1410 cm⁻¹ (carboxylic acid), at 1060 cm⁻¹ (C-O), at 880 cm⁻¹ (aromatic), and at 550 cm⁻¹ (Ca).

From the results, it can be concluded that the heating ramp and Ar flow rate do not influence the surface compounds, as they are solely influenced by the pyrolysis temperature.

Table 3 summarises the general vibration characteristics and wavenumbers of the compounds present in the FTIR spectra of the raw materials and the resulting biochars, comparing them to the literature [35].

Table 3. Main vibrations of the compounds present in the FTIR spectra of raw materials and biochars.

Group	Vibration	Experimental (cm ⁻¹)	Literature (cm ⁻¹)	Reference
Carboxylic acid and water	ν (O-H)	3600–3100, 1630	3600–3000, 1632	[35]
Alkyl, aliphatic, and aromatic	ν (C-H)	2925, 2860, 1400	2970–2860, 1402	[35]
Ketone and carbonyl	ν (C=O)	1730–1713, 1560	1730–1700, 1560–1510	[35]
Carboxylic acid	ν (O-H)	1410	1440–1400	[42]
Ether	ν (C-O)	1064–1000	1300–1000	[42]
Aromatic hydrogens	ν (C-H)	880–800	700–900	[44]
Calcium	ν (Ca-O)	550–600	550–600	[43]

3.4. Bio-Oil Characterisation

The bio-oils obtained were characterised using a gas chromatograph coupled to a mass spectrometer in order to perform a tentative qualitative analysis of the major compounds present in the resulting bio-oils under different pyrolysis conditions.

3.4.1. Temperature Influence

To assess the effect of temperature, the chromatograms of the bio-oils obtained from OW and OP at different pyrolysis temperatures, namely 400 and 600 °C, were compared (Tables 4 and 5, respectively), keeping constant in both cases the rest of the conditions (150 mL Ar·min⁻¹, 10 °C·min⁻¹, 2 h).

Table 4. Compounds detected in bio-oils chromatograms and their relative area percentages obtained in the pyrolysis of orange waste at different temperatures.

Compound	Pyrolysis Temperature (°C)	
	600	400
	Area (%)	
Propanoic acid	2.97	3.84
Toluene	24.63	29.43
2,4-Dimethyl-2-oxazoline-4-methanol	8.57	4.88
Furfural	2.98	8.09
2-Pentanone, 4-hydroxy-4-methyl-	3.08	5.94
2-Furanmethanol	3.17	2.70
2,5-Furandione, dihydro-3-methylene-	1.63	-
2-Furancarboxaldehyde, 5-methyl-	4.07	6.19
Phenol	3.00	2.41
Maltol	1.66	1.31
Pyranone	2.31	2.83
5-Hydroxymethylfurfural	23.01	32.37
4-Hydroxy-3-methylbenzoic acid, methyl ester	5.80	-
1-Methyl-8-propyl-3,6-diazahomoadamantan-9-ol	2.53	-
9-Octadecenamide, (Z)-	2.92	-
Hexadecanoic acid, 2-hydroxy-ethyl ester	5.18	-
Octadecanoic acid, 2,3-dihydroxypropyl ester	2.50	-

Table 4 shows the values of the areas and the main compounds in the chromatograms of bio-oils obtained in the pyrolysis of OW at 400 and 600 °C. Both bio-oils presented toluene and 5-hydroxymethylfurfural (HMF) as the components of the highest intensity and area, these areas being higher at the lowest temperature (400 °C).

In the experience at 600 °C, the third major compound was 2,4-dimethyl-2-oxazoline-4-methanol. However, in the experience at 400 °C, the same compound had a much smaller area. Finally, furfural was identified, the concentration of which was higher in bio-oil obtained at 400 °C.

Table 5. Compounds detected in bio-oils chromatograms and their relative area percentages obtained in the pyrolysis of orange pruning at different temperatures.

Compound	Pyrolysis Temperature (°C)	
	600	400
	Area (%)	
Toluene	2.15	2.6
3-Penten-2-one, 4-methyl-	1.85	-
2-Pentanone, 4-hydroxy-4-methyl-	94.73	92.62
2-Furanmethanol	-	1.29
Phenol, 2-methoxy-	-	1.24
Phenol, 2,6-dimethoxy-	1.27	2.25

Table 5 shows the values of the areas and the main compounds in the chromatograms of bio-oils obtained in the pyrolysis of OP at 400 and 600 °C. The main compounds detected were 4-hydroxy-4-methyl-2-pentanone and toluene. Although the area of the first was higher at 600 °C, the area of the second was higher in the bio-oil obtained at 400 °C. However, the differences between the two experiences were very small.

Furthermore, the differences between the compounds obtained from each raw material were great (Tables 4 and 5). The main compound found in OP bio-oils was 4-hydroxy-4-methyl-2-pentanone, while the main compounds in OW bio-oils were toluene and furfural-related compounds.

3.4.2. Influence of Argon Flow Rate

In order to evaluate the influence of the atmosphere under which pyrolysis was performed, the GS-MS chromatograms of the bio-oils obtained from OW (Table 6) and OP (Table 7) using different inert gas flow rates (30, 150, and 300 mL Ar·min⁻¹) during the pyrolysis process have been compared, keeping the rest of the conditions (600 °C, 10 °C·min⁻¹, 2 h) constant in all three cases.

Table 6. Compounds detected in orange waste bio-oils chromatograms and their relative area percentages using different argon flow rates during the pyrolysis.

Compound	Argon Flow Rate (mL·min ⁻¹)		
	300	150	30
	Area (%)		
Propanoic acid	2.97	2.97	-
Pyrrolidine, 1-methyl-	-	-	6.12
Toluene	28.47	24.63	29.43
2,4-Dimethyl-2-oxazoline-4-methanol	6.70	8.57	5.23
Pyridine, 3-methyl-	-	-	6.29
Furfural	8.06	2.98	-
2-Pentanone, 4-hydroxy-4-methyl-	6.70	3.08	9.55
2-Furanmethanol	2.54	3.17	5.05
2,5-Furandione, dihydro-3-methylene-	-	1.63	1.78
2-Furancarboxaldehyde, 5-methyl-	5.34	4.07	-
Phenol	1.98	3.00	4.09
1,2-Cyclopentanedione, 3-methyl-	-	-	1.85
Maltol	-	1.66	2.30
Pyranone	3.51	2.30	3.86
5-Hydroxymethylfurfural	25.89	23.01	4.61
Hydroquinone	-	-	4.61
4-Hydroxy-3-methylbenzoic acid, methyl ester	-	5.80	3.34
1-Methyl-8-propyl-3,6-diazahomoadamantan-9-ol	-	2.53	2.89

Table 6. Cont.

Compound	Argon Flow Rate (mL·min ⁻¹)		
	300	150	30
	Area (%)		
9-Octadecenamide, (Z)-	-	2.92	-
Hexadecanoic acid, 2-hydroxy-ethyl ester	6.27	5.18	7.33
Octadecanoic acid, 2,3-dihydroxypropyl ester	1.57	2.50	3.25

Table 7. Compounds detected in orange pruning bio-oils chromatograms and their relative area percentages using different argon flow rates during the pyrolysis.

Compound	Argon Flow Rate (mL·min ⁻¹)		
	300	150	30
	Area (%)		
Pyrrolidine, 1-methyl-	1.61	-	6.91
Toluene	2.72	2.15	31.42
2,4-Dimethyl-2-oxazoline-4-methanol	-	-	5.90
3-Penten-2-one, 4-methyl-	-	1.85	-
Pyridine, 3-methyl-	-	-	3.39
2-Pentanone, 4-hydroxy-4-methyl-	89.03	94.73	10.77
2-Furanmethanol	1.46	-	5.70
2,5-Furandione, dihydro-3-methylene-	-	-	2.01
Phenol	-	-	4.62
Phenol, 2-methoxy-	1.89	-	-
Maltol	-	-	2.59
Pyranone	-	-	4.35
5-Hydroxymethylfurfural	-	-	5.20
Hydroquinone	-	-	5.20
Phenol, 2,6-dimethoxy-	1.89	-	-
Hexadecanoic acid, 2-hydroxy-ethyl ester	-	-	8.27
Octadecanoic acid, 2,3-dihydroxypropyl ester	-	-	3.67

Chromatograms using 150 and 300 mL Ar·min⁻¹ showed toluene and HMF as the components of the greatest intensity and area (Table 6). Regarding the experience carried out using 30 mL Ar·min⁻¹, although the main peak also corresponded to toluene, HMF had a much smaller area and intensity. A greater number of compounds also appeared, probably because, when pyrolysis was performed at such a low Ar flow rate, a 100% inert atmosphere was not ensured. As a result, some ambient oxygen could enter the vertical tubular pyrolytic furnace, leading to the oxidation of compounds. This explanation is coherent, since, as observed in Table 6, the compounds from the experience under 30 mL Ar·min⁻¹ have more oxygen in their molecular formula. Finally, furfural was found using 300 and 150 mL Ar·min⁻¹, with relative areas of 8.06% and 2.98%, respectively.

With regard to the bio-oils obtained from the pyrolysis of OP (Table 7), those resulting from pyrolysis using 300 mL and 150 mL Ar·min⁻¹ contained 4-hydroxy-4-methyl-2-pentanone as the main component. However, the bio-oil produced using 30 mL Ar·min⁻¹ had a wider range of compounds, in which toluene and 4-hydroxy-4-methyl-2-pentanone were the main components, the latter at a much lower concentration than in the pyrolyses using 300 mL and 150 mL Ar·min⁻¹.

Furthermore, the differences between the two raw materials were large. Orange waste produced a bio-oil with a wider range of components, while orange pruning produced a bio-oil with mainly one component: 4-hydroxy-4-methyl-2-pentanone.

3.4.3. Influence of the Heating Ramp

In order to study the influence of the heating ramp on the bio-oils obtained from OW (Table 8) and OP (Table 9) pyrolysis, the chromatograms obtained using the different heating ramps (5, 10, and 20 °C·min⁻¹) were compared, keeping the rest of the conditions constant (150 mL Ar·min⁻¹; 400 °C, 2 h).

Table 8. Compounds detected in orange waste bio-oils chromatograms and their relative area percentages using different heating ramps in the pyrolysis.

Compound	Heating Ramp (°C·min ⁻¹)	
	10	5
Area (%)		
Propanoic acid	3.84	2.69
Toluene	29.43	14.85
2,4-Dimethyl-2-oxazoline-4-methanol	4.88	1.37
Furfural	8.09	8.23
2-Pentanone, 4-hydroxy-4-methyl-	5.94	13.02
2-Furanmethanol	2.71	2.04
2-Furancarboxaldehyde, 5-methyl-	6.19	6.49
Phenol	2.41	2.76
Maltol	1.31	2.37
Pyranone	2.83	9.02
5-Hydroxymethylfurfural	32.37	37.16

Table 9. Compounds detected in orange pruning bio-oils chromatograms and their relative area percentages using different heating ramps in the pyrolysis.

Compound	Heating Ramp (°C·min ⁻¹)		
	20	10	5
Area (%)			
Pyrrolidine, 1-methyl-	-	-	1.82
Propanoic acid	1.68	-	-
Toluene	2.45	2.60	2.78
2-Pentanone, 4-hydroxy-4-methyl-	60.44	92.62	89.9
2-Furanmethanol	2.18	1.29	1.28
Phenol	3.63	-	-
1,2-Cyclopentanedione, 3-methyl-	3.76	-	-
Phenol, 2-methoxy-	3.81	1.24	1.56
Catechol	5.76	-	-
1,2-Benzenediol, 3-methoxy-	3.12	-	-
Phenol, 2,6-dimethoxy-	7.32	2.25	2.76
Hexadecanoic acid, 2-hydroxy-ethyl ester	2.27	-	-
Octadecanoic acid, 2,3-dihydroxypropyl ester	3.58	-	-

Bio-oils obtained from OW pyrolysis using 5 and 10 °C·min⁻¹ presented as components of the highest intensity and area toluene and HMF (Table 8). The area of toluene was approximately double for the experience at 10 °C·min⁻¹, but the relative areas of HMF were quite similar, somewhat higher for that of the bio-oil obtained using 5 °C·min⁻¹ heating ramp.

In the pyrolysis using the 5 °C·min⁻¹ heating ramp, the third major compound found was 4-hydroxy-4-methyl-2-pentanone. In addition, both experiences had the area corresponding to furfural, their relative areas being similar and greater than 8.

It can be concluded that the main compounds present in the bio-oils obtained from OW were, regardless of the pyrolysis conditions tested, toluene and HMF, compounds that usually appear in the bio-oils of fruit residues [20,45,46] and agri-food waste [47]. The literature also corroborates the presence of furfural and phenolic compounds, among

other identified components [46]. The most suitable conditions for obtaining toluene were $10\text{ }^{\circ}\text{C}\cdot\text{min}^{-1}$, $30\text{ mL Ar}\cdot\text{min}^{-1}$, and $400\text{ }^{\circ}\text{C}$, while the conditions for the production of HMF were $5\text{ }^{\circ}\text{C}\cdot\text{min}^{-1}$, $300\text{ mL Ar}\cdot\text{min}^{-1}$, and $400\text{ }^{\circ}\text{C}$.

5-Hydroxymethylfurfural has been used in agrochemistry as a fungicide, in galvanochemistry as a corrosion inhibitor, in the cosmetic industry, and as a flavour agent [48]. HMF is also a starting material for the synthesis of precursors of various pharmaceuticals, thermo-resistant polymers, and complex macrocycles (2,5-furandicarbaldehyde and 2,5-furandicarboxylic acid) [48]. For this reason, OW bio-oils could be regarded as a valuable source of HMF.

Table 9 shows the main compounds found in bio-oils from orange pruning pyrolysis using different heating ramps, among which 4-hydroxy-4-methyl-2-pentanone stands out. However, its content was reduced by 30% in pyrolysis using a heating ramp of $20\text{ }^{\circ}\text{C}\cdot\text{min}^{-1}$. Furthermore, the composition of the bio-oils obtained using the heating ramps of 10 and $5\text{ }^{\circ}\text{C}\cdot\text{min}^{-1}$ was similar. Other minor compounds such as toluene and 2-furanmethanol had the same area in the three bio-oil chromatograms. In summary, the OP bio-oils were mainly composed of 4-hydroxy-4-methyl-2-pentanone regardless of the pyrolysis conditions assayed. The most suitable conditions for obtaining this compound were $10\text{ }^{\circ}\text{C}\cdot\text{min}^{-1}$ heating ramp, $150\text{ mL Ar}\cdot\text{min}^{-1}$ flow rate, and $600\text{ }^{\circ}\text{C}$ pyrolysis temperature.

4-Hydroxy-4-methyl-2-pentanone is used as an intermediate in the manufacturing of dyes, inhibitors, pharmaceuticals, and insecticides and as a solvent in some industries (to adjust the solubility of paint resins and regulate the evaporation rate). It can also be used for the treatment of textiles and leather, in chemical synthesis, or as a cleaning solvent. Its current market price is 140 € per 2.5 L product (Fisher Scientific S.L., Madrid, Spain). As it can account for up to 94% of OP bio-oils (Tables 5 and 7), its production from orange pruning may be feasible.

3.5. Sulphur Removal Using Biochars from Pyrolysis of Sweet Orange Waste and Orange Pruning

Once the OW and OP biochars were obtained and characterised, the possibility of adsorbing sulphur from waste cooking oils, despite their low specific surface area, was tested. The WCO used contained a sulphur concentration of $36\text{ mg}\cdot\text{kg}^{-1}$, a concentration above the threshold indicated in the EN 14,214 and ASTM D7467 standards.

Tables 10 and 11 show the pyrolysis conditions for the obtaining of OW and OP biochars, respectively, as well as their specific surface areas and desulphurisation yields. It can be seen that the specific surface area of the OW biochars did not influence the removal of sulphur (Table 10). The highest sulphur removal (78.3%) was achieved with the biochar obtained in the pyrolysis at $400\text{ }^{\circ}\text{C}$, $5\text{ }^{\circ}\text{C}\cdot\text{min}^{-1}$, and $150\text{ mL}\cdot\text{min}^{-1}$.

Table 10. Desulphurisation of waste cooking oil with orange waste biochars obtained under different conditions.

T ($^{\circ}\text{C}$)	H _{ramp} ($^{\circ}\text{C}\cdot\text{min}^{-1}$)	Ar Flow ($\text{mL}\cdot\text{min}^{-1}$)	S _{BET} ($\text{m}^2\cdot\text{g}^{-1}$)	Sulphur Removal (%)
400	5	150	≤ 1	78.3 ± 0.01
400	10	150	≤ 1	77.4 ± 0.03
600	10	30	≤ 1	76.3 ± 0.01
600	10	150	≤ 1	75.5 ± 0.03
600	10	300	≤ 1	76.2 ± 0.02

H_{ramp}: heating ramp; S_{BET}: BET-specific surface.

In contrast to OW biochars, the specific surface area of the OP biochars had an influence on the sulphur removal from waste cooking oil (Table 11). Notwithstanding, the performance of both OW and OP biochars was similar, ranging from 66.4% to 78.8%. The highest yield (78.8%) was obtained with the biochar obtained in the pyrolysis at $600\text{ }^{\circ}\text{C}$, $10\text{ }^{\circ}\text{C}\cdot\text{min}^{-1}$, and $150\text{ mL}\cdot\text{min}^{-1}$, which had a specific surface area of $7.52\text{ m}^2\cdot\text{g}^{-1}$. The biochar obtained at $600\text{ }^{\circ}\text{C}$, $10\text{ }^{\circ}\text{C}\cdot\text{min}^{-1}$, and $30\text{ mL Ar}\cdot\text{min}^{-1}$, despite having the largest

surface area ($24.28 \text{ m}^2 \cdot \text{g}^{-1}$), was not the one that adsorbed the most sulphur (66.4%). Thus, there was no direct and clear relationship between the specific surface area of OP biochars and their ability to adsorb sulphur (Figure 7). The literature illustrates that the specific surface area and the pore size are inversely proportional [24]. That is, as the specific surface area increases, the pore size decreases, which could explain the obtained results.

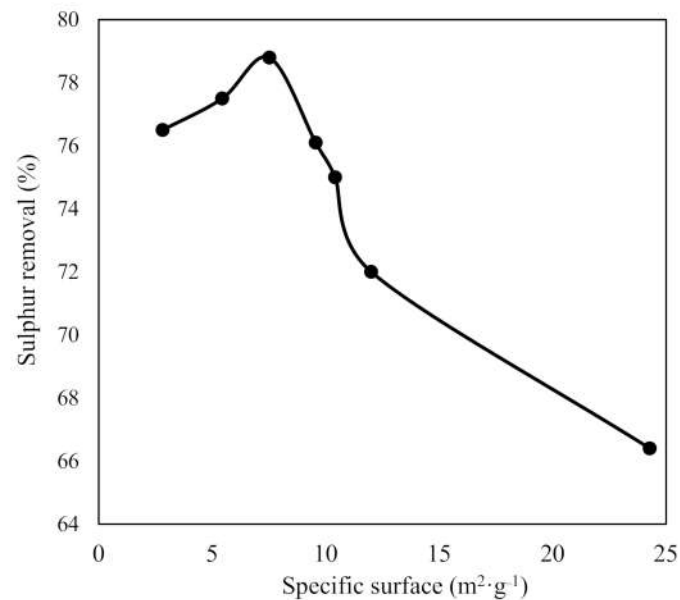


Figure 7. Effect of BET specific surface area of orange pruning biochars on sulphur removal.

Table 11. Desulphurisation of waste cooking oil with orange pruning biochars obtained under different conditions.

T (°C)	H _{ramp} (°C·min ⁻¹)	Ar Flow (mL·min ⁻¹)	S _{BET} (m ² ·g ⁻¹)	Sulphur Removal (%)
400	5	150	2.82	76.5 ± 0.01
400	10	150	5.44	77.5 ± 0.03
600	10	30	24.28	66.4 ± 0.01
600	10	150	7.52	78.8 ± 0.01
600	10	300	12.01	72.0 ± 0.03
600	20	150	10.42	75.0 ± 0.04

H_{ramp}: heating ramp; S_{BET}: BET-specific surface.

A comparison was made between the FTIR spectra of the biochars that led to the highest and lowest yield in sulphur removal to assess changes in the surface compounds (Figure 8). As can be observed, two new bands appeared in the FTIR spectra after the WCO desulphurisation process. The first, at 1127 cm^{-1} , was related to the C=S bond, while the second, at 1200 cm^{-1} , was related to the O=S=O bond [49]. Finally, it should be noted that the intensity of these bands in the FTIR spectra of the biochars that led to the lowest sulphur removal yields (Figure 8B) was less intense than those of the biochars that achieved the highest sulphur removal from WCO (Figure 8A).

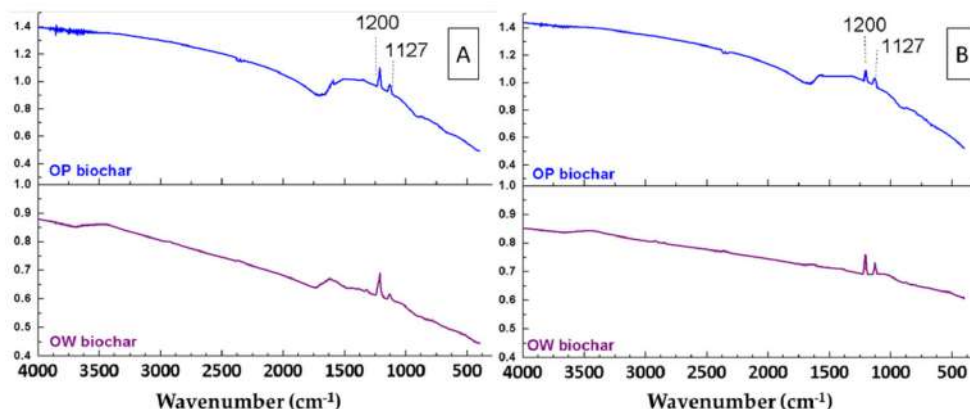


Figure 8. FTIR spectra of orange waste (OW) and orange pruning (OP) biochars after their use for sulphur removal from waste cooking oil. (A) Biochars that achieved the highest sulphur removal. (B) Biochars that achieved the lowest sulphur removal.

After all of these studies, it was clear that the most suitable OW biochar for the desulphurisation of waste cooking oils was obtained at 400 °C, 5 °C·min⁻¹, and 150 mL·min⁻¹. The OP biochar with the highest performance for the desulphurisation of waste cooking oil was obtained at 600 °C, 10 °C·min⁻¹, and 150 mL·min⁻¹.

4. Conclusions

The TGA of the raw materials showed that OP presents higher thermal stability than OW due to its higher lignin content (20% and 5%, respectively). This could also be responsible for the obtaining of higher percentages of biochar from OP than from OW when both raw materials were subjected to pyrolysis under the same conditions. The higher the pyrolysis temperature, the lower the biochar production from both raw materials. The most suitable conditions for producing biochar from the pyrolysis of OP were found to be 400 °C, 150 mL Ar·min⁻¹, and 10 °C·min⁻¹, while those for obtaining biochar from the pyrolysis of OW were 400 °C, 150 mL Ar·min⁻¹, and 5 °C·min⁻¹. The biochars produced from OP had higher specific surface area (up to 24.28 m²·g⁻¹) than those produced from OW (≤ 1 m²·g⁻¹).

With regard to bio-oils, those obtained from OW were mostly composed of toluene and 5-hydroxymethylfurfural, reaching relative areas of up to 29.43% and 37.16%, respectively. By contrast, the bio-oils obtained from OP were mainly formed by 4-hydroxy-4-methyl-2-pentanone (up to 94.73% relative area).

Finally, the biochars obtained from the pyrolysis of OW and OP proved to be useful for the removal of sulphur from WCO, despite their low specific surface areas. Thus, the biochar obtained from the pyrolysis of OP at 600 °C, 150 mL Ar·min⁻¹, and 10 °C·min⁻¹ achieved a reduction of 78.8% of the initial sulphur content of WCO. Similarly, the biochar obtained from pyrolysis of OW at 400 °C, 150 mL Ar·min⁻¹ and 5 °C·min⁻¹ led to 78.3% sulphur removal from WCO.

All in all, the results obtained in this work demonstrate that pyrolysis could be an interesting option for the treatment of OW and OP. Both the obtaining of biochars for sulphur absorption from WCO and the extraction of high-added-value compounds from bio-oils could be real, feasible alternatives for this waste.

Author Contributions: Conceptualisation, P.Á.-M.; methodology, P.Á.-M.; formal analysis, F.-J.S.-B., N.G.-C., P.Á.-M. and J.F.G.-M.; investigation, F.-J.S.-B. and N.G.-C.; resources, P.Á.-M.; writing original draft preparation, F.-J.S.-B. and J.F.G.-M.; writing review and editing, J.F.G.-M.; supervision, P.Á.-M. and J.F.G.-M.; project administration, P.Á.-M.; funding acquisition, P.Á.-M. All authors have read and agreed to the published version of the manuscript.

Funding: This research was funded by the European Union under the LIFE 13 BIOSEVILLE Programme, grant number ENV/ES/1113 (analysis, materials and salaries) and by the European Regional Development Fund (ERDF) through the CARBOENERGY project (materials and salaries) granted by the FEDER INNTERCONECTA call.

Institutional Review Board Statement: Not applicable.

Informed Consent Statement: Not applicable.

Data Availability Statement: The data presented in this study are available on request from the corresponding author. The data are not publicly available due to confidentiality agreements with the funding companies.

Conflicts of Interest: The authors declare that they have not known competing financial interests or personal relationships that could have appeared to influence the work reported in this paper.




References

1. FAOSTAT. Available online: <http://www.fao.org/faostat/es/#data/QC> (accessed on 23 May 2020).
2. Ministerio de Agricultura, Pesca y Agricultura. Superficies y Producciones Anuales de Cultivos (2017). Available online: <https://www.mapa.gob.es/es/estadistica/temas/estadisticas-agrarias/agricultura/superficies-producciones-anuales-cultivos/> (accessed on 28 November 2019).
3. García-Martín, J.F.; Olmo, M.; García, J.M. Effect of ozone treatment on postharvest disease and quality of different citrus varieties at laboratory and at industrial facility. *Postharvest Biol. Technol.* **2018**, *137*, 77–85. [CrossRef]
4. Rodríguez, A.; Rosal, A.; Jiménez, L. Biorefinery of agricultural residues by fractionation of their components through hydrothermal and organosolv processes. *Afinidad* **2009**, *545*, 14–19.
5. Wilkins, M.R.; Suryawati, L.; Maness, N.O.; Chrz, D. Ethanol production by *Saccharomyces cerevisiae* and *Kluyveromyces marxianus* in the presence of orange-peel oil. *World J. Microbiol. Biotechnol.* **2007**, *23*, 1161–1168. [CrossRef]
6. Rezzadori, K.; Benedetti, S.; Amante, E.R. Proposals for the residues recovery: Orange waste as raw material for new products. *Food Bioprod. Processing* **2012**, *90*, 606–614. [CrossRef]
7. Crawshaw, R. *Co-Product Feeds: Animal Feeds from the Food and Drinks Industries*; Nottingham University Press: Nottingham, UK, 2001; p. 285.
8. Guerrero, C.C.; Carrasco de Brito, J.; Lapa, N.; Oliveira, J.F.S. Re-use of industrial orange wastes as organic fertilizers. *Bioresour. Technol.* **1995**, *53*, 43–51. [CrossRef]
9. Elías Castells, X. *Reciclaje de Residuos Industriales: Residuos Sólidos Urbanos y Fangos de Depuradora*; Ediciones Díaz de Santos, S.A.: Madrid, Spain, 2009; p. 1320.
10. Restrepo Duque, A.M.; Rodríguez Sandoval, E.; Manjarrés Pinzón, K. Edible orange peels: An approximation to the development of products with added value from agricultural products. *Producción + Limpia* **2011**, *6*, 47–57.
11. Boluda-Aguilar, M.; López-Gómez, A. Production of bioethanol by fermentation of lemon (*Citrus limon* L.) peel wastes pretreated with steam explosion. *Ind. Crops Prod.* **2013**, *41*, 188–197. [CrossRef]
12. Siles, J.Á.; Martín, M.D.L.Á.; Martín, A.; Raposo, F.; Borja, R. anaerobic digestion of wastewater derived from the pressing of orange peel generated in orange juice production. *J. Agric. Food Chem.* **2007**, *55*, 1905–1914. [CrossRef]
13. Calabrò, P.S.; Fazzino, F.; Sidari, R.; Zema, A. Optimization of orange peel waste ensiling for sustainable anaerobic digestion. *Renew. Energy* **2020**, *154*, 849–862. [CrossRef]
14. Feng, C.H.; García-Martín, J.F.; Broncano Lavado, M.; del López-Barrera, M.; Álvarez-Mateos, P. Evaluation of different solvents on flavonoids extraction efficiency from sweet oranges and ripe and immature Seville oranges. *Int. J. Food Sci. Technol.* **2020**, *55*, 3123–3134. [CrossRef]
15. Volpe, M.; Panno, D.; Volpe, R.; Messineo, A. Upgrade of citrus waste as a biofuel via slow pyrolysis. *J. Anal. Appl. Pyrolysis* **2015**, *115*, 66–76. [CrossRef]
16. Bagnato, G.; Sanna, A.; Paone, E.; Catizzone, E. Recent catalytic advances in hydrotreatment processes of pyrolysis bio-oil. *Catalysts* **2021**, *11*, 157. [CrossRef]
17. Sánchez-Borrego, F.J.; Álvarez-Mateos, P.; García-Martín, J.F. Biodiesel and other value-added products from bio-oil obtained from agrifood waste. *Processes* **2021**, *9*, 797. [CrossRef]
18. García Martín, J.F.; Cuevas, M.; Feng, C.H.; Álvarez Mateos, P.; Torres García, M.; Sánchez, S. Energetic valorisation of olive biomass: Olive-tree pruning, olive stones and pomaces. *Processes* **2020**, *8*, 511. [CrossRef]
19. Association European Biomass Industry Pyrolysis. Available online: <https://www.eubia.org/cms/> (accessed on 26 May 2020).
20. Basu, P. *Biomass Gasification and Pyrolysis*, 1st ed.; Academic Press: Cambridge, MA, USA, 2010; p. 376.
21. Bhattacharjee, N.; Baran Biswas, A. Pyrolysis of orange bagasse: Comparative study and parametric influence on the product yield and their characterization. *J. Environ. Chem. Eng.* **2019**, *7*, 102903. [CrossRef]
22. Bradley, D.; Svebio, B.H.; Ab, H.; Wild, M.; Deutmeyer, M.; Schouwenberg, P.P.; Essent, R.; Hess, R.; Tumuluru, J.S.; Bradburn, K. Low Cost, Long Distance Biomass Supply Chains. In *Task 40: Sustainable International Bioenergy Trade*; Goh, C.S., Junginger, M., Eds.; IEA Bioenergy: Paris, France, 2013; pp. 1–65.

23. Encinar, J.M.; Beltran, F.J.; Gonzalez, J.F.; Moreno, M.J. Pyrolysis of maize, sunflower, grape and tobacco residues. *Chem. Technol. Biotechnol.* **1997**, *70*, 400–410. [[CrossRef](#)]
24. Wu, L.; Wan, W.; Shang, Z.; Gao, X.; Kobayashi, N.; Luo, G.; Li, Z. Surface modification of phosphoric acid activated carbon by using non-thermal plasma for enhancement of Cu(II) adsorption from aqueous solutions. *Sep. Purif. Technol.* **2018**, *197*, 156–169. [[CrossRef](#)]
25. Roy, M.; Mohanty, K. Valorization of de-oiled microalgal biomass as a carbon-based heterogeneous catalyst for a sustainable biodiesel production. *Bioresour. Technol.* **2021**, *337*, 125424. [[CrossRef](#)]
26. Sánchez-Borrego, F.J.; Barea de Hoyos-Limón, T.J.; García-Martín, J.F.; Álvarez-Mateos, P. Production of bio-oils and biochars from olive stones: Application of biochars to the esterification of oleic acid. *Plants* **2021**, *11*, 70. [[CrossRef](#)] [[PubMed](#)]
27. Álvarez-Mateos, P.; García-Martín, J.F.; Guerrero-Vacas, F.J.; Naranjo-Calderón, C.; Barrios-Sánchez, C.C.; Pérez-Camino, M.C. Valorization of a high-acidity residual oil generated in the waste cooking oils recycling industries. *Grasas Aceites* **2019**, *70*, e335. [[CrossRef](#)]
28. García Martín, J.F.; Carrión Ruiz, J.; Torres García, M.; Feng, C.H.; Álvarez Mateos, P. Esterification of free fatty acids with glycerol within the biodiesel production framework. *Processes* **2019**, *7*, 832. [[CrossRef](#)]
29. García-Martín, J.F.; Alés-Álvarez, F.J.; Torres-García, M.; Feng, C.H.; Álvarez-Mateos, P. Production of oxygenated fuel additives from residual glycerine using biocatalysts obtained from heavy-metal-contaminated *Jatropha curcas* L. roots. *Energies* **2019**, *12*, 740. [[CrossRef](#)]
30. Cárdenas, J.; Orjuela, A.; Sánchez, D.L.; Narváez, P.C.; Katryniok, B.; Clark, J. Pre-treatment of used cooking oils for the production of green chemicals: A review. *J. Clean. Prod.* **2021**, *289*, 125129. [[CrossRef](#)]
31. Shan, Y.; Erika, G.; Gray, D.; Yuan, Y.; Simeon, R. *Cost-Effective Waste to Biodiesel Production at a Wastewater Treatment Plant*; East Bay Municipal Utility District: Oakland, CA, USA, 2019.
32. Aguiar Trujillo, L.; Márquez-Montesinos, F.; Gonzalo, A.; Sánchez, J.L.; Arauzo, J. Influence of temperature and particle size on the fixed bed pyrolysis of orange peel residues. *J. Anal. Appl. Pyrolysis* **2008**, *83*, 124–130. [[CrossRef](#)]
33. Lopez-Velazquez, M.A.; Santes, V.; Balmaseda, J.; Torres-García, E. Pyrolysis of orange waste: A thermo-kinetic study. *J. Anal. Appl. Pyrolysis* **2013**, *99*, 170–177. [[CrossRef](#)]
34. Aburto, J.; Moran, M.; Galano, A.; Torres-García, E. Non-isothermal pyrolysis of pectin: A thermochemical and kinetic approach. *J. Anal. Appl. Pyrolysis* **2015**, *112*, 94–104. [[CrossRef](#)]
35. Álvarez-Mateos, P.; Alés-Álvarez, F.J.; García-Martín, J.F. Phytoremediation of highly contaminated mining soils by *Jatropha curcas* L. and production of catalytic carbons from the generated biomass. *J. Environ. Manag.* **2019**, *231*, 886–895. [[CrossRef](#)]
36. Yang, H.; Yan, R.; Chen, H.; Lee, D.H.; Zheng, C. Characteristics of hemicellulose, cellulose and lignin pyrolysis. *Fuel* **2007**, *86*, 1781–1788. [[CrossRef](#)]
37. Martínez-Cartas, M.L.; Sánchez, S.; Cuevas, M. Thermal characterization and pyrolysis kinetics of six types of tropical timber from Central Africa. *Fuel* **2022**, *307*, 121824. [[CrossRef](#)]
38. Miranda, R.; Bustos, D.; Sosa Blanco, C.; Gutiérrez Villarreal, M.H.; Rodríguez Cantú, M.E. Pyrolysis of sweet orange (*Citrus sinensis*) dry peel. *J. Anal. Appl. Pyrolysis* **2008**, *86*, 245–251. [[CrossRef](#)]
39. Monteiro Santos, C.; Dweck, J.; Silva Viotto, R.; Henrique Rosa, A.; de Morais, L.C. Application of orange peel waste in the production of solid biofuels and biosorbents. *Bioresour. Technol.* **2015**, *196*, 469–479. [[CrossRef](#)] [[PubMed](#)]
40. Abdelaal, A.; Pradhan, S.; Al-Nouss, A.; Tong, Y.; Al-Ansari, T.; McKay, G.; Mackey, H.R. The impact of pyrolysis conditions on orange peel biochar physicochemical properties for sandy soil. *Waste Manag. Res.* **2021**, *39*, 995–1004. [[CrossRef](#)] [[PubMed](#)]
41. Del Pozo, C.; Rego, F.; Yang, Y.; Puy, N.; Bartolí, J.; Fábregas, E.; Bridgwater, A.V. Converting coffee silverskin to value-added products by a slow pyrolysis-based biorefinery process. *Fuel Processing Technol.* **2021**, *214*, 106708. [[CrossRef](#)]
42. Charusiri, W.; Vitidsant, T. Biofuel production via the pyrolysis of sugarcane (*Saccharum officinarum* L.) leaves: Characterization of the optimal conditions. *Sustain. Chem. Pharm.* **2018**, *10*, 71–78. [[CrossRef](#)]
43. Lugo, C.; García, E.; Rondón, J.; Briceño, J.; Pérez, P.; Rodríguez, P.; del Castillo, H.; Imbert, F. Study of reactions catalyzed as methane reforming and selective catalytic reduction of NO_x on perovskites of Type La_{0.7}Sr_{0.3}Ni_{1-x}Co_xO₃ obtained via SCS. Part II. *Rev. Cienc. Ing.* **2020**, *41*, 35–146.
44. De Almeida, C.F.; de Andrade, R.C.; de Oliveira, G.F.; Suegama, P.H.; de Arruda, E.J.; Texeira, J.A.; de Carvalho, C.T. Study of porosity and surface groups of activated carbons produced from alternative and renewable biomass: Buriti petiole. *Orbital* **2017**, *9*, 18–26. [[CrossRef](#)]
45. Kim, J.W.; Lee, S.-H.; Kim, S.-S.; Park, S.H.; Jeon, J.-K.; Park, Y.-K. The pyrolysis of waste mandarin residue using thermogravimetric analysis and a batch reactor. *Korean J. Chem. Eng.* **2011**, *28*, 1867–1872. [[CrossRef](#)]
46. Özbay, N.; Apaydin-Varol, E.; Burcu Uzun, B.; Eren Pütünb, A. Characterization of bio-oil obtained from fruit pulp pyrolysis. *Energy* **2008**, *33*, 1233–1240. [[CrossRef](#)]
47. Van de Beld, B.; Funke, A.; Lindfors, C.; Sandström, L. Country Reports 2019. In *Task 34: Direct Thermochemical Liquefaction*; Funke, A., Ed.; IEA Bioenergy: Paris, France, 2019; pp. 1–20.
48. Lewkowsky, J. Synthesis, chemistry and applications of 5-hydroxymethylfurfural and its derivatives. *Arkivoc* **2001**, *1*, 17–54. [[CrossRef](#)]
49. Huang, S.; Liang, Q.; Geng, J.; Luo, H.; Wei, Q. Sulfurized biochar prepared by simplified technic with superior adsorption property towards aqueous Hg(II) and adsorption mechanisms. *Mater. Chem. Phys.* **2019**, *238*, 121919. [[CrossRef](#)]

Article

Production of Bio-Oils and Biochars from Olive Stones: Application of Biochars to the Esterification of Oleic Acid

Francisco José Sánchez-Borrego , Tomás Juan Barea de Hoyos-Limón, Juan Francisco García-Martín * 
and Paloma Álvarez-Mateos * 

Departamento de Ingeniería Química, Facultad de Química, Universidad de Sevilla, 41012 Sevilla, Spain; fsanchez25@us.es (F.J.S.-B.); tbareadehoyoslimn@gmail.com (T.J.B.d.H.-L.)

* Correspondence: jfgarmar@us.es (J.F.G.-M.); palvarez@us.es (P.Á.-M.)

Abstract: Olive stones are a by-product of the olive oil industry. In this work, the valorisation of olive stones through pyrolysis was attempted. Before pyrolysis, half of the samples were impregnated with sulphuric acid. Pyrolysis was carried out in a vertical tubular furnace with a ceramic support. The pyrolysis conditions assayed were: temperature between 400 and 600 °C, heating ramp between 5 and 20 °C·min⁻¹, and inert gas flow rate between 50 and 300 mL Ar·min⁻¹. Among them, temperature was the only parameter that influenced the pyrolysis product distribution. The most suitable temperature for obtaining biochar was 400 °C for both non-treated and pre-treated raw material, while for obtaining bio-oil, it was 600 °C for impregnated olive stones and 400 °C for the raw material. The impregnated olives stones led to bio-oils with much higher amounts of high-added-value products such as levoglucosenone and catechol. Finally, the biochars were impregnated with sulphuric acid and assayed as biocatalysts for the esterification of oleic acid with methanol in a stirred tank batch reactor at 60 °C for 30 min. Biochars from non-treated olive stones, which had lower specific surfaces, led to higher esterification yields (up to 96.2%).

Keywords: biodiesel; bio-oil; levoglucosenone; olive stones; pyrolysis



Citation: Sánchez-Borrego, F.J.; Barea de Hoyos-Limón, T.J.; García-Martín, J.F.; Álvarez-Mateos, P. Production of Bio-Oils and Biochars from Olive Stones: Application of Biochars to the Esterification of Oleic Acid. *Plants* **2022**, *11*, 70. <https://doi.org/10.3390/plants11010070>

Academic Editor:
Georgios Koubouris

Received: 2 December 2021

Accepted: 23 December 2021

Published: 27 December 2021

Publisher's Note: MDPI stays neutral with regard to jurisdictional claims in published maps and institutional affiliations.



Copyright: © 2021 by the authors. Licensee MDPI, Basel, Switzerland. This article is an open access article distributed under the terms and conditions of the Creative Commons Attribution (CC BY) license (<https://creativecommons.org/licenses/by/4.0/>).

1. Introduction

The agricultural exploitation of olive tree accounts for 11×10^6 ha in the world, most of them in Mediterranean countries, for example, Spain, Italy, Greece, Morocco, etc. As a result, 20×10^6 t [1] olives a year are produced worldwide. The main exploitation is the production of olive oil, which produces large amounts of by-products. Another main products of olives are table olives, known throughout the world as pickles and used as an ingredient in cooking.

In some olive oil companies, the olives are first de-stoned before entering the olive oil extraction system, in which the olives go through a decanter of two or three outlets to obtain olive oil and pomace (containing 65–75 wt.% moisture), or olive oil, pomace (containing 45–55 wt.% moisture), and wastewater, respectively [1,2]. This work focuses mainly on olive stones (OS), which have an estimated production of 42,900 t/year in Spain [3].

OS are made up of cellulose, hemicellulose, and lignin. Their composition of these components is different depending on the olive variety, ranging between 27.1 and 36.4 wt.% of cellulose; 24.5 and 32.2 wt.% of hemicellulose, and 23.1 and 40.4 wt.% of lignin [1,4–6].

One of the potential uses of OS is the production of renewable energy through their biochemical transformation into biofuels (bioethanol) [7]. Furthermore, they could be used as a lightweight aggregate in construction mortars [8], as a feed flour with high protein, fibre, and omega-3 content [9], and as a bioplastic precursor [10].

However, the most frequent use of this by-product is combustion to obtain thermal energy. Its high calorific value and low cost make olive stones an excellent lignocellulosic material for energy. Combustion generates pollution for the environment, emitting gases

such as CO₂, CO, SO, SO₂, and polycyclic aromatic hydrocarbons. There are alternative processes, less harmful in their use, for specific other thermochemical treatments such as pyrolysis, torrefaction, and gasification [11].

Pyrolysis is a thermochemical process carried out at high temperatures, between 400 and 700 °C, under an inert atmosphere (total absence of oxygen). During the pyrolysis process, each lignocellulose material undergoes different reaction mechanisms (that is, decarboxylation, dehydration, and demethylation) resulting in the production of bio-oil, syngas, and biochar [12].

In addition to the characteristics of the raw material used, there are several factors that influence the process, namely temperature, heating ramp, and gas flow rate [13]. It is important to note the effect of temperature on obtaining of pyrolysis products, since higher percentages of bio-oil are obtained at high temperatures (500–700 °C), while a higher proportion of biochar is obtained at low temperatures (350–400 °C) [14].

Pyrolysis can be fast or slow, depending on the heating ramp and residence time. Lower process temperatures and heating ramps and longer gas residence times improve biochar production. Approximately 35% of the weight of dry biomass can be turned into biochar, although higher pressure can provide significantly higher performance [15].

Bio-oil is a mixture of organic compounds such as esters, acids, and aromatic compounds depending on the composition of the raw material; thus, research has been carried out in recent years on the use of these components. One of these applications is the extraction of some aromatic components, such as phenols, and other compounds of high added value such as levoglucosenone or catechol. Furthermore, it is important to mention that bio-oil is also used for the manufacture of high-quality biofuels for internal combustion engines [16]. However, no information can be found in the available literature on the composition of bio-oils from olive stones.

Non-condensable gases (syngas) are a mixture of basic components such as carbon monoxide (CO) and hydrogen (H₂). The higher heating value of syngas (4.37–5.68 MJ/m³) plays an important role in the generation of energy in cogeneration plants [17].

Biochar is a non-volatile carbon-rich solid residue composed of the non-hydrocarbon residues of biomass, mainly parts of lignin, oxides (usually metallic), and heavy metals, depending on the composition of the feedstock. Among all the applications that biochar currently has, its use as a catalyst can be highlighted, for example, in the esterification reaction of oleic acid with methanol to obtain biodiesel [18,19]. Many researchers have found that biochar can be used as an alternative adsorbent to remove different types of pollutants, such as heavy metals, nutrients, and pharmaceuticals, from aqueous solutions [20]. Many raw materials and their resulting biochars have low specific surface or low catalytic activity, so these materials are pre-treated (activated) with acids, such as sulphuric acid [21] or phosphoric acid [22]. To the best of our knowledge, biochars from olives stones have not been applied as biocatalyst so far.

Based on all the considerations mentioned above, the objectives of this work were as follows:

- Valorise olive stones through pyrolysis;
- Assess the most suitable pyrolysis conditions for the production of biochar and bio-oil;
- Characterize the biochars and bio-oils obtained;
- Establish the most suitable conditions for obtaining levoglucosenone and catechol in bio-oils;
- Apply the biochar obtained under the most suitable pyrolysis conditions as a biocatalyst for the esterification reaction of free fatty acids with methanol to obtain biodiesel.

2. Results

2.1. Characterisation of the Raw Material

2.1.1. Thermogravimetric Analysis (TGA)

The OS were analysed by thermogravimetry using the thermobalance under the conditions described in Section 3.4.1 in order to study their decomposition and obtain information on the optimum carbonisation temperature.

Figure 1 shows the different peaks corresponding to the mass loss during heating. Mass loss at temperatures around 100 °C was associated with moisture content. In this case, the loss occurred around 70 °C, with a total loss of 15 wt.%, corresponding to physically adsorbed water that interacts only with other water molecules, a band that extended up to 120 °C [23].

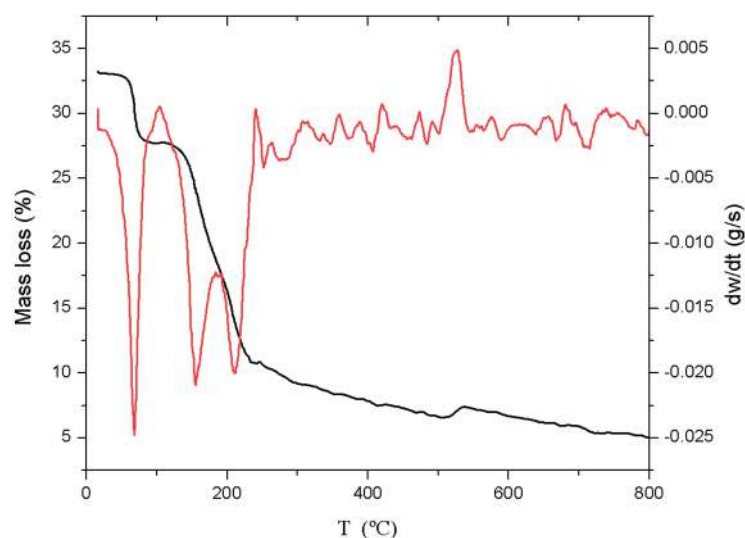


Figure 1. TG (black line) and DTG (red line) curves obtained from the carbonisation of OS.

Cellulose polymers degraded between 150 and 200 °C [24], and in this case showed a maximum degradation rate at 165 °C, as observed in the peak of the DTG curve. This loss was 24% of the total weight of the sample.

On the other hand, degradation of hemicellulose was observed from 200 to 250 °C [24], accounting for 27 wt.% of the sample.

In Figure 1, lignin did not show a well-defined degradation peak. On the contrary, the degradation process started at 200 °C and continued gradually up to 800 °C, a temperature at which more than 80 wt.% of the initial mass had been decomposed [24], corresponding to approximately 15 wt.% of the total weight of the raw material.

As can be seen in the TGA, a large part of the weight loss (70%) had already occurred at 400 °C (Figure 1), which indicated that the sample consisted mainly of water, cellulose, and hemicellulose. It was also observed that 80 wt.% degradation of the initial mass was reached at 600 °C. Therefore, either of the two maximum temperatures assayed in the pyrolysis process ensured the carbonisation of most of the olive stones.

Finally, at 800 °C, there was still around 20 wt.% of the olive stones undegraded by pyrolysis, which corresponds to carbon residues and metallic compounds.

When comparing these data with previous work carried out with OS [25], it could be seen that the product yield was very similar. Cellulose and lignin yields were lower (24.0 vs. 26.8 wt%. and 15.0 vs. 20.0 wt.%, respectively), but that of hemicellulose was higher (27.0 vs. 25.5 wt.%).

2.1.2. FTIR Analysis

The FTIR spectra of OS pre-treated with sulphuric acid (OS + H₂SO₄) were compared with those of the non-treated raw material (OS), with the purpose of evaluating the influence of this pre-treatment on the structure (Figure 2).

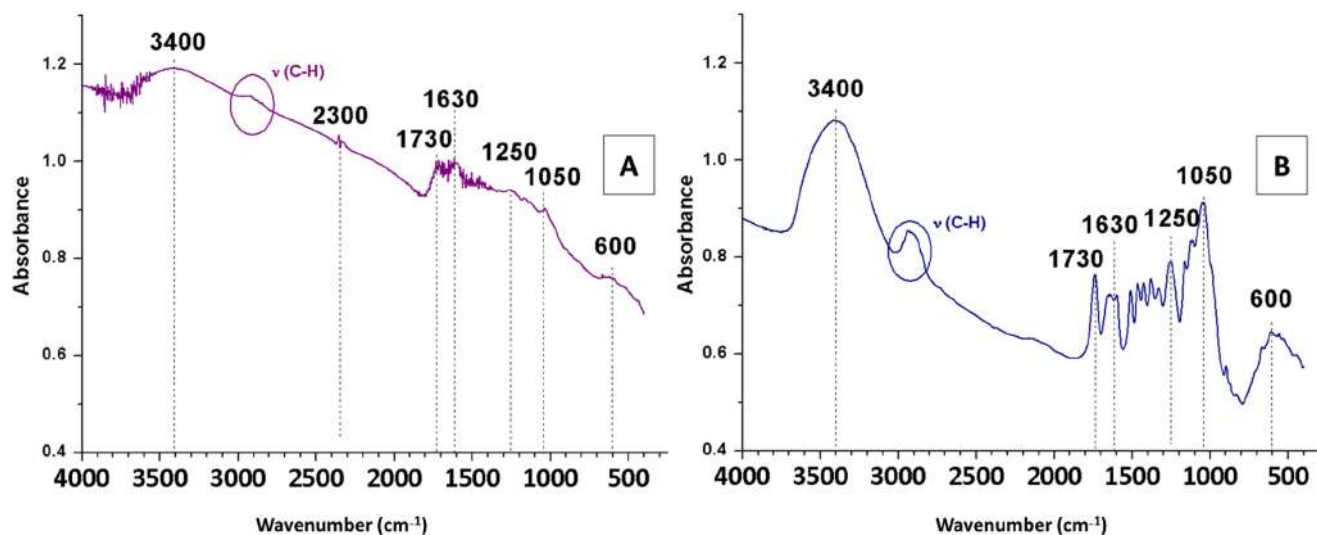


Figure 2. FTIR spectra of OS + H₂SO₄ (A) and OS (B).

The spectrum of OS + H₂SO₄ (Figure 2A) showed differences in most bands compared to the FTIR spectrum or the raw material (Figure 2B). This was explained by the fact that sulphuric acid degraded hemicellulose and cellulose, which could be seen in the 3500–3100 cm⁻¹ bands corresponding to OH vibrations (due to the presence of cellulose and hemicellulose with their abundant alcoholic hydroxyl groups or the symmetric and asymmetric stretching vibrations related to H₂O molecules) and in the aliphatic bands around 2900 cm⁻¹. The band at 2300 cm⁻¹ corresponded to the asymmetric tension vibration of the CO₂ molecule, which was higher in intensity in the spectrum of OS + H₂SO₄ compared to that of OS. Regarding the band at 1730 cm⁻¹, it had a lower intensity with pre-treatment (Figure 2A) than without pre-treatment (Figure 2B), due to the degradation of hemicellulose by sulphuric acid. Furthermore, sulphuric acid degraded not only hemicellulose and cellulose, but also lignin. Although lignin degradation was lower, it can be seen reflected in the C=C bands (at 1630 cm⁻¹), which are characteristic of lignin aromatics [23]. Since the bands at 1250 and 1050 cm⁻¹ were related to glycosidic bonds (found mainly in hemicellulose and cellulose), their intensity was greatly reduced after treatment. Finally, the band at 600 cm⁻¹, characteristic of calcium, remained completely unchanged.

2.2. Pyrolysis Yields

Table 1 shows the yield of each product obtained in the different pyrolysis processes according to the operational conditions.

Regarding the pyrolysis temperature, it was inversely proportional to the biochar production (Table 1), but directly proportional to the fluent products (biogas and bio-oil) [26].

Regarding the heating ramp, pyrolysis from OS + H₂SO₄ led to the same biochar yield. However, modifying the heating ramp achieved a reduction in the pyrolysis process time while leading to the same biochar yield, that is, the use of a heating ramp of 20 °C·min⁻¹ resulted in time savings of 20 min and 1 h when compared to the use of heating ramps of 10 and 5 °C·min⁻¹, respectively. In addition, the reduction of the pyrolysis process time also resulted in energy savings, with 20 °C·min⁻¹ being the optimal heating ramp. Similarly, the resulting percentages of biochar were again similar in the pyrolysis of OS. However, the influence on bio-oil should be highlighted, because the lower the heating ramp, the higher

the bio-oil yield. Therefore, $5\text{ }^{\circ}\text{C}\cdot\text{min}^{-1}$ is the optimal heating ramp when the objective is to obtain bio-oil.

Table 1. Biochar, syngas, and bio-oil yields obtained under different pyrolysis conditions.

Pyrolysis	Raw Material	SAT (min)	T ($^{\circ}\text{C}$)	H _{ramp} ($^{\circ}\text{C}\cdot\text{min}^{-1}$)	Ar Flow ($\text{mL}\cdot\text{min}^{-1}$)	Y _{Biochar} (wt.%)	Y _{syngas} (wt.%)	Y _{Bio-oil} (wt.%)
1	OS + H ₂ SO ₄	4	600	10	150	44.6	38.2	17.1
2	OS + H ₂ SO ₄	4	500	10	150	51.2	35.2	13.5
3	OS + H ₂ SO ₄	4	400	10	150	57.8	35.6	6.7
4	OS + H ₂ SO ₄	4	400	5	150	59.6	33.4	7.0
5	OS + H ₂ SO ₄	4	400	20	150	60.2	31.6	8.2
6	OS + H ₂ SO ₄	8	400	10	150	60.0	33.0	7.0
7	OS + H ₂ SO ₄	8	400	20	300	57.2	41.2	1.6
8	OS + H ₂ SO ₄	8	400	20	50	57.8	37.3	4.9
9	OS + H ₂ SO ₄	8	600	10	150	50.0	47.4	2.6
10	OS	-	600	10	150	27.2	52.6	20.3
11	OS	-	500	10	150	27.7	48.8	23.5
12	OS	-	400	10	150	31.2	45.5	23.4
13	OS	-	400	20	150	29.3	40.5	30.2
14	OS	-	400	20	50	29.7	29.5	40.8
15	OS	-	400	5	150	31.7	36.2	32.2
16	OS	-	400	5	50	33.5	30.3	36.2
17	OS	-	400	5	300	30.3	44.3	25.3

Furthermore, in terms of argon flow rate, the pyrolysis of OS + H₂SO₄ under $150\text{ mL Ar}\cdot\text{min}^{-1}$ produced the highest amounts of biochar and bio-oil. When OS was used as raw material (without sulphuric acid pre-treatment), there were hardly any differences in the yields of pyrolysis products when the argon flow rate was varying. Pyrolysis under $50\text{ mL Ar}\cdot\text{min}^{-1}$ should be highlighted, as it was the one that achieved the highest biochar and bio-oil yields from non-treated OS, as well as the lowest Ar expenditure.

Finally, in light of these data (Table 1), it could be said that feedstock that was previously pre-treated (OS + H₂SO₄) led to higher biochar yields. These higher biochar yields are due to the formation of chemical bonds between two polymer chains (cross-link) and the retention of low-molecular-weight carbonaceous species in the solid phase, stabilising the cellulose structure [27]. The results showed that acid pre-treatment resulted in 60% of biochar yield, compared to only about 31% of biochar yield without pre-treatment [28].

Pyrolyses 1 and 9 and Pyrolyses 3 and 6 were performed under the same conditions, respectively (Table 1). However, the product yields showed some differences even though the OS were from the same batch. This is because two pre-treatments were performed at different times during the execution of the experiments in this research. The first involved the first to the fifth samples, while the second involved from the sixth to the ninth samples.

These differences were based on the sulphuric actuation time (4 vs. 8 min) in the pre-treatment with sulphuric acid. The longer the residence time, the greater the retention of carbonaceous biomass, which had a direct influence on product yields (Table 1), as the longer the contact time with H₂SO₄, the higher the biochar yield [27].

2.3. Bio-Oil Characterisation

The bio-oils were subjected to gas chromatography–mass spectroscopy analysis in order to obtain a qualitative and semi-quantitative analysis of the major compounds. The samples selected were those from Pyrolyses 3 and 12, as they were obtained from pyrolysis under the same conditions, but with different raw material. Specifically, the bio-oil obtained from Pyrolysis 3 was obtained from OS + H₂SO₄ and that from Pyrolysis 12 was from OS. Table 2 illustrates the compounds identified by GC–MS, with a probability of matching with the database greater than 40%.

Table 2. Bio-oils composition.

Compound	Bio-Oils Samples	
	Pyrolysis 3	Pyrolysis 12
	Area (%)	
Toluene	1.18	-
Furfural	5.30	3.80
4-Hydroxy-4-methylpentan-2-one	2.53	-
2-Furanmethanol	-	3.49
Ethylbenzene	3.03	2.34
o-Xylene	6.26	3.40
p-Xylene	2.74	1.51
Cyclopenta-1,2-dione	1.15	2.42
5-Methyl-2-furancarboxaldehyde	2.15	1.61
Phenol	3.60	-
N-Butyl-tert-butylamine	-	2.59
3-Methylcyclopentan-1,2-dione	-	2.60
2-Methylphenol	1.55	1.20
3-Methylphenol	3.53	-
2-Methoxyphenol	5.28	7.87
Levoglucosenone	9.57	-
Catechol	6.17	3.33
Creosol	6.94	7.32
1,4:3,6-Dianhydro- α -D-glucopyranose	3.51	-
3-Methylbenzene-1,2-diol	1.71	1.27
3-Methoxybenzene-1,2-diol	2.35	3.28
4-Ethyl-2-methoxyphenol	2.14	5.02
4-Methylbenzene-1,2-diol	1.59	1.55
2-Methoxy-4-vinylphenol	5.38	14.30
Eugenol	-	2.00
Vanillin	3.65	1.50
3,5-Dimethoxy-4-hydroxytoluene	6.07	5.70
Trans-isoeugenol	-	5.75
1,6-Anhydro- β -D-glucopyranose	2.88	1.51
5-Tert-butylpyrogallol	1.73	-
1-(4-Hydroxy-3-methoxyphenyl)-propan-2-one	1.52	2.02
4-Ethanoyl-2,6-dimethoxy-phenol	-	3.56
Butyrovaniolone	3.15	-
4-Hydroxy-3,5-dimethoxy-benzaldehyde	1.73	-
(E)-2,6-Dimethoxy-4-(prop-1-en-1-yl)-phenol	-	4.56
Coniferyl aldehyde	-	2.15
Syringylacetone	-	2.37
Butylsyringone	1.64	-

The influence of OS pre-treatment on the bio-oil composition can be observed in Table 2. Some of the compounds found in the bio-oil produced from OS + H₂SO₄ are more valuable than those obtained from OS, such as levoglucosenone, catechol, or vanillin. This could be explained by the transformation of lignocellulosic compounds into levoglucosenone under acidic conditions [29–31].

Levoglucosenone was one of the most abundant compounds in the bio-oil obtained from the pyrolysis of pre-treated OS, accounting for almost 10% of the bio-oil. This compound has a high market value: 10 mg of levoglucosenone (95%) as a laboratory reagent currently cost 165 euros (Sigma Aldrich, St Louis, MO, USA, 11/2021).

2.4. Biochar Characterisation

FTIR spectroscopy was used for the analysis of the surface functional groups in the biochars obtained under different conditions (acid pre-treatment, temperature, heating ramp, and argon flow rate).

2.4.1. Temperature Influence

In order to assess the effect of temperature, the FTIR spectra of the raw materials (OS + H₂SO₄ and OS) were compared with those of the biochars obtained from them at different maximum pyrolysis temperatures, keeping the rest of the conditions constant (150 mL Ar·min⁻¹ and 10 °C·min⁻¹) (Figure 3).

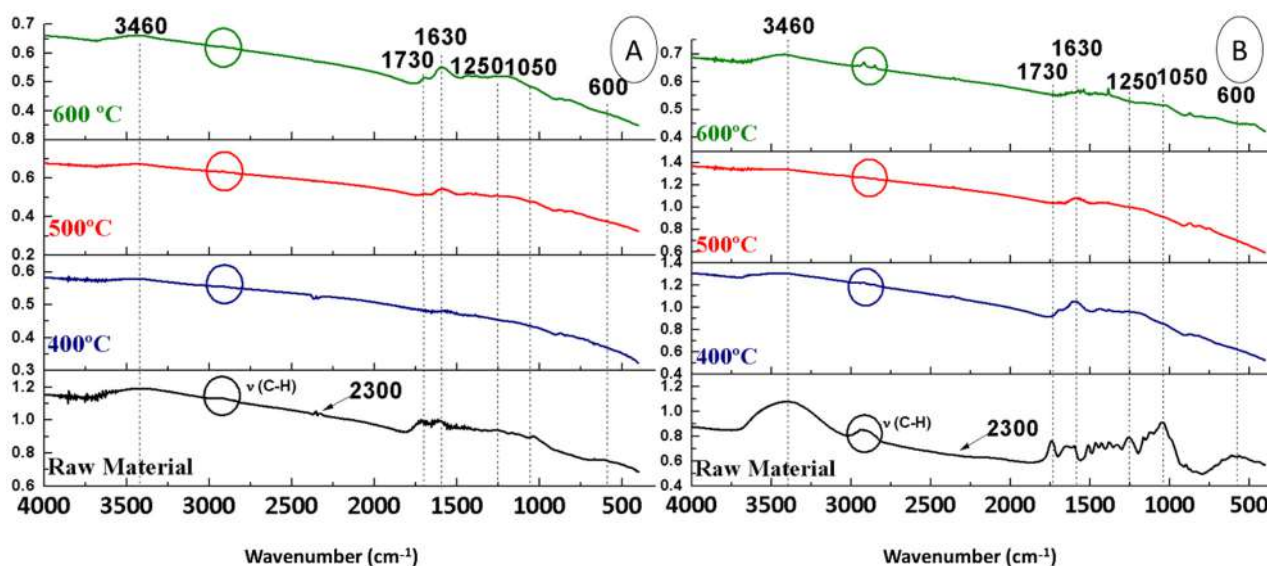


Figure 3. FTIR spectra of biochars from OS + H₂SO₄ (A) and OS (B) at different temperatures.

The first band observed in both Figure 3A,B was at 3400 cm⁻¹. This is usually associated with water absorption (OH vibration), which is explained by the fact that the analysis was carried out under ambient conditions (with humidity in the atmosphere).

Regarding the OS + H₂SO₄ biochars (Figure 3A), it could be seen that at 600 °C there were no traces of aliphatic hydrocarbons (2900 cm⁻¹). The band at 2300 cm⁻¹ (CO₂) appeared only at 400 °C. On the contrary, the bands at 1730 cm⁻¹ (C=O) and 1630 cm⁻¹ (C=C) remained constant and only disappeared when pyrolysed at 400 °C. The peaks observed at 1250 and 1050 cm⁻¹, related to CO in glycosidic bonds, were inversely proportional to temperature. The aromatic compounds, which appeared at 700–900 cm⁻¹, did not seem affected by the temperature. Finally, the peak at 600 cm⁻¹ (Ca) disappeared completely in the FTIR spectra of biochars from OS + H₂SO₄ (Figure 3A).

Regarding the OS biochars (Figure 3B), the band at 2900 cm⁻¹ was only appreciated at the temperature of 600 °C. The band at 2300 cm⁻¹ (CO₂) was barely appreciated after pyrolysis. When the raw material is pyrolysed at 600 °C, the band at 1730 cm⁻¹ (C=O) and at 1630 cm⁻¹ (C=C) disappeared completely. While the one at 1250 cm⁻¹ was not influenced by the temperature, the one at 1050 cm⁻¹ was directly proportional to the temperature. In addition, aromatic compounds were present in all biochars (region 700–900 cm⁻¹), even at 600 °C. Finally, the peak at 600 cm⁻¹ completely disappeared in all experiments after the pyrolytic treatment.

2.4.2. Influence of the Heating Ramp

To assess the effect of the heating ramp, the FTIR spectra of the raw materials (OS + H₂SO₄ and OS) were compared with those of the biochars obtained from them at different heating ramps, keeping the rest of the conditions constant (400 °C and 150 mL Ar·min⁻¹) (Figure 4).

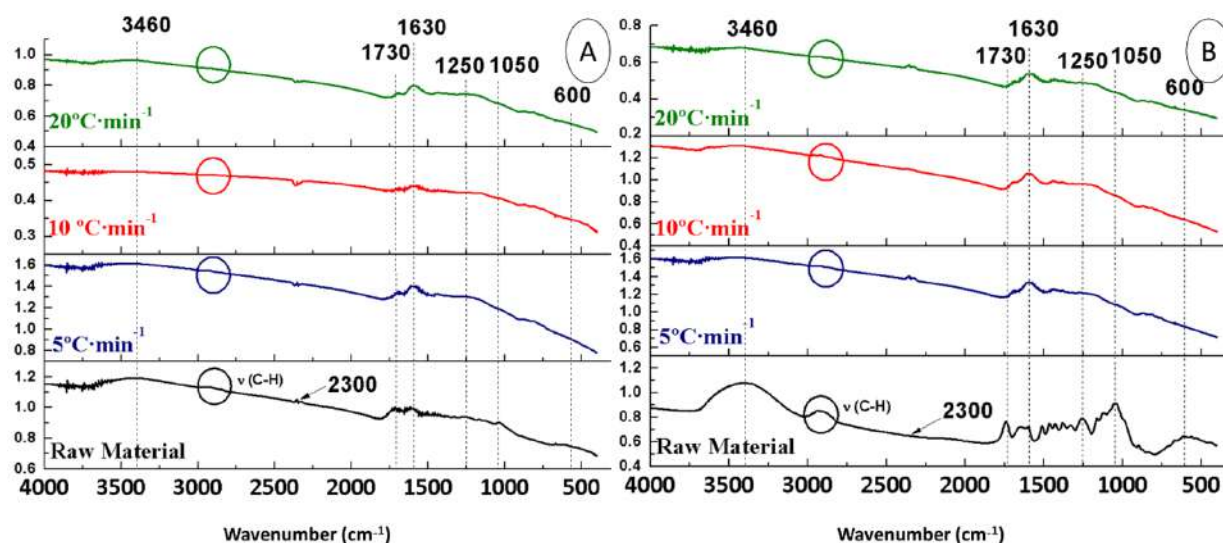


Figure 4. FTIR spectra of biochars from OS + H₂SO₄ (A) and OS (B) at different heating ramps.

Regarding the OS + H₂SO₄ biochars (Figure 4A), it could be seen that the absorbance band in the 3400 cm⁻¹ region was still present due to absorption of humidity. However, the aliphatic band (2900 cm⁻¹) was not present in the samples. The band at 2300 cm⁻¹ (CO₂) was kept stable in all samples. The bands at 1730 cm⁻¹ (C=O) and at 1630 cm⁻¹ (C=C) still appeared, being lower at 10 °C·min⁻¹. The peaks observed at 1250 and 1050 cm⁻¹ (CO) disappeared after pyrolysis, so both bands did not rely on the heating ramp. The band at 700–900 cm⁻¹ was kept stable in all the samples. Finally, the peak at 600 cm⁻¹ (Ca) did not change with the heating ramp.

As for OS biochars (Figure 4B), the band at 3400 cm⁻¹ (H₂O) remained in all samples. On the contrary, the band at 2900 cm⁻¹ was not present in the samples. The band at 2300 cm⁻¹ (CO₂) remained stable in all samples. The band at 1730 cm⁻¹ (C=O) and at 1630 cm⁻¹ (C=C) remained constant, being lower at 20 °C·min⁻¹. The bands at 1250 and 1050 cm⁻¹ (CO) disappeared after pyrolysis. There was no influence of the heating ramp on the band at 700–900 cm⁻¹. Finally, the peak at 600 cm⁻¹ (Ca) disappeared completely after pyrolysis.

2.4.3. Argon Flow Influence

To assess the effect of the argon flow during pyrolysis, the FTIR spectra of the raw materials (OS + H₂SO₄ and OS) were compared with those of the biochars obtained at different argon flows, keeping the rest of conditions constant (400 °C and 20 °C·min⁻¹ (to OS + H₂SO₄) and 5 °C·min⁻¹ (to OS)) (Figure 5).

Regarding the OS + H₂SO₄ biochars (Figure 5A), it could be seen that the 3400 cm⁻¹ band was still present due to the absorption of water from the atmosphere. However, aliphatic hydrocarbons (2900 cm⁻¹) were not present in the samples. The band at 2300 cm⁻¹ (CO₂) only appeared at 150 mL Ar·min⁻¹. The bands at 1730 cm⁻¹ (C=O) and at 1630 cm⁻¹ (C=C) still appeared, being lower at 150 mL Ar·min⁻¹. The peaks observed at 1250 and 1050 cm⁻¹ (CO) disappeared after pyrolysis. Aromatic compounds (800 cm⁻¹) did not appear to be affected by argon flow. Finally, the peak at 600 cm⁻¹ due to Ca disappeared completely.

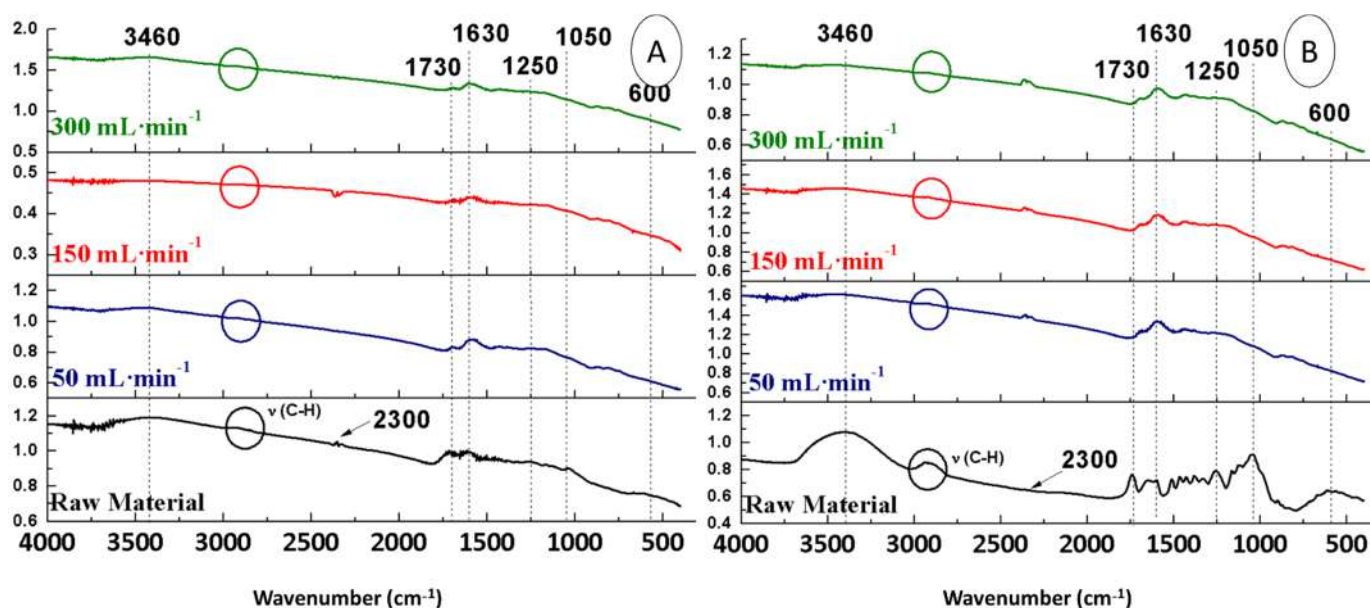


Figure 5. FTIR spectra of biochars from OS + H₂SO₄ (A) and OS (B) at different Ar flows.

Finally, with respect to the OS biochars (Figure 5B), the band at 3400 cm⁻¹ (H₂O) remained in all samples. On the contrary, the band at 2900 cm⁻¹ was not present in the samples. The band at 2300 cm⁻¹ (CO₂) remained stable. The band at 1730 cm⁻¹ (C=O) and at 1630 cm⁻¹ (C=C) still occurred, keeping stable in all samples. The bands at 1250 and 1050 cm⁻¹ (CO) disappeared after pyrolysis. Argon flow did not influence aromatic compounds (800 cm⁻¹). Finally, the characteristic peak of calcium (600 cm⁻¹) disappeared completely.

In summary, it could be concluded that the most influential parameter on biochar spectra was the maximum pyrolysis temperature, which is reflected in Section 2.4.1.

2.4.4. Specific Surface of Biochars

The specific surface area is an important parameter, as it could influence the use of biochars from OS as a catalyst for esterification reactions. The specific surface area of the biochars obtained under the different pyrolysis conditions is illustrated in Table 3.

It could be observed that the sulphuric pre-treatment of OS increased the specific surface area in biochars. Therefore, all biochars obtained from pyrolysis of OS + H₂SO₄ had higher specific surface area than those obtained from OS without pre-treatment under the same conditions. Therefore, the highest BET surface was obtained at 600 °C with OS + H₂SO₄ as a raw material.

Table 3. Specific surface of the biochars obtained under different pyrolysis conditions.

Raw Material	T (°C)	H _{ramp} (°C·min ⁻¹)	Ar Flow Rate (mL·min ⁻¹)	S _{BET} (m ² ·g ⁻¹)
OS + H ₂ SO ₄	600	10	150	418.60
OS + H ₂ SO ₄	500	10	150	263.38
OS + H ₂ SO ₄	400	10	150	5.80
OS + H ₂ SO ₄	400	5	150	13.75
OS + H ₂ SO ₄	400	20	150	21.50
OS + H ₂ SO ₄	400	10	150	42.09
OS + H ₂ SO ₄	400	20	300	106.11
OS + H ₂ SO ₄	400	20	50	52.95
OS + H ₂ SO ₄	600	10	150	367.93
OS	600	10	150	242.70
OS	500	10	150	230.40
OS	400	10	150	4.55
OS	400	20	150	8.18
OS	400	20	50	3.94
OS	400	5	150	8.90
OS	400	5	50	6.57
OS	400	5	300	12.37

2.5. Application of Biochars as Biocatalyst for the Esterification Reaction

The acid index of the commercial oleic acid was 182.18 mg KOH/g oil. The acid index was used to follow the reaction. Two phases were obtained: the organic phase (upper phase) composed of methyl esters, and the aqueous phase (lower phase). Table 4 shows the percentage of both phases in each esterification reaction carried out with the different biochars obtained from pyrolysis (activated and non-activated).

Table 4. Resulting acid index, esterification yield, and percentages of organic (OP) and aqueous (AP) phases obtained after esterification.

Biochar	Impregnation	Acid Index	Esterification Yield	OP (%)	AP (%)
1	No	172.2	5.5	-	-
2	No	180.7	0.3	-	-
4	Yes	13.1	92.8	63.9	32.1
5	Yes	16.1	91.2	64.1	22.8
6	No	183.7	0.0	-	-
6	Yes	26.7	85.3	52.1	26.9
7	Yes	17.4	90.4	60.8	36.8
8	Yes	12.9	92.9	58.5	26.5
9	Yes	8.8	95.2	61.0	28.5
10	Yes	9.8	94.6	62.8	23.7
11	Yes	7.1	96.1	55.3	25.3
12	Yes	7.0	96.2	63.7	26.6
13	Yes	10.3	94.3	57.7	23.0
15	Yes	8.7	95.2	49.2	28.9
16	Yes	8.4	95.4	67.3	24.8
17	Yes	7.8	95.7	59.9	25.7

The esterification yields obtained were similar to those found in the literature using biochars from the pyrolysis of *Jatropha curcas* L. [18] and microalgae [19], whose authors reported esterification yields of up to 83.6 and 94.2%, respectively.

The esterifications using the biochars from OS, which had low specific surfaces (Table 3), provided better yields than when using the biochars from OS + H₂SO₄ (Table 4). This could be explained by the fact that the lower the specific surface, the larger the pore size. The larger the pore size, the better the absorption of large molecules such as sulphuric

acid [32]. Furthermore, the pyrolysis temperature at which the biochar was obtained seemed to influence the esterification reaction, with 400 °C being the optimal temperature to obtain biochars for the esterification reaction.

The organic phase of Experiment 12, which achieved the highest esterification yield (96.2%), was analysed as described in Section 3.5.2. In Table 5, the compounds with a probability of matching with the database greater than 40% were identified, along with their relative area.

Table 5. Composition of the organic phase obtained after esterification of commercial oleic acid.

Area (%)	Compound
5.65	Dodecanoic acid methyl ester
2.78	Methyl myristoleate
9.49	Palmitic acid methyl ester
12.79	Palmitoleic acid methyl ester
5.83	Cis-10-heptadecenoic acid methyl ester
48.78	Oleic acid methyl ester
13.50	Linoleic acid methyl ester
1.18	11-Eicosenoic acid methyl ester

3. Materials and Methods

3.1. Raw Materials

The OS were provided by the Cooperativa Agrícola Olivarera Virgen del Campo S.C.A. (Cañete de las Torres, Córdoba, Spain). The reagents used were sulphuric acid (H₂SO₄) 98.0 wt.% (PanReac, Barcelona, Spain), methanol (CH₃OH) 99.5 wt.% (PanReac, Barcelona, Spain), and oleic acid 65.0–88.0 wt.% (PanReac, Barcelona, Spain). The inert gas used in the pyrolysis was argon (Ar) (Al Air Liquid España, Madrid, Spain).

3.1.1. Pre-treatment of Olive Stones

The OS grinding was carried out in a planetary ball mill (Retsch PM 200, Düsseldorf, Germany). The mill was programmed at 500 rpm for 20 min. Grinding was carried out to obtain an OS particle diameter size of less than 150 µm.

Once all OS were homogenized, a fraction was treated before pyrolysis with H₂SO₄. The pre-treatment consisted of pouring 1 mL of 98 wt.% H₂SO₄ per gram of OS, after which it was homogenised and washed with excess distilled water until it had neutral pH and dried in an oven at 45 °C for 24 h to remove moisture. Finally, the mixture was homogenised in a mortar.

3.2. Pyrolysis

The OS pre-treated with sulphuric acid and the OS without previous treatment were subjected to pyrolysis under an inert gas atmosphere (Ar) (Figure 6). The pyrolytic furnace (16 cm height, 3.5 cm diameter) was a vertical tubular furnace with a ceramic support with a pore size of 3 mm. Its maximum temperature is 900 °C and it is controlled by a CN300-P self-tuning PID controller (Conatec, Irún, Spain).

Between 5 g of OS pre-treated with H₂SO₄ or 6 g of OS untreated were introduced into the reactor. The temperatures to which the samples were subjected for 2 h were 400, 500, and 600 °C, with heating ramps of 5, 10, and 20 °C·min⁻¹. Argon flow rates of 50, 150, and 300 mL·min⁻¹ were used during the experiments (Table 6).

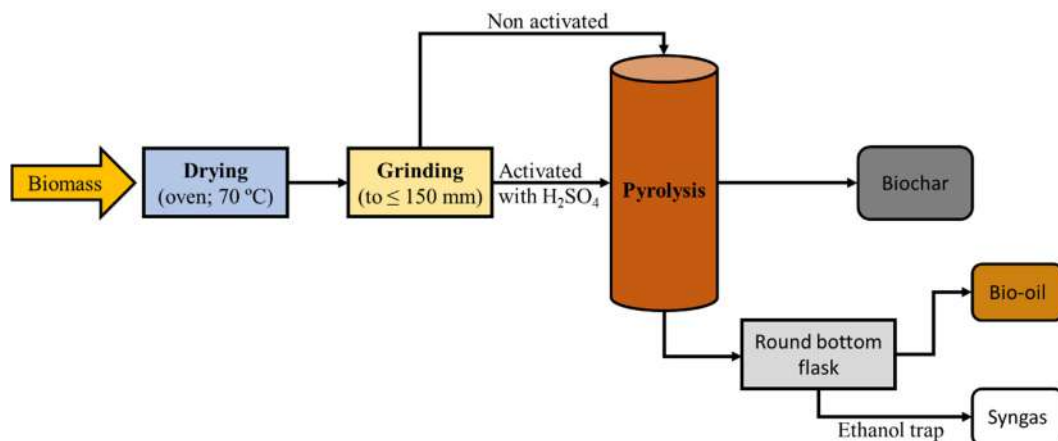


Figure 6. Process scheme for biomass pyrolysis.

Table 6. Pyrolysis conditions for olive stones (OS).

Pyrolysis	Raw Material	T (°C)	H _{ramp} (°C·min ⁻¹)	Ar Flow (mL·min ⁻¹)
1	OS + H ₂ SO ₄	600	10	150
2	OS + H ₂ SO ₄	500	10	150
3	OS + H ₂ SO ₄	400	10	150
4	OS + H ₂ SO ₄	400	5	150
5	OS + H ₂ SO ₄	400	20	150
6	OS + H ₂ SO ₄	400	10	150
7	OS + H ₂ SO ₄	400	20	300
8	OS + H ₂ SO ₄	400	20	50
9	OS + H ₂ SO ₄	600	10	150
10	OS	600	10	150
11	OS	500	10	150
12	OS	400	10	150
13	OS	400	20	150
14	OS	400	20	50
15	OS	400	5	150
16	OS	400	5	50
17	OS	400	5	300

3.3. Bio-Oil Characterisation

The liquid phase was recovered by transferring it from the two-neck flask of the pyrolytic equipment to a previously tared round bottom flask. After that, to remove the remaining residue from the bottom of the two-neck flask, a few microliters of acetone were introduced and poured into the round bottom flask. Subsequently, bio-oil was taken to a rotary evaporator (Heidolph, Schwabach, Germany) to evaporate the acetone and obtain pure bio-oil.

A qualitative analysis of the bio-oil composition from pyrolysis was performed with a TSQ8000 mass spectrometer (Thermo Fisher Scientific, Waltham, MA, USA) coupled to a triple quadrupole gas chromatograph (GC-MS) equipped with an autosampler. A Zebron ZB-5MS (Phenomenex, CA, USA) column (30 m × 0.25 mm × 0.25 μm; 5% phenylarylene, 95% dimethylpolysiloxane) and N₂ as carrier gas were used. The analyses were carried out under the following conditions: 50 °C initial temperature, 7 °C·min⁻¹ heating ramp for 30 min, and final temperature 310 °C.

The identification of the peaks was performed using the database of the Quan Browser tool of the XCalibur software (Thermo Fisher Scientific, Waltham, MA, USA). To limit the number of compounds, several factors were taken into account: relative area of the

compound greater than 1, match probability of the compound in the database greater than 40%, and occurrence of the compound in a greater number of samples.

3.4. Biochar Characterisation

3.4.1. Thermogravimetric Analysis

The thermogravimeter with which this analysis was carried out was a SDT Q600 electrobalance (TA Instruments, Inc., New Castle, DE, USA), which has a sensitivity of $\pm 0.5 \mu\text{g}$. The system responsible for the generation of heat was a vertical furnace that allows a maximum pyrolysis temperature of $1200 \text{ }^\circ\text{C}$ to be reached.

The raw material (OS) was treated at a heating ramp of $6 \text{ }^\circ\text{C}\cdot\text{min}^{-1}$ up to $800 \text{ }^\circ\text{C}$, with a constant flow of $100 \text{ mL Ar}\cdot\text{min}^{-1}$. This treatment was carried out until the complete decomposition of the organic matter, which was then burned in air, obtaining only inorganic ash.

3.4.2. Fourier-Transform Infrared Spectroscopy (FTIR)

A Nicolet TM iSTM5 FTIR Fourier transform infrared spectrometer (Thermo Fisher Scientific, Waltham, MA, USA) was used to characterise the feedstock and all biochars. This homogenised feedstock was compacted in a uniaxial press under pressure.

For transmission measurements, pellets were prepared using potassium bromide (KBr) as diluent, with a final sample concentration of 5 wt.%, and spectra were recorded in the $500\text{--}4000 \text{ cm}^{-1}$ wavenumber range.

3.4.3. BET Specific Surface

The BET method was used to calculate the specific surface area (SBET). A Gemini V-2365/V.1.00 adsorption equipment (Micromeritics Instrument Corporation, Norcross, GA, USA) was used. The biochars were previously degassed at $150 \text{ }^\circ\text{C}$ for 2 h under a N_2 atmosphere.

3.5. Esterification Reaction

The esterification reactions of olive stones, whether pre-treated (impregnated) with H_2SO_4 or not, were carried out in a stirred tank batch reactor (25 cm height, 12 cm diameter), equipped with a temperature regulator and a gas condenser (Liebig refrigerant cooled with water at room temperature) at $60 \text{ }^\circ\text{C}$ for 30 min.

The mixture was heated at $60 \text{ }^\circ\text{C}$ for 30 min by means of a Fibroman-C heating mantle (J.P. SELECTA, Barcelona, Spain) connected to a temperature controller. Two additional openings were used to extract the sample and introduce the thermocouple, which continuously measured the temperature.

Before esterification, all biochars, except biochars obtained from Pyrolyses 1, 2, and 6 (Table 6), were subjected to activation with sulphuric acid. Similar to the pre-treatment of the raw material (Section 3.1.1), the activation of the biochars was carried out by impregnation of 1 g of biochar with 1 mL of sulphuric acid (98 wt.%). The conditions under which the esterifications were carried out were: 10 g oleic acid, 17.2 g methanol (1:15 oleic acid to methanol molar ratio), and 1 g biochar. These conditions were selected from previous studies available in the literature [33].

Finally, the interesting products were obtained in the organic phase, which was subjected to two determinations. The first was the measurement of its acid index, and the second was the determination of the fatty acid methyl esters (FAME) by gas chromatography–mass spectroscopy in the TSQ8000 mass spectrometer (Thermo Fisher Scientific, Waltham, MA, USA) described in Sections 3.5.1 and 3.5.2.

3.5.1. Acid Index

Before the esterification started, it was important to know the acid index of the oleic acid, as the reduction of its value indicates the extent of the esterification reaction and allows the calculation of its yield. UNE-EN 14104:2003 was followed to determine the

acidity of oleic acid and the esterification product. A detailed description of this procedure can be found in [34].

3.5.2. Gas Chromatography-Mass Spectroscopy

The percentage of different FAME in the samples was determined by gas chromatography using methyl heptadecanoate as the internal standard. A HP 5890 series II gas chromatograph (Hewlett Packard, Palo Alto, CA, USA) equipped with a SP2380 capillary column (Sigma-Aldrich, St Louis, MO, USA) [60 m × 0.25 mm internal diameter × 0.25 µm film thickness] was used. The column temperature was set at 185 °C and then the temperature program was increased to 220 °C with a heating ramp of 3 °C min⁻¹. The injection was operated in splitless mode, with injector and detector temperatures of 210 °C and 250 °C, respectively. The FAMES were identified by mass spectrometry by comparing the spectra with those of the database for this type of compound (Wiley, NIST).

4. Conclusions

Thermogravimetric analysis showed that OS have a low percentage of lignin. The FTIR spectrum of the OS + H₂SO₄ feedstock did not show differences in spectral bands compared to that of the OS feedstock, but did show a much lower intensity of the bands. The most suitable conditions to obtain the highest biochar yield from OS + H₂SO₄ were 400 °C, 20 °C·min⁻¹ and 150 mL Ar·min⁻¹. The optimal conditions to obtain the highest bio-oil yield from OS were 400 °C, 5 °C·min⁻¹ and 50 mL Ar·min⁻¹. The highest specific surface area (approximately 400 m²/g) was obtained in the biochar from the pyrolysis at 600 °C from OS + H₂SO₄. The FTIR spectra of the biochars obtained from OS + H₂SO₄ and OS did not show noticeable differences. However, increasing the pyrolysis temperature decreases the intensity of the bands. The use of biochar from OS as catalyst in the esterification reaction showed better yield compared to the biochar from OS + H₂SO₄. The pyrolysis conditions in terms of biochar characteristics did not affect the esterification yield.

Author Contributions: Conceptualisation, P.Á.-M.; methodology, P.Á.-M.; formal analysis, F.J.S.-B., T.J.B.d.H.-L., P.Á.-M. and J.F.G.-M.; investigation, F.J.S.-B. and T.J.B.d.H.-L.; resources, P.Á.-M.; writing—original draft preparation, F.J.S.-B. and J.F.G.-M.; writing—review and editing, J.F.G.-M.; supervision, P.Á.-M. and J.F.G.-M.; project administration, P.Á.-M.; funding acquisition, P.Á.-M. All authors have read and agreed to the published version of the manuscript.

Funding: This research was funded by the European Union under grant LIFE 13-Bioseville ENV/1113, and by the FEDER funds through the CARBOENERGY project (FEDER INNTERCONNECTA 2018 call).

Data Availability Statement: The data presented in this study are available on request from the corresponding author. The data are not publicly available due to confidentiality agreements with the funding companies.

Conflicts of Interest: The authors declare no conflict of interest.

References

1. García Martín, J.F.; Cuevas, M.; Feng, C.H.; Álvarez Mateos, P.; Torres García, M.; Sánchez, S. Energetic valorisation of olive biomass: Olive-tree pruning, olive stones and pomaces. *Processes* **2020**, *8*, 511. [[CrossRef](#)]
2. Donner, M.; Radić, I. Innovative circular business models in the olive oil sector for sustainable mediterranean agrifood systems. *Sustainability* **2021**, *13*, 2588. [[CrossRef](#)]
3. Sánchez, F.; San Miguel, G. Improved fuel properties of whole table olive stones via pyrolytic processing. *Biomass Bioenergy* **2016**, *92*, 1–11. [[CrossRef](#)]
4. Rodríguez, G.; Lama, A.; Rodríguez, R.; Jiménez, A.; Guillén, R.; Fernández-Bolaños, J. Olive stone an attractive source of bioactive and valuable compounds. *Bioresour. Technol.* **2008**, *99*, 5261–5269. [[CrossRef](#)]
5. Martín Lara, M.A.; Hernáinz, F.; Calero, M.; Blázquez, G.; Tenorio, G. Surface chemistry evaluation of some solid wastes from olive-oil industry used for lead removal from aqueous solutions. *Biochem. Eng. J.* **2009**, *44*, 151–159. [[CrossRef](#)]
6. Fernández Bolaños, J.; Felizón, B.; Heredia, A.; Rodríguez, R.; Guillén, R.; Jiménez, A. Steam-explosion of olive stones: Hemicellulose solubilization and enhancement of enzymatic hydrolysis of cellulose. *Bioresour. Technol.* **2001**, *79*, 53–61. [[CrossRef](#)]

7. Cuevas, M.; García-Martín, J.F.; Bravo, V.; Sánchez, S. Ethanol production from olive stones through liquid hot water pre-treatment, enzymatic hydrolysis and fermentation. Influence of enzyme loading, and pre-treatment temperature and time. *Fermentation* **2021**, *7*, 25. [CrossRef]
8. Merino, M.R.; Guijarro Rodríguez, J.; Fernández Martínez, F.; Santa Cruz Astorqui, J. Viability of using olive stones as lightweight aggregate in construction mortars. *Rev. Constr.* **2017**, *16*, 431–438. [CrossRef]
9. Harina de Semilla de Aceituna Premio a la Innovación en Sial Paris-Elayo. Available online: <https://www.elayo.es/harina-de-semilla-de-aceituna-premio-a-la-innovacion-en-sial/> (accessed on 27 October 2021).
10. AIMPLAS and OLIFE Use Olive Stones to Develop a New Sustainable Plastic Material for Oil Product Packaging | Plateforme des Acteurs Européens de L'économie Circulaire. Available online: <https://circulareconomy.europa.eu/platform/fr/good-practices/aimplas-and-olife-use-olive-stones-develop-new-sustainable-plastic-material-oil-product-packaging> (accessed on 27 October 2021).
11. Won Seo, M.; Hon Lee, S.; Nam, H.; Lee, D.; Tokmurzin, D.; Wang, S.; Park, Y.-K. Recent advances of thermochemical conversion processes for biorefinery. *Bioresour. Technol.* **2022**, *343*, 126109. [CrossRef]
12. Collard, F.X.; Blin, J. A review on pyrolysis of biomass constituents: Mechanisms and composition of the products obtained from the conversion of cellulose, hemicelluloses and lignin. *Renew. Sustain. Energy Rev.* **2014**, *38*, 594–608. [CrossRef]
13. Bhattacharjee, N.; Baran Biswas, A. Pyrolysis of orange bagasse: Comparative study and parametric influence on the product yield and their characterization. *J. Environ. Chem. Eng.* **2019**, *7*, 102903. [CrossRef]
14. Guo, J.; Zheng, L.; Li, Z.; Zhou, X.; Cheng, S.; Zhang, L.; Zhang, Q. Effects of various pyrolysis conditions and feedstock compositions on the physicochemical characteristics of cow manure-derived biochar. *J. Clean. Prod.* **2021**, *311*, 127458. [CrossRef]
15. Basu, P. *Pyrolysis and Torrefaction*, 1st ed.; Elsevier: Amsterdam, The Netherlands, 2010; ISBN 9780123749888.
16. Sánchez Borrego, F.J.; Álvarez Mateos, P.; García Martín, J.F. Biodiesel and other value-added products from bio-oil obtained from agrifood waste. *Processes* **2021**, *9*, 797. [CrossRef]
17. Bradley, D.; Hektor, B.; Wild, M.; Deutmeyer, M.; Schowenberg, P.P.; Hess, J.R.; Shankar Tumuluru, J.; Bradburn, K. Low cost, long distance biomass supply chains. In *Task 40: Sustainable International Bioenergy Trade*; Goh, C.S., Junginger, M., Eds.; IEA Bioenergy: Paris, France, 2013; pp. 1–65.
18. Álvarez-Mateos, P.; García-Martín, J.F.; Guerrero-Vacas, F.J.; Naranjo-Calderón, C.; Barrios, C.C.; Pérez Camino, M.C.; Barrios, C.C. Valorization of a high-acidity residual oil generated in the waste cooking oils recycling industries. *Grasas Y Aceites* **2019**, *40*, e335. [CrossRef]
19. Roy, M.; Mohanty, K. Valorization of de-oiled microalgal biomass as a carbon-based heterogeneous catalyst for a sustainable biodiesel production. *Bioresour. Technol.* **2021**, *337*, 125424. [CrossRef]
20. Sun, Y.; Gao, B.; Yao, Y.; Fang, J.; Zhang, M.; Zhou, Y.; Chen, H.; Yang, L. Effects of feedstock type, production method, and pyrolysis temperature on biochar and hydrochar properties. *Chem. Eng. J.* **2014**, *240*, 574–578. [CrossRef]
21. Islam, M.K.; Rehman, S.; Guan, J.; Lau, C.Y.; Tse, H.Y.; Yeung, C.S.; Leu, S.Y. Biphasic pretreatment for energy and carbon efficient conversion of lignocellulose into bioenergy and reactive lignin. *Appl. Energy* **2021**, *303*, 117653. [CrossRef]
22. Laurenza, A.G.; Losito, O.; Casiello, M.; Fusco, C.; Nacci, A.; Pantone, V.; D'Accolti, L. Valorization of cigarette butts for synthesis of levulinic acid as top value-added chemicals. *Sci. Rep.* **2021**, *11*, 15775. [CrossRef]
23. Hasanin, M.S.; Kassem, N.; Hassan, M.L. Preparation and characterization of microcrystalline cellulose from olive stones. *Biomass Convers. Biorefinery* **2021**. [CrossRef]
24. Yang, H.; Yan, R.; Chen, H.; Lee, D.H.; Zheng, C. Characteristics of hemicellulose, cellulose and lignin pyrolysis. *Fuel* **2007**, *86*, 1781–1788. [CrossRef]
25. Alshuaib, S.M.; Al-Ghouthi, M.A. Multivariate analysis for FTIR in understanding treatment of used cooking oil using activated carbon prepared from olive stone. *PLoS ONE* **2020**, *15*, e0232997. [CrossRef]
26. Bartocci, P.; D'Amico, M.; Moriconi, N.; Bidini, G.; Fantozzi, F. Pyrolysis of olive stone for energy purposes. *Energy Procedia* **2015**, *82*, 374–380. [CrossRef]
27. Salimi, M.; Salehi, Z.; Heidari, H.; Vahabzadeh, F. Production of activated biochar from *Luffa cylindrica* and its application for adsorption of 4-nitrophenol. *J. Environ. Chem. Eng.* **2021**, *9*, 105403. [CrossRef]
28. Zhao, L.; Zheng, W.; Mašek, O.; Chen, X.; Gu, B.; Sharma, B.K.; Cao, X. Roles of phosphoric acid in biochar formation: Synchronously improving carbon retention and sorption capacity. *J. Environ. Qual.* **2017**, *46*, 393–401. [CrossRef] [PubMed]
29. Cao, F.; Schwartz, T.J.; McClelland, D.J.; Krishna, S.H.; Dumesic, J.A.; Huber, G.W. Dehydration of cellulose to levoglucosenone using polar aprotic solvents. *Energy Environ. Sci.* **2015**, *8*, 1808–1815. [CrossRef]
30. Kudo, S.; Goto, N.; Sperry, J.; Norinaga, K.; Hayashi, J.I. Production of levoglucosenone and dihydrolevoglucosenone by catalytic reforming of volatiles from cellulose pyrolysis using supported ionic liquid phase. *ACS Sustain. Chem. Eng.* **2017**, *5*, 1132–1140. [CrossRef]
31. Comba, M.B.; Tsai, Y.; Sarotti, A.M.; Mangione, M.I.; Suárez, A.G.; Spanevello, R.A. Levoglucosenone and its new applications: Valorization of cellulose residues. *Eur. J. Org. Chem.* **2018**, *5*, 590–604. [CrossRef]
32. Wu, L.; Wan, W.; Shang, Z.; Gao, X.; Kobayashi, N.; Luo, G.; Li, Z. Surface modification of phosphoric acid activated carbon by using non-thermal plasma for enhancement of Cu(II) adsorption from aqueous solutions. *Sep. Purif. Technol.* **2018**, *197*, 156–169. [CrossRef]

33. Ben-Youssef, C.; Chávez-Yam, A.; Zepeda, A.; Rivera, J.M.; Rincón, S. Simultaneous esterification/transesterification of waste cooking oil and *Jatropha curcas* oil with MOF-5 as a heterogeneous acid catalyst. *Int. J. Environ. Sci. Technol.* **2021**, *18*, 3313–3326. [[CrossRef](#)]
34. García Martín, J.F.; Carrión Ruiz, J.; Torres García, M.; Feng, C.H.; Álvarez Mateos, P. Esterification of free fatty acids with glycerol within the biodiesel production framework. *Processes* **2019**, *7*, 832. [[CrossRef](#)]